WET SCRUBBING OF BIOMASS PRODUCER GAS TARS USING VEGETABLE OIL

By

PRAKASHBHAI RAMABHAI BHOI

Bachelor of Engineering in Mechanical Engineering
Sardar Patel University
Vallabh Vidyanagar, Gujarat, India
1999

Master of Technology in Mechanical Engineering
(Specialization: Turbo Machines)
Sardar Vallabhbhai National Institute of Technology
Surat, Gujarat, India
2005

Submitted to the Faculty of the
Graduate College of the
Oklahoma State University
in partial fulfillment of
the requirements for
the Degree of
DOCTOR OF PHILOSOPHY
May, 2014

WET SCRUBBING OF BIOMASS PRODUCER GAS

TARS USING VEGETABLE OIL

Dissertation Approved:

Dr. Raymond L. Huhnke

Committee Chair & Dissertation Advisor

Dr. Krushna N. Patil

Dr. Ajay Kumar

Dr. James R. Whiteley

ACKNOWLEDGEMENTS

Financial support for this research received from the National Science Foundation EPSCoR program under Grant number EPS-0814361 and Oklahoma Agricultural Experimentation Station is greatly appreciated.

I would like to express my sincere appreciation and gratitude to my Research Advisor and Committee Chair Dr. Raymond L. Huhnke for his expert guidance, valuable suggestions and recommendations, consistent encouragement and sharing experience during every stage of my doctoral research program. I greatly improved my useful skills such as critical thinking ability through one-on-one interaction, planning of experimental design, data interpretation, writing and presentation skills. I am extremely grateful to Dr. James R. Whiteley for his expert advice and valuable suggestions. One-on-one meetings with Dr. Whiteley helped me a lot in improving my understanding of the research subject and the quality of my research. I am extremely grateful to my research advisory committee members Dr. Krushna Patil and Dr. Ajay Kumar for their expert guidance, suggestions, valuable contributions and support to my research program.

It would have been impossible to finish this work on time without a great support from BAE Laboratory staff members. I am obliged to Mr. Wayne Kiner and his team for fabricating a wet scrubbing column and a liquid distributor. I am also thankful to Mr. Mike Veldman for helping me in the electrical connections, instrumentation and data recording.

I also appreciate the help provided by Mr. Jason Walker whenever I needed it most. I greatly appreciate the support extended by Mr. Mark Gilstrap in preparing GC/MS for the sample analysis, for helping me in calibration of GC/MS, developing procedure for hazard analysis (PHA) and sharing his expert knowledge and experiences. I am also thankful to BAE staff members including Ms. Nancy Rogers, Ms. Hicks Jannice, Mr. Craig Trible and other staff members for their great help.

I am extremely thankful to Dr. Mark Payton for his valuable guidance and performing statistical analysis of the wet scrubbing experimental data. I am also thankful to Dr. Khaled Gasem for allowing me to audit Advanced Thermodynamics course and sharing his immense knowledge of thermodynamic modeling which was very much useful in understanding the process modeling of my doctoral research project.

I am very much grateful to Dr. Tony Cai for helping me in procuring random packing materials for the packed bed column used in this research. I am also grateful to Dr. Josh Ramsey for having a technical discussion and helping me in understanding fundamentals of the absorption process. A special thanks to Dr. Mark Wilkins for allowing me to complete my teaching practicum in his Renewable Energy Engineering course and providing me an opportunity to develop teaching skills.

I am extremely thankful to Mr. Solomon Gebreyohannes for sharing his knowledge in developing a process model. I am also thankful to Dr. Anand Vennavelli, Mr. Anil Krishna Jammula and Mr. Yash Tamhankar, Dr. Karthikeyan Ramachandriya, Mr. Anand Govindarajan, and Mr. Kumar Singarapu for their involvement in technical discussion and contributing their valuable time. I greatly appreciate the support from Mr. Vinayak Shenoy for his help in experiments. Social support from family friends (Dr.

Ashok Sharma, Dr. Amit Khanchi, Dr. Bhavna Sharma, Dr. Karthic Ramachandriya, Dr. Jasreen Sekhon, Dr. Dinesh Babu, and Dr. Hiren Bhavsar) and their families are greatly appreciated.

I will always be thankful to my previous mentors: Dr. B. S. Pathak and Mr. S. R. Patel for developing my expertise in thermochemical conversion technologies and nurturing my career, Dr. S. A. Channiwala for his expert guidance and widening my expertise in the field of combustion, Mr. Y. D. Mishra for sharing his immense knowledge and developing my project management and leadership skills in addition to technical skills in the field of power plant engineering.

I am extremely grateful to my wife (Rita) and beautiful daughter (Kavya) for their love, care and extraordinary support. A smiling face of my daughter encouraged me every day. My elder brothers (Mr. Rameshbhai, Mr. Bharatbhai and Mr. Dineshbhai) are a great source of motivation and helped me every stage of my career. I missed my late father (Shri Ramabhai Babubhai Bhoi) a lot and will always be thankful to him for contributing to what I achieved so far.

Last but not least, I thank God for giving me every opportunity to learn, develop and excel in my career.

Name: PRAKASHBHAI RAMABHAI BHOI

Date of Degree: MAY, 2014

Title of Study: WET SCRUBBING OF BIOMASS PRODUCER GAS TARS USING VEGETABLE OIL

Major Field: BIOSYSTEMS ENGINEERING

Abstract:
The overall aims of this research study were to generate novel design data and to develop an equilibrium stage-based thermodynamic model of a vegetable oil based wet scrubbing system for the removal of model tar compounds (benzene, toluene and ethylbenzene) found in biomass producer gas. The specific objectives were to design, fabricate and evaluate a vegetable oil based wet scrubbing system and to optimize the design and operating variables; i.e., packed bed height, vegetable oil type, solvent temperature, and solvent flow rate. The experimental wet packed bed scrubbing system includes a liquid distributor specifically designed to distribute a high viscous vegetable oil uniformly and a mixing section, which was designed to generate a desired concentration of tar compounds in a simulated air stream. A method and calibration protocol of gas chromatography/mass spectroscopy was developed to quantify tar compounds. Experimental data were analyzed statistically using analysis of variance (ANOVA) procedure. Statistical analysis showed that both soybean and canola oils are potential solvents, providing comparable removal efficiency of tar compounds. The experimental height equivalent to a theoretical plate (HETP) was determined as 0.11 m for vegetable oil based scrubbing system. Packed bed height and solvent temperature had highly significant effect (p<0.0001) while, the solvent flow rate did not have a significant (p>0.05) effect on the removal of model tar compounds. The packing specific constants, C_h and $C_{P,0}$, for the Billet and Schultes pressure drop correlation were determined as 2.52 and 2.93, respectively. The equilibrium stage based thermodynamic model predicted the removal efficiency of model tar compounds in the range of 1-6%, 1-4% and 1-2% of experimental data for benzene, toluene and ethylbenzene, respectively, for the solvent temperature of 30°C. The NRTL-PR property model and UNIFAC for estimating binary interaction parameters are recommended for modeling absorption of tar compounds in vegetable oils. Bench scale experimental data from the wet scrubbing system would be useful in the design and operation of a pilot scale vegetable oil based system. The process model, validated using experimental data, would be a key design tool for the design and optimization of a pilot scale vegetable oil based system.

TABLE OF CONTENTS

Chapter Page

Chapter Page

LIST OF TABLES

Table Page

Table Page

LIST OF FIGURES

Figure Page

Figure Page

Figure Page

Figure Page

Figure Page

CHAPTER I

INTRODUCTION AND LITERATURE REVIEW

The sustainable supply of energy is challenging due to growing concerns over climate change, national energy security and increasing global demands. This leads to an urgent need for developing sustainable biofuels, bioproducts, biopower, and bioenergy (DOE, 2012). Biomass has been identified as a potential source of energy to address continued rising demand of imported oils. Over a billion tons of renewable biomass is available in the United States (DOE, 2012). The major biomass sources include dedicated energy crops, woody crops, agricultural and forest residues, perennial grasses, municipal solid waste, urban solid and food waste, and algae. In Oklahoma, perennial grasses, primarily switchgrass, are potential biomass feedstocks for the production of biofuels (Kenkel et al., 2006).

The lignocellulosic to 2nd generation biofuels conversion technologies are categorized by two major pathways: (1) biochemical and (2) thermochemical. The technical challenges of biochemical conversion technologies include variability of biomass feedstocks, expensive and specific cellulosic enzymes and microorganism requirement, low yield of biofuels because the lignin content of biomass is unreacted, expensive pretreatment processing, and inhibitory effect during pretreatment of biomass (Hoekman, 2009). In comparison, thermochemical conversion technologies overcome many of the above mentioned challenges. Thermochemical conversion pathways include gasification and pyrolysis technologies. Gasification is a thermal decomposition of lignocellulosic biomass at high temperature in the presence of limited amount of oxygen or air.

The producer gas generated through gasification consists mainly of hydrogen, carbon monoxide, methane, carbon dioxide, and nitrogen. Producer gas also contains solid particulate matters (SPM), ash, water, organic impurities (mainly tars), and inorganic impurities such as ammonia, hydrogen sulfide, sulfur dioxide, and nitrogen dioxide (Torres et al., 2007). Some of the major challenges of gasification technology are minimization of tar formation and removal of tars from producer gas (Hoekman, 2009).

1.1 Biomass producer gas tars

1.1.1 Tar generation

Many definitions of biomass producer gas tars are reported in the literature. One definition is "organics produced through thermal or partial oxidation of any organic material are called tars" (Milne et al., 1998).

Yield and composition of tar depends on gasifier type, operating pressure and temperature, feedstock, and residence time. Reaction conditions inside each type of gasifier system are different and as a result, tar generation varies (Baker et al., 1988). Fixed bed gasifiers, such as downdraft and updraft, are considered to have separate zones of temperatures including drying, pyrolysis, combustion, and reduction zones. Tars are produced mainly in the pyrolysis zone. The yield of tar from an updraft gasifier is high compared to the downdraft unit due to the difference in flow of producer gas through the gasifier. In an updraft gasifier system, the tar passes through a pyrolysis and drying section which is at a very low temperature (80-200°C). At these temperatures, tar entrained in the producer gas remains in the form of condensed droplets. In a downdraft gasifier, tar-contained producer gas passes through a high temperature (above 1000°C) combustion zone which further reduces tar yield through thermal cracking and oxidizing process (Baker et al., 1988). Consequently, there is a large difference between the tar yields from downdraft and updraft gasifiers. In a fluidized bed gasifier, a high temperature (600-900°C) and gas-solid contact enhances tar cracking (Baker et

al., 1988). Tars produced in a fluidized bed gasifier are far less than the updraft gasifier while higher than the downdraft gasifier. A typical concentration range of tars is 10-100 g/m^3, 2-10 g/m^3, and 1 g/m^3 for updraft, fluidized bed, and downdraft gasifiers, respectively (Milne et al., 1998).

1.1.2 Compositions of tars

The amount and composition of tar depend on the type of gasifier and the severity of operating condition (mainly reactor temperature and residence time). Another important variable that affects tar composition is biomass composition (cellulose, hemicellulose and lignin content). The tar development scheme (Elliott, 1988), which illustrates the tar degradation phases as a function of process temperatures, is shown in Figure 1.1.

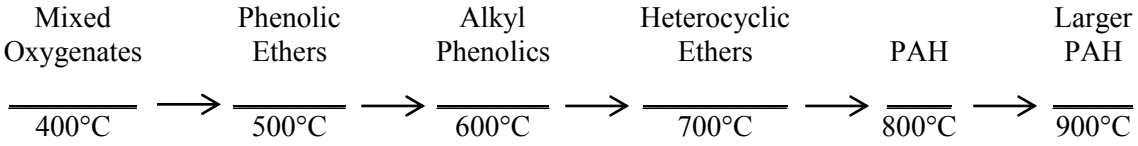

Figure 1.1 Biomass producer gas tar maturation scheme (Elliott, 1988)

Tars produced from initial pyrolysis of biomass are referred as primary tars, mainly consisting of mixed oxygenates (as shown in Figure 1.1), which further reduce to secondary tars mainly consisting of phenolic compounds and alkyl phenolics through thermal reaction of primary tars. The secondary compounds then convert into ternary tar compounds that mainly include heterocyclic ethers, poly aromatic hydrocarbon (PAH), and larger PAH.

The primary tars are extremely oxygenated and consequently are soluble in water. As mixed oxygenates pass through the high temperature zones, they successively convert to phenolic compounds through thermal deoxygenation and dehydrogenation, which further reduce to aromatic and poly aromatic hydrocarbons. The ternary tars, largely PAHs, are highly insoluble in water. When the operating temperature of a downdraft gasifier is above 800°C, it is postulated that the major composition of tar is mainly aromatic and poly aromatic hydrocarbons (Milne et al., 1998).

The compositional analyses of biomass producer gas tars have been reported by many researchers (Cateni, 2007; Coll et al., 2001; Milne et al., 1998). The major composition of wood waste-based producer gas tars, as reported by Milne et al. (1998) and Coll et al. (2001), consist of benzene (37.9%), toluene (14.3%), other one-ring aromatic hydrocarbons (13.9%), phenolic compounds (4.6%), with the remaining being the high molecular weight hydrocarbons. Cateni (2007) provided compositional analyses for tars generated from fluidized bed gasification of switchgrass. The weight distributions of the top 10 major tar compounds were: benzene (29%), toluene (18%), phenol (14%), ethylbenzene (10%), methyl phenol (8%), styrene (6%), xylene (5%), naphthalene (4%), dimethyl naphthalene (3%) and methyl naphthalene (3%), which represent about 75% of the total mass of the tar. As expected, the tar compounds reported by Cateni (2007) consisted mainly of deoxygenated hydrocarbons and PAH at the gasification temperature of 700 to 800°C, which are comparable to the tar maturation scheme given in Figure 1.1.

Table 1.1 Classifications of tars (Boerrigter et al., 2005)

Class	Type	Property	Examples
1	GC-undetectable	Very heavy tars	Heaviest tars (pitch), and biomass fragments
2	Heterocyclic tars compounds	Highly water soluble compounds	Pyridine, cresol, phenol, quinolone
3	Light aromatic – 1 ring	Do not pose problem with condensation	Toluene, styrene, ethylbenzene, and xylene
4	Light poly aromatic hydrocarbon – 2-3 rings PAH	Condense at comparatively high concentrations and intermediate temperature	Indene, naphthalene, biphenyl, and antracene
5	Heavy poly aromatic hydrocarbons – ≥ 4 rings PAH	Condense at comparatively high temperature low concentrations	Pyrene, crysene, and fluoranthene
6	GC detectable	-	unknowns

According to the Energy Research Center of the Netherlands (ECN) (Boerrigter et al., 2005), tars are categorized as six classes based on the molecular weight of tars compounds (Table 1.1). Boerrigter et al. (2005) reported that an increase in temperature leads to a decomposition of class 1 and 2 tars, while the concentration of class 3 and 5 tars increases.

Anis & Zainal (2011) reported that problems associated with tar is fundamentally related to its properties and composition rather than its quantity. Researchers also stated that the condensation behavior of tars is related with the properties of tar compounds. Bergman et al. (2002) stated that the tar dew-point temperature is the key parameter in designing producer gas cleaning devices. Tar dew-point temperature is the saturation temperature of tar, i.e., tar starts condensing when the producer gas temperature drops below tar dew-point temperature. A typical tar dew-point temperature varies from 150 to 350°C depending on the tar's specific compounds and associated concentrations. Condensation of heavy tar leads to a reduction in the tar dew-point temperature consequently allowing light tar to remain in vapor phase. Phuphuakrat et al. (2011) observed that the lighter tar compounds are difficult to condense. The most commonly used model tar compounds reported in the literature include benzene and toluene (Mudinoor, 2010) which are considered light tars.

In this study, benzene, toluene, and ethylbenzene were selected as model tar compounds because these tars are difficult to condense, i.e., least soluble tar compounds in chronological order. According to Cateni (2007), these three compounds account for 60% of the 10 major tar compounds in switchgrass-based producer gas.

1.1.3 Acceptable limits of tars

A typical tar concentration in the biomass producer gas varies from 1 to 100 g/Nm^3 (Milne et al., 1998). The acceptable tar content in producer gas depends largely on the end use applications. Producer gas can be used as a fuel in boilers and kilns for the production of thermal energy, as a fuel in internal combustion engines and gas turbines for power generation, or as a feedstock for the production of liquid biofuels, such as ethanol, methanol, hydrocarbons, and chemicals. The use of producer gas for thermal applications often does not result in a limit on the tar content because tars burn along with the producer gas, increasing the calorific value of producer gas (Baker et al., 1986). Such an application requires an adjacent installation of gasifier and burner to avoid condensation of tars and subsequent plugging of pipelines. In internal combustion engines, the allowable tar content

limit ranges from 50-100 mg/Nm^3 to avoid an accumulation and condensation in the gas mixing section and inlet valves (Baker et al., 1986; Xu et al., 2010). The producer gas may need to be compressed for gas turbines and internal compression engines resulting in higher partial pressures of tar compounds that may lead to condensation of tars (Anis & Zainal, 2011). In addition, a severe problem of erosion and corrosion in direct-fired gas turbines limits tar content to no higher than 5 mg/Nm^3. Though the permissible tar content for the liquid biofuels (such as ethanol, methanol, and hydrocarbons) and chemicals are not well-defined, a few studies reported the adverse effect on the catalysts, enzymes and microorganisms due to presence of tars and recommended a tar content limit to less than 0.1 mg/Nm^3 (Ahmed et al., 2006; Baker et al., 1986; Xu et al., 2010). Overall, the presence of tars in the producer gas creates challenges for downstream applications.

1.2 Biomass producer gas tar removal techniques

Tar removal techniques are mainly classified as primary or secondary depending on the location of processes implemented. Primary tar removal methods are employed in the gasification reactor, while secondary methods are installed downstream of the gasifier system.

1.2.1 Primary methods of tar removal

Primary methods of tar reduction include the selection of biomass feedstock, optimum gasifier design and operating conditions and proper bed catalysts or additives. The operating variables, such as pressure, temperature, gasifying agent, equivalence ratio (ER), and residence time have major effects on the formation and decomposition of tars. Additionally, these operating variables influence the performance parameters, primarily the temperature profile of the gasifier reactor, producer gas composition, carbon conversion efficiency, and gasification efficiencies.

Knight (2000) studied the effect of gasification system pressure on tars of whole tree chips and reported that as the system pressure increased from 8 to 21.4 bar, the oxygenated compounds, i.e., phenols, were removed completely. To achieve high carbon conversion efficiency and low tar

contents in the producer gas and, gasifier reactor operating temperature is recommended to be above 800°C. High temperature reduces the amount of tars and alters its composition through changes in the gasification chemical reactions. Kinoshita et al. (1994) studied the effect of temperature on tar composition, yield and concentration using a fixed bed gasification with sawdust as the feedstock. They reported that a significant amount of oxygen-containing compounds, predominantly phenol, benzo-furan and cresol, exists only at gasification temperatures below 800°C. As the gasification temperature is increased above 800°C, oxygen-containing compounds greatly reduce, and single-ring and two-ring compounds reduce (except benzene and naphthalene) while three-ring and four-ring compounds increase. A similar observation was reported by other researchers (Brage et al., 2000; Yu et al., 1997). In addition, Brage et al. (2000) observed more than 40% reduction in tar yield and increase in gas formation when the temperature increased from 700 to 900°C.

Equivalence ratio (ER) is defined as the ratio of actual air supplied to the stoichiometric air required for the complete combustion of feedstock. ER has influence on yield, concentration and composition of tars, producer gas calorific value, and carbon conversion and gasification efficiencies. According to Kinoshita et al. (1994), as ER increases, yield and concentration of tars decrease because more oxygen is available to react with volatiles in pyrolysis zone. However, there is a practical limitation on ER because at high ER, carbon monoxide and hydrogen decrease and carbon dioxide increases; consequently, the calorific value of producer gas reduces significantly. Kinoshita et al. (1994) also observed that as the ER increases from 0.22 to 0.32, the yields of benzene and naphthalene increase, yields of toluene and indane slightly increase initially and then decrease, while yields of xylene and styrene reduce linearly for producer gas generated from sawdust. Narvaez et al. (1996) observed similar trends for the effect of ER on tars using pine sawdust as the feedstock.

Air, steam, steam-oxygen and carbon dioxide have been studied as gasifying mediums (Devi et al., 2003). Gasifying medium has a significant influence on the producer gas composition, especially carbon monoxide, hydrogen and carbon dioxide, calorific value and tars. When air is used

as a gasifying medium, the calorific value of producer gas is low because of the dilution effect by nitrogen. To overcome this limitation, steam is used as a gasifying media which results in nitrogen free producer gas with high hydrogen concentration (often over 50%); consequently, the calorific value of producer gas increases substantially compared to air gasification. Herguido et al. (1992) found that as the steam-to-biomass (S/B) ratio increased from 0.5 to 2.5, hydrogen increased to over 50% (vol.), carbon dioxide increased from 10 to 30%, carbon monoxide decreased from 35 to 10%, while tar yield greatly reduced from 8% to nearly zero. Though tar yield reduces substantially at S/B ratio of 2.5, calorific value of producer gas also reduces significantly compared to lower S/B ratio of 0.5 because of reduction in carbon monoxide (Herguido et al., 1992). Steam gasification reactions are endothermic, requiring continuous heat energy during the process. The oxygen supply, along with the steam, provides the necessary heat energy to maintain the steam-gasification process. Gil et al. (1997) reported that as the gasifying ratio (GR), i.e., (steam + oxygen)/biomass, was increased from 0.6 to 1.7, tar content reduced from 50 to 5 g/m^3. The recommended ratio of steam-to-oxygen is 3 (mol/mol) for the low tar content. Gil et al. (1997) also reported reductions in hydrogen and carbon monoxide concentrations from 30 to 20% and 50 to 30%, respectively, while carbon dioxide increased from 14 to 30% as the GR increased from 0.6 to 1.7. Carbon dioxide (CO_2) gasification is also promising because the tar reduction is favored through dry reforming reactions of CO_2. Minkova et al. (2000) observed that a mixture of CO_2 and steam favors effective separation of volatiles from the carbonizing materials and increases the surface area of the solid products. Minkova et al. (2000) also stated that the CO_2-steam mixture also enhances formation of gaseous products and reduces liquid and solid products resulting in reduced tar content.

Kinoshita et al. (1994) determined that even though residence time has a little effect on the tar yield, it influences tar composition significantly. They also stated that as the residence time increases, oxygen-containing components and single-ring and two-ring components (except benzene and naphthalene) decrease, while three-ring and four-ring components increase. The type of biomass

feedstock also plays an important role on the concentration of tar compounds. Milne et al. (1998) reported that the nature of tar depends strongly on the type of feedstock gasified because the primary tar compounds are formed from cellulose while ternary tar compounds are made from cellulose and lignin content of biomass feedstocks. In addition, fuel-bound sulfur, nitrogen, alkali and chlorine are converted to inorganic impurities such as hydrogen sulfide, hydrogen cyanide, ammonia, hydrochloric acids and alkali compounds.

The use of in-bed additives not only reduces tars but also varies the gas composition and resulting high heating value. The catalytically active in-bed additives enhance char gasification, and reduce tars to useful product gas compositions. Devi et al. (2003) reported that the widely studied catalysts include dolomite, olivine, alkali carbonate and nickel-based, metal oxide, and bio-char. They also reported that even though in-bed catalysts can improve producer gas and reduce tar content, problems of catalysts deactivation, attrition, and fines carry-over must be addressed to make it a viable application.

The design of the gasifier reactor influences the heating value of producer gas, gasification efficiency, and tar yield. Secondary air injection significantly reduces tar yield by increasing reactor temperature. Pan et al. (1999) recommended a secondary to primary air ratio of about 20% to reduce the tar content by approximately 90%. Two-stage gasifier designs also significantly reduce gas tar content. The fundamental principle of a two-stage design is to separate the pyrolysis zone from the reduction zone of the gasifier system. The secondary air injection in the reduction zone increases the gasification temperature causing the tar content to reduce significantly. A two-stage gasification system developed by Asian Institute of Technology (AIT), Thailand (Bui et al., 1994) reported a reduction in tar content about 40 times less than a single stage reactor under similar operating conditions. An alternative two-stage gasifier design developed at the Technical University of Denmark (Henriksen & Christensen, 1994) includes a stage to combine gasification of char and biomass pyrolysis products. In this design, pyrolysis gases pass through a char bed, which enhances

tar reduction due to partial oxidation of pyrolysis gases in addition to the catalytic effect. Susanto & Beenackers (1996) developed a moving bed gasifier design with internal recycle with the aim to develop a design appropriate for scaling-up the downdraft gasifier with low tar content. Biomass was first pyrolyzed and char was moved to the reduction zone. The pyrolyzed gas was mixed with the gasifying media and burned in a separate combustion chamber. The flue gas acted as a gasifying medium in the reduction zone. A tar content of 100 mg/Nm^3 was reported.

Overall, primary methods of tar removal are considered as the best approach. However, primary methods do not reduce tar contents to levels required for most applications and may have an adverse effect on the other performance parameters such as calorific value, compositions, and yield of producer gas (Anis & Zainal, 2011). Consequently, secondary methods of tar removal are mandatory for most downstream applications.

1.2.2 Secondary methods of tars removal

Secondary tar removal systems are installed downstream of the gasifier system that are based, primarily, on mechanical or physical methods, and catalytic and thermal cracking. Thermal cracking is the process of converting or cracking tars into lighter gaseous compounds through heating at a specific temperature and residence time. Bridgwater (1995) found that tar levels can be reduced through thermal cracking process at temperatures of 800-1000°C. However, tars derived from biomass are more refractory and difficult to crack through thermal cracking only. To crack tars effectively, Bridgwater (1995) suggests the following methods:

- Increasing the residence time, which is somewhat effective,
- Direct interaction with an autonomously heated surface, which requires a huge energy supply, making it partly effective thus reducing the overall efficiency, and
- Partial oxidation using air or oxygen which increases levels of carbon dioxide, reduces the efficiency, and increases cost due to oxygen use.

Partial oxidation method is only effective if the temperature increases above 1300°C, which can be obtained through oxygen gasification (Bridgwater, 1995). In another study, Brandt & Henriksen (2000) reported that temperature and residence time of 1250°C and 0.5s, respectively, is required to achieve high tar cracking. In addition, tar levels and composition depend on biomass feedstock. Myrén et al. (2002) studied thermal cracking of tars derived from birch, miscanthus and rice straw at temperatures of 700, 850 and 900°C. They reported that the benzene and naphthalene increased while light tar compounds decreased as the temperature increased from 700 to 900°C for all three biomasses. In conclusion, thermal cracking partially reduces tars, while increasing cost due to high operating temperature.

Catalytic cracking is another group of secondary methods and is a promising technology due to advantages of conversion of tar into useful gaseous compounds and adjusting compositions of producer gas. The criteria of the catalyst described by Sutton et al. (2001) are: catalyst should be capable of reforming methane if the desired product is producer gas, provide proper syngas ratio for the projected processes, resilient to deactivation due to carbon fouling and sintering, easily regenerated, economical and must be effective in removing tars. Anis & Zainal (2011) reviewed catalysts for tar cracking and provided six categories: 1) nickel-based catalysts, 2) non-nickel based catalysts, 3) alkali metal catalysts, 4) basic catalysts, 5) acid catalysts, and 6) activated carbon catalysts. They concluded that although, basic and acid catalysts are effective in improving gaseous product quality, these catalysts increase ash content after char gasification and deactivate quickly due to coke formation. Char or activated carbon is the cheapest catalyst due to naturally being produced inside the gasifier; however, the problem of blocking of the pores through coke formation is a major challenge. Non-nickel metal catalysts, mainly rhodium-based catalysts, are promising; however, they are more costly than nickel catalysts. Nickel-based catalysts are the most active catalysts among all catalysts to convert tars. Co-impregnation of nickel on olivine, zeolite and dolomite can increase the stability to resists carbon deposition, i.e., coke formation, and the cost can also be reduced. Thermal

and catalytic cracking are promising due to high energy conversion efficiency; however, they require a huge energy supply to maintain a high operating temperature. Thus, there is a need of an economical and effective method of tar removal.

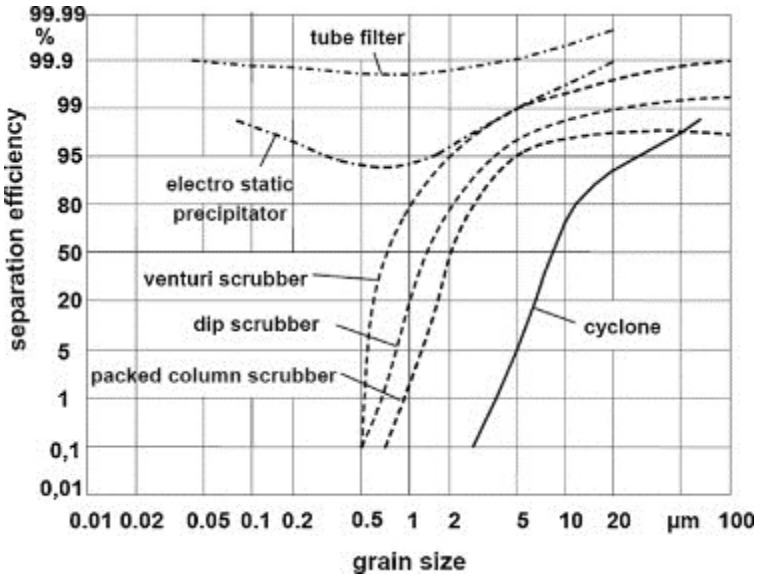

Figure 1.2 Particulate removal efficiencies of physical methods (Hasler & Nussbaumer, 1999)

Alternatively, physical or mechanical systems are low energy intensive methods of tar removal, which are categorized into dry and wet gas treatment depending on the application. Dry cleaning systems are employed before gas cooling where the gas temperature is above 500°C and is dropped to less than 200°C after cooling. Typical equipment for dry cleaning include primarily cyclone, electrostatic precipitators (ESP), rotating particle separators (RPS), bag filters, ceramic filters, baffle filters, fabric/tube filters, sand bed filters, and adsorbers. These devices are mainly used for particulate removal from the producer gas. The particulate removal efficiencies of some of the physical methods are highlighted in Figure 1.2. As shown, the least and the most effective method are cyclone and tube filter, respectively.

Several researchers reported the performance of physical devices for the removal of biomass producer gas tar (Baker et al., 1986; Hasler & Nussbaumer, 1999; Rabou et al., 2009). Hasler & Nussbaumer (1999) stated that tar removal efficiencies of RPS and fabric filter are 70% and 50%, respectively. They also stated that RPS and fabric filter are unable to remove tar to the same degree

as wet gas cleaning devices. Thus, an activated carbon based adsorber was added in between the RPS filter and fabric filter, achieving tar removal efficiency more than 70%.

For sand bed filters, Hasler & Nussbaumer (1999) reported tar removal efficiencies of 50-97%, while Pathak et al. (2007) reported tar and particulate efficiencies of more than 90%. In sand bed filters, tars are deposited on sand particles which lead to plugging issues. The regeneration of the sand is laborious and expensive.

de Jong et al. (2003) studies hot gas ceramic filtration of quartz and glass fiber types and found tar removal efficiencies were 77-97.9% and 75.6-97%, respectively. However, ceramic filters have not been recommended due to complexity and cost. A recently developed catalytic filter combines the filtration of particulates and catalytic tar reduction in a single operation. A catalytic candle filter contains nickel-based catalysts which are more effective in removing benzene and naphthalene at the temperature above 850°C (Anis & Zainal, 2011).

Wet gas cleaning technologies are typically installed after gas cooling with gas temperatures in the range of 20-60°C (Anis & Zainal, 2011). For wet gas cleaning, spray towers, venturi scrubbers, packed bed scrubber, impingement scrubbers, wet electrostatic precipitators, wet cyclones, and oil based gas washer (OLGA) are the major equipment. The performance of these equipment has been demonstrated at both laboratory and industrial scale under various operating conditions. Wet gas cleaning equipment have been applied at commercial biomass gasification plants located at Gussing, Harboore, Wiener Neustadt, Pyroforce, Interstate Waste Technologies, Inc (IWT) test facility/shaft gasifier, and Technical University of Denmark (DTU) test facility/two-stage gasifier (Lettner et al., 2007). Anis & Zainal (2011) reported that tars and particulates removal efficiencies of wet electrostatic precipitator (ESP) were 40-70% and 99%, respectively, at commercial gasification plants located at Harboore, Wiener Neustadt and the Energy Research Center of the Netherlands (ECN). Though the wet ESP is effective in removing particulates and condensed tar particles, the size and cost of the ESP is very high compared to other wet gas cleaning equipment (Anis & Zainal, 2011).

1.3 Wet scrubbing solvents

Wet scrubbing of producer gas is a prominent technique for the removal of tars through use of various kinds of scrubbing solvents. Wet scrubbing offers several advantages such as both gaseous impurities and particulates can be removed simultaneously. Also, wet scrubbing reduces gas temperatures, decreasing the volume of gases, resulting in a smaller overall size of the downstream systems.

Wet scrubbing of tars involves absorption of gaseous tar compounds in the scrubbing solvents. Selection of the scrubbing solvent is primarily governed by its absorption capacity of the targeted contaminants. In addition, environmental, safety and health issues must be considered during the solvent selection (Curzons et al., 1999). For a very dilute and ideal gas-liquid mixture, Henry's law governs the solubility of gaseous compounds in the liquid. It states that "the partial pressure of the species in the vapor phase is directly proportional to its liquid-phase mole fraction" (Smith & Ness, 2011). Henry's law is defined as

$$\frac{H}{P} = \frac{yi}{xi} \qquad \text{Eq. (1)}$$

where, H is Henry's constant, atm

P is the total pressure, atm

y_i is the mole fraction of solute in gaseous phase

x_i is the mole fraction of solute in liquid phase

The lower the value of Henry's constant (H), the higher the solubility of gases in liquid and vice versa. For highly concentrated and non-ideal gas-liquid mixtures, a thermodynamic phase equilibrium diagram is used to determine the solubility of gaseous compounds in liquid.

Water has been reported as a common wet scrubbing solvent for tar removal (Bhave et al., 2008; Hasler & Nussbaumer, 1999; Hindsgaul et al., 2000; Khummongkol & Tangsathitkulchai, 1989). The main drawbacks with water as a scrubbing solvent are the low absorption capacity of tar

compounds, mainly poly aromatic hydrocarbons (PAHs). In addition, waste water treatment is costly because the separation of phenolic compounds from water is difficult. A few studies have been reported on the use of various oils such as engine, biodiesel, vegetable, and waste cooking oils as solvents for the removal of tars (Boerrigter et al., 2005; Phuphuakrat et al., 2011). Boerrigter et al. (2005) studied oils as solvents for producer gas tar removal using an oil based gas washer (OLGA) technology. However, the types and properties of oils are not stated in the published report. Phuphuakrat et al. (2011) studied the effectiveness of diesel fuel, waste cooking oil based biodiesel fuel, engine oil and vegetable oil (soybean and canola oil in 60:40 ratio) for tar removal using a bubbler unit. Tars produced from wood-chip pyrolysis were heated to 800°C in the reformer to crack the higher molecular weight tar compounds into lighter molecules such as benzene, toluene, xylene, styrene, phenol and indane which were then scrubbed using a bubbler unit. Phuphuakrat et al. (2011) reported that though diesel has the highest absorption efficiency of all tar compounds, it is not recommended due to high volatility and cost; thus the next efficient 60:40 ratio soybean and canola oil mixture, which has the highest removal efficiency for all tar compounds, is recommended.

A few studies have been also reported on the use of various oils such as vegetable, engine, biodiesel, and waste cooking oils as solvents for the removal of volatile organic compounds (VOCs) (Ozturk & Yilmaz, 2006; Pierucci et al., 2005). Ozturk & Yilmaz (2006) investigated vegetable (sunflower), waste vegetable, lubricant and waste lubricant oils for removal of VOCs such as toluene, benzene, carbon tetrachloride and methanol independently in a bubble column. They stated that fresh vegetable oil (sunflower oil), fresh and waste lubricant oil showed more than 90% removal efficiencies while waste vegetable oil showed nearly 90% removal efficiency for toluene and benzene. Pierucci et al. (2005) investigated an absorption of VOCs, such as toluene, xylene, ethyl estate, butyl acetate, methyl ethyl ketone and acetone generated from spray paint booths using plant oil (colza oil) in a tray column. The absorption unit operated at an air flow rate of 14000 Nm^3/h, which had VOCs in the range of 1200 to 2500 ppm. The average removal efficiency was about 90%.

Tar compounds, mainly poly aromatic hydrocarbons (PAHs), such as benzene, toluene, ethylbenzene, styrene, xylene, and naphthalene, being lipophilic in nature, can mix comparatively well in plant-based oils because these oils have varied fatty acid (FA) compounds, such as saturated (palmitic and steric acids) and unsaturated (oleic, linolenic and linoleic acids) that are also lipophilic in nature. Soybean oil is the largest source of the vegetable oils in the U.S. (USDA, 2012). Soybean and other oils, like canola and sunflower, are less expensive than organic solvents such as acetone and isopropanol (EIA, 2012). In addition, vegetable oils are renewable, CO_2 neutral, and hazard free. In this study, soybean and canola oils have been selected as solvents for the removal of model tar compounds.

1.4 Wet scrubbing system for the removal of biomass producer gas tars

Wet scrubbing systems have been used as the most common biomass producer gas cleaning processes world-wide. Wet scrubbing devices include wet impingers, spray towers, venturi scrubbers and packed bed columns (Bhave et al., 2008; Cateni, 2007; Dogru et al., 2002; Khummongkol & Tangsathitkulchai, 1989; Phuphuakrat et al., 2011; Phuphuakrat et al., 2010). In wet impinger units, a jet of producer gas is impacted on the water surface which enhances the condensation of tars due to drop in the temperature, achieving efficiencies of about 70% (Khummongkol & Tangsathitkulchai, 1989). In spray towers, water is sprayed at the top while the gas is supplied from the bottom, i.e., a counter current flow of gas and liquid. In this technology, tars are condensed by contact with spraying water and form particles, which are washed away by the liquid along with solid particulates. The tar-contained water flows to a decanter where condensed tar particles and solid particulates settle and separate from the water. Spray towers and wet impingers generate a low pressure drop; however, tar removal efficiencies are comparatively low (Baker et al., 1986).

Venturi scrubber is the most effective in removal of tars and particulate; however, it is a complex process. The water contacts the tar and particulate laden gas in a throat section. Solid particulates and condensed tar particles are collected through collision with water droplets. Tar

removal efficiencies of venturi scrubbers range from 50% to 90%, while generating very high pressure drops (Hasler & Nussbaumer, 1999). Compared to venturi scrubbers, packed bed columns offer high tars and particulates removal efficiencies (as much as 99%) while generating low pressure drops across the column.

1.4.1 Wet packed bed scrubbing system

A packed bed column is a good choice considering its high removal efficiency and a low pressure drop across the column. A few studies have been reported on packed bed scrubbers for the removal of producer gas tars and particulates (Bhave et al., 2008; Boerrigter et al., 2005). Bhave et al. (2008) developed a water-based scrubbing system which combines wet and dry-packed bed scrubbing sections in a single unit. The wet packed bed column consists of 15-mm raschig ring bed of 40 cm high (bottom), 15-30-mm pebbles bed of 10 cm high (middle) and 6-mm raschig ring bed of 20 cm high (top). The system was tested for 50 m^3/h producer gas generated through a throat-less downdraft gasifier. Producer gas tar and particulate removal efficiency using the packed bed scrubber varied from 70% to 90%. With oil based gas washer (OLGA) technology, Boerrigter et al. (2005) reported reduction in producer gas tar concentration from 7000 to 50 mg/Nm^3. However, the details of the packed bed scrubbers and oil types were not provided.

A few studies also reported research on organic solvent, vegetable oils, and fuel oils based wet scrubbing system for the removal of volatile organic compounds (VOCs) (Heymes et al., 2006; Ozturk & Yilmaz, 2006). The objective of the study conducted by Heymes et al. (2006) was to identify an efficient organic solvent for the removal of hydrophobic VOCs compound, i.e., toluene. They stated that the properties of the organic absorbent must have high absorption capacity for VOCs, low viscosity, high diffusion coefficient which regulates absorption kinetics, low vapor pressure to avoid loss of solvent during regeneration, no toxicity, no fire or explosion hazard, and low cost. Of the four studied solvents (polyethylene glycols, phthalates, adipate and silicon oils), adipate, i.e.,

di (2-ethylhexyl) adipate, was the most effective solvent owing to high toluene absorption capacity, low vapor pressure, low viscosity and high diffusion coefficient for toluene.

Ozturk & Yilmaz (2006) studied fresh and waste vegetable, and lubrication oils as solvents in a bubble column to remove VOCs consisting of benzene, carbon tetrachloride, methanol and toluene. They reported that waste oils as the cost competitive solvents for the removal of VOCs. Phuphuakrat et al. (2011) reported that fuel oils, such as diesel and plant-based biodiesel fuels, in the bubble column reactor showed a high removal efficiency for tar compounds; however, the loss of solvent due to high volatility was the major issue, resulting in fuel oils not recommended as solvents.

Overall, vegetable oils are promising solvents for the removal of tars owing to characteristics of high absorption capacity for tar compounds, availability in large quantities, less volatile, no health or explosion hazards, and low cost. However, no study on the vegetable oil based wet packed bed scrubbing system for the removal of tars was found in the literature.

1.4.2 Packed bed materials

Though structured packings are considerably expensive than random packings, these generate a lower pressure drop per theoretical stage and offer a higher efficiency and capacity (Seader et al., 2011). Biomass producer gas tars have a tendency to condense when the temperature decreases. Therefore, random packings have been selected due to its low maintenance. Wide varieties (type, size and material) of random packings are available commercially. Usually, metal packings are recommended due to its strength and good wettability (Seader et al., 2011). As the size of the packing increases, removal efficiency reduces due to poor mass transfer. Fundamentally, packings nominal size of less than one-eighth of the column diameter is recommended to minimize the liquid maldistribution (Seader et al., 2011).

1.4.3 Design and operating parameters of wet packed bed scrubbers

In industry, a significant difference is observed between predicted and actual packing bed height of scrubbing systems (Doan & Fayed, 2001). This occurs because the height of transfer unit used in bed height estimation varies with the bed height. Also, use of predictive models show poor estimation of bed height (Doan & Fayed, 2001). Overall, parameters such as type, size and material of packing and packed bed height are important for designing packed bed columns. The method of packing and liquid distribution also significantly affect the performance of the absorption system (Wu et al., 2010; Yin et al., 2000).

In addition to design parameters, Wu et al. (2010) reported that packed bed column performance was influenced by air flux, liquid flux, concentration of absorbent solution and concentration of pollutants. Heymes et al. (2006) indicated that the lower the viscosity of vegetable oils, the higher the mass transfer of VOCs due to decrease in thickness of interface layer on the liquid side that enhances diffusion process. Noureddini et al. (1992) stated that the viscosity of vegetable oils is inversely proportional to its temperature. Liquid viscosity also has an effect on the liquid flow and the wetting of the packing, consequently influencing the mass transfer efficiency (Doan & Fayed, 2001).

The focus of this research is to determine the effectiveness of vegetable oils (soybean and canola oils) as scrubbing solvents for removal of model tar compounds and the effects of bed heights and operating variables (solvent flow rates and temperatures) on tar removal efficiency.

1.5 Process modeling of wet packed bed scrubbing system

Equilibrium stage based (thermodynamic) and rate based (mass transfer) models are mainly used for absorption process simulation. Equilibrium stage based models assume that phases leaving the stage are in thermodynamic equilibrium. For example, the leaving streams, i.e. vapor (V_j) and liquid (L_j) of stage j are in thermodynamic equilibrium as shown in Figure 1.3. Seader et al. (2011)

stated that the major assumptions of equilibrium stage model are: "1) phase equilibrium is achieved at each stage, 2) no chemical reactions occur and 3) entrainment of liquid drops in vapor and occlusion of vapor bubbles in liquid are negligible". Equilibrium stage based modeling involves the major governing equation of material, equilibrium, summation and enthalpy balance which are known as MESH equations (Seader et al., 2011).

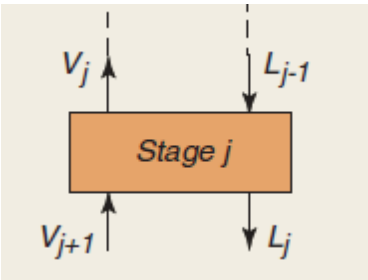

Figure 1.3 Equilibrium stage (Taylor et al., 2003)

Rate based models (Figure 1.4) involve mass transfer between the contacting phases which governs the separation process and equilibrium exist at the gas-liquid interface (AspenTech, 2001). Rate based models include mass and heat transfer rate and hydraulic equations in addition to material, equilibrium, summation and enthalpy balance equations which are known as MERSHQ equations. The major difference between equilibrium and rate based modeling is the way the balance equations are used. In equilibrium stage models, the sum of phase balances yields the mass and energy balances of the whole stage, while in the rate based models separate balance equations are solved for each phase including mass and heat transfer terms for mass and energy balance equations, respectively (Taylor et al., 2003).

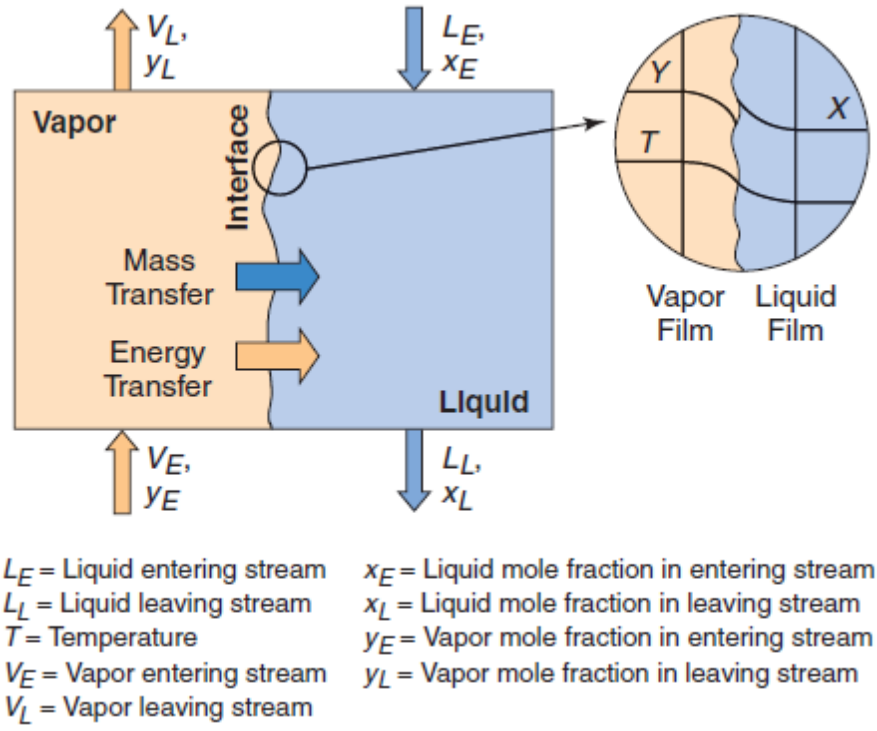

Figure 1.4 Non-equilibrium stage (Taylor et al., 2003)

The accuracy of equilibrium and rate based models depends on an accurate prediction of phase behavior properties of chemical species. There are two approaches: (φ/φ) and (φ/γ) for prediction of phase behavior. In the first approach (φ/φ), the fugacity coefficient (φ) is used to account for non-ideal behavior of both vapor and liquid phases, while in the second approach (φ/γ), the fugacity coefficients (φ) and an activity coefficients (γ) are used to account for non-ideal behavior of vapor and liquid phase, respectively (Gebreyohannes et al., 2012). Selection of the approach influences the estimation of the equilibrium ratio (K-value), which governs the interphase composition and departing stream composition for rate based and equilibrium based models, respectively. Fugacity coefficients are estimated using equation of state (EOS) models, while the activity coefficients are predicted using excess Gibbs energy (G^E) models. Several EOS and G^E models have been developed for various applications (Sandler, 1999). The prediction capability of

phase behavior mainly depends on the selection of activity coefficient (G^E) models and the quality of experimental vapor-liquid equilibrium (VLE) data for the given system (Gebreyohannes et al., 2012).

Studies have also been reported on various thermodynamic models for predicting vapor-liquid equilibrium (Carlson, 1996; Kuramochi et al., 2009; Mateescu et al., 2011; Ravindranath et al., 2007). Mateescu et al. (2011) reported that the UNIQUAC (UNIversal QUAsiChemical) functional-group activity coefficients (UNIFAC) method reliably predicted the vapor-liquid equilibrium (VLE) of VOCs (such as toluene, xylene, and acetone) in biodiesel fuels (methyl palmitate, methyl oleate, methyl lenolenate, and ethyl stearate). Kuramochi et al. (2009) stated that the VLE of methanol-soybean based biodiesel and methanol-glycerin systems is predicted accurately by UNIFAC and Dortmund-UNIFAC models. Ravindranath et al. (2007) and Carlson (1996) stated that the nonrandom two-liquid (NRTL) and universal quasi chemical (UNIQUAC) activity coefficient models provide better VLE property predictions than the UNIFAC model for highly non-ideal vapor-liquid equilibrium system. Therefore, NRTL model was selected to estimate the activity coefficients for the present study.

The NRTL equation developed by Renon & Prausnitz (1969) for a binary mixture is given below. Researchers developed the NRTL equation using Wilson's local composition theory and Scott's two-liquid solution theory.

$$\frac{g^E}{RT} = x_1 x_2 \frac{\tau_{21} G_{21}}{x_1 + x_2 G_{21}} + \frac{\tau_{12} G_{12}}{x_2 + x_1 G_{12}} \quad \text{Eq. (2)}$$

The activity coefficients of NRTL equation for a binary mixture are

$$\ln \gamma_1 = {x_2}^2 \left(\tau_{21} \frac{\exp(-2\,\alpha_{12}\tau_{21})}{[x_1 + x_2 \exp(-\alpha_{12}\tau_{21})]^2} + \tau_{12} \frac{\exp(-\alpha_{12}\tau_{12})}{[x_2 + x_1 \exp(-\alpha_{12}\tau_{12})]^2} \right) \quad \text{Eq. (3)}$$

$$\ln \gamma_2 = {x_1}^2 \left(\tau_{12} \frac{\exp(-2\,\alpha_{12}\tau_{12})}{[x_2 + x_1 \exp(-\alpha_{12}\tau_{12})]^2} + \tau_{21} \frac{\exp(-\alpha_{12}\tau_{21})}{[x_1 + x_2 \exp(-\alpha_{12}\tau_{21})]^2} \right) \quad \text{Eq. (4)}$$

where

$$G_{12} = \exp\ (-\alpha_{12}\tau_{12}) \quad \text{Eq. (5)}$$

$$G_{21} = \exp\ (-\alpha_{12}\tau_{21}) \quad \text{Eq. (6)}$$

$with\ g_{12} = g_{21}$

$$\tau_{12} = \frac{(g_{12} - g_{22})}{RT} = \frac{a_{12}}{T} \quad \text{Eq. (7)}$$

$$\tau_{21} = \frac{(g_{21} - g_{11})}{RT} = \frac{a_{21}}{T} \quad \text{Eq. (8)}$$

g_{12}, g_{21}, g_{11} *and* g_{22} are energy parameters describing interactions between two molecules

α_{12} is the non-randomness factor = 0.3 (Seader et al., 2011)

x_1 *and* x_2 are the mole fraction of component 1 and 2, respectively

R is the universal gas constant

T is the temperature of the binary mixture

The three main parameters, i.e., a_{12}, a_{21} and α_{12}, are required to estimate the activity coefficients of the NRTL equation. Gebreyohannes et al. (2012) stated that the variation in non-randomness parameter (α_{12}) has little effect on VLE property prediction. Seader et al. (2011) stated that α_{12} is independent of temperature and depends on molecule properties. They also stated that the recommended value of α_{12} of 0.3 for non-polar compounds. To estimate the temperature dependent binary energy interaction parameters (a_{12} and a_{21}), an experimental phase equilibrium data over a range of compositions are required.

In absence of experimental phase equilibrium data, various predictive models can be used to estimate the binary interaction parameters. The most commonly used group contribution models are universal functional activity coefficient (UNIFAC) and analytical solution of groups (ASOG) (Gebreyohannes et al., 2012). Both UNIFAC and ASOG models were developed extensively; however, UNIFAC is more widely accepted due to flexible, simple and applicable to many group parameters. Therefore, in the present study binary interaction parameters for NRTL model were predicted using UNIFAC model.

A few studies have been reported on process modeling of water-based and oil based tar removal process (Seethamraju et al., 2013; Tisdale, 2004). Tisdale (2004) described a process model

of the spray chamber type water based scrubber system for tar removal. The scrubbing system includes two scrubbers in series. Flash3 was used to model first scrubber (spray chamber) and Flash2 was used to model second scrubber (spray chamber) (Tisdale, 2004). To model the amount of saturated tars in water, Flash3 was used in the first scrubber which separates two liquids and one vapor stream through liquid-liquid-vapor equilibrium. Tisdale (2004) used Redlich-Kwong-Soave (RK-SOAVE) property method for the process model, and also stated that Peng Robinson (PENG-ROB) is comparable to RK-SOAVE property method.

Seethamraju et al. (2013) reported the simulation of diesel, canola, and biodiesel oil based high pressure absorption system for tars removal considering NRTL as a vapor-liquid equilibrium model and UNIFAC method is used to determine the missing binary interaction parameters. Vegetable oil based process model of atmospheric pressure packed bed wet scrubbing system for tar removal has not been reported. The proposed study involves process modeling of a wet packed bed scrubbing system using an equilibrium stage based approach. Peng Robinson (PENG-ROB) EOS was used to estimate fugacity coefficient for the vapor phase and NRTL model was used to predict the activity coefficient for the liquid phase. The missing interaction parameters for NRTL model were predicted using UNIFAC model.

1.6 Statement of problem

As per the published studies indicated above, water based wet scrubbing systems have major drawbacks of costly waste water treatment and a low absorption capacity of tar compounds in water. Vegetable oils-based wet scrubbing studies using a bubble column showed a great potential for the tar removal. Vegetable oils are renewable in nature, being plant-based they are CO_2 neutral, less volatile, low cost and hazard free. Experimental and modeling studies on the effects of bed height, solvent temperature and flow rates on the removal efficiency of model tar compounds using plant-based oils as scrubbing solvents in a wet packed bed scrubbing system are not reported in the literature.

1.7 Objectives

The overall goals of the present study were to develop novel design data and process model of vegetable oil based wet packed bed scrubbing system for the removal of model tar compounds. The specific objectives were:

1. Design a bench scale wet packed bed scrubbing system to study the absorption of model tar compounds in vegetable oils (soybean and canola oils).
2. Using a wet packed bed scrubbing system, determine the effects of vegetable oil type, bed height, solvent temperature, and solvent flow rate on the removal efficiencies of the model tar compounds composed of benzene, toluene and ethylbenzene.
3. Develop a process model of the wet packed-bed scrubbing system evolved under objectives 1 and 2 using equilibrium-stage based modeling capability of Aspen Plus™ and validate using the experimental data obtained through objective 2.

CHAPTER II

MATERIALS AND METHODS

A vegetable oil based wet packed bed scrubbing system was designed and fabricated to study the removal of tars from biomass producer gas. Soybean and canola oils were used as solvents. The model tar compounds used in this study were benzene, toluene and ethylbenzene. The effect of vegetable oil type, packed bed height, and solvent operating variables, i.e., temperature and flow rate, on tar removal efficiencies were studied using a bench-scale wet packed bed scrubber. A process model of the wet packed bed scrubbing system was also developed using an equilibrium stage-based modeling capability of Aspen Plus™. The detailed experimental procedures are described below.

2.1 Materials characterization

2.1.1 Vegetable oils (Solvent)

Soybean and canola oils, as purchased from Jedwards International, Inc., Quincy, MA, were used as solvents in this study. The properties of these oils are given in the Table 2.1. The numbers in the bracket of each fatty acid compound represent the carbon atoms and number of double bonds. For example, palmitic acid (16:0) means that this acid has 16 carbon atoms and no double bonds. Fatty acids are classified based on the presence or absence of double bonds. Fatty acids with no double bonds, one double bond and two or more double bonds are called saturated, mono saturated and poly saturated fatty acids, respectively.

Table 2.1 Properties of vegetable oils

Parameters	Soybean oil	Canola oil
Palmitic acid (16:0), %	9	4.8
Steric acid (18:0), %	4.4	1.8
Oleic acid (18:1), %	26.4	57.4
Linoleic acid (18:2), %	51.6	22.3
Linolenic acid (18:3), %	6.8	4.5
Density, kg/m^3	922.5	917
Viscosity, mm^2/s	65.4	39.2
Heating value, MJ/kg	37	37
Flash point, °C	> 288	> 230

As shown in the Table 2.1, the saturated compounds (palmitic and steric acids) in soybean oil are more than double than that of canola oil. Consequently, the viscosity of soybean is much higher than canola oil. The other unsaturated compounds (sum of oleic, linoleic and linolenic acids), heating value and density are comparatively equal.

Another important parameter is the surface tension (σ) of vegetable oils which is in the range of 30 to 32 mN/m for the temperature range of 30 to 50°C (Esteban et al., 2012; O'Meara, 2012). A low surface tension ($\sigma < 25$ mN/m) is recommended for the solvent because higher surface tensions (>70 mN/m) lead to poor wettability which reduces mass transfer efficiency, increasing height equivalent to a theoretical plate (HETP) of the packed column.

2.1.2 Model tar compounds

The model tar compounds used in this study were benzene, toluene and ethylbenzene. The purity of benzene, toluene and ethylbenzene as procured from Sigma Aldrich Inc., Atlanta, GA, was 99.5, 99.7, and 99.8%, respectively. Properties of these compounds provided by Sigma Aldrich Inc. are shown in Table 2.2.

Table 2.2 Properties of model tar compounds

Compound	Formula	Molecular Weight, g/mole	Melting Point, °C	Boiling Point, °C
Benzene	C_6H_6	78.11	5.5	80
Toluene	C_7H_8	92.14	-93	110-111
Ethylbenzene	C_8H_{10}	106.17	-95	136

2.2 Vegetable oil based wet packed bed scrubbing system

This study explores the absorption of benzene, toluene and ethylbenzene in vegetable oils. Perry et al. (1984) stated that the design condition (pressure, temperature and liquid-to-gas ratio) is normally selected by volatility or solubility of the least soluble compound when there are no chemical reactions involved. The solubility data are determined at equilibrium conditions. The equilibrium conditions are important for the design of an absorption column because the absorption efficiency reaches zero when the equilibrium conditions are attained. The equilibrium condition, i.e., vapor-liquid equilibrium ratio (K-value), is defined as "the ratio of mole fractions of a species in two phases at equilibrium" (Seader et al., 2011).

$$K_i = \frac{y_i}{x_i} \qquad \text{Eq. (9)}$$

where, K_i is the K-value of the component i (benzene, toluene and ethylbenzene)

y_i and x_i are the mole fractions of component i in the vapor and liquid phases, respectively. The K-value of the tar compounds was determined through a flash calculation using a non-random two-liquid (NRTL) model because NRTL provides a better vapor-liquid equilibrium (VLE) prediction than the other thermodynamic models (Ravindranath et al., 2007). In addition, K-values were determined using atmospheric conditions (1 atmosphere and 50°C) which were selected based on preliminary studies. The K-values of benzene, toluene and ethylbenzene were 0.30, 0.10 and 0.04, respectively. Benzene is the least soluble compound due to its higher vapor-

liquid equilibrium ratio (K-value) compared to toluene and ethylbenzene. Therefore, benzene was used to design the packed bed column.

The actual liquid-to-gas (L/G) ratio is usually greater than the minimum L/G by as much as 25 to 100% (Perry et al., 1984). The estimated value of L/G is determined by economic consideration, judgment and experience. Perry et al. (1984) stated that the molar L/G ratio should be 20 to 50% higher than the minimum L/G required based on the optimization of L/G ratio in terms of total annual cost. Accordingly, the designed (operating) liquid-to-gas (L/G) ratio of 0.45 was used which is 50% higher than the minimum L/G ratio.

2.2.1 Diameter of the column

The minimum column diameter is limited by flooding, and the typical design considers the operating gas velocity in the range of 50 to 70% of the flood velocity, i.e., the velocity of gas which prevents the flow of liquid causing a substantial increase in the pressure drop across the column and limits the mixing of gas and liquid phase (Seader et al., 2011). Usually, the design (operating) gas velocity of the column is determined using the vendor's pressure drop correlation for the given packings. In the absence of vendor's data, it is recommended to use generalized pressure drop correlations with superimposed experimental data given by Kister (1992).

The diameter of the column was determined using a generalized pressure-drop correlation (GPDC) of Eckert (1963, 1970, 1975) as modified by Strigle (1994) as shown in Figure 2.1. The maximum capacity factor was determined using GPDC and flooding point correlation provided by Kister et al. (2007). The pressure drop at flood point can be determined using following correlation provided by (Kister, 1992).

$$\Delta P_{FL} = 0.12\, F_P^{0.7} \qquad \text{Eq. (10)}$$

where, ΔP_{FL} is the pressure drop at flood point, in H_2O/ft of packing

F_P is the packing factor, 1/ft

The x-axis of Figure 2.1 represents the flow parameter (F_{LG}) is given below.

$$F_{LG} = \frac{L}{G}\left(\frac{\rho_G}{\rho_L}\right)^{0.5} \quad \text{Eq. (11)}$$

where, L is the liquid low rate, lb/h

G is the gas flow rate, lb/h

ρ_G is the gas density, lb/ft^3

ρ_L is the liquid density, lb/ft^3

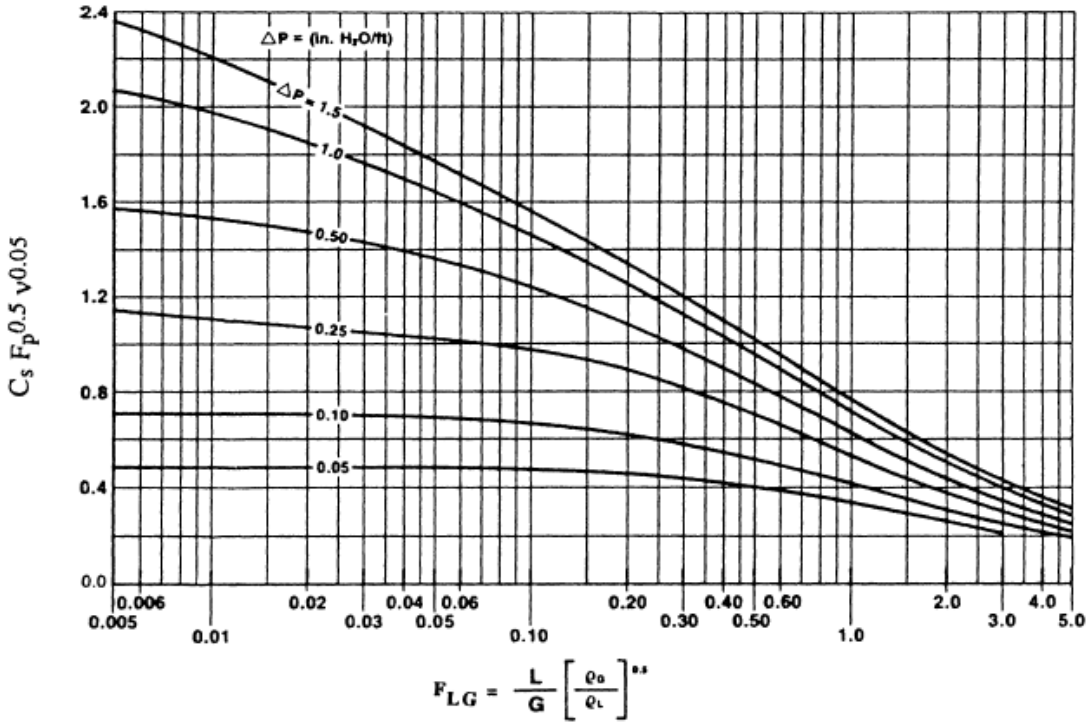

Figure 2.1 Generalized pressure drop correlation (GPDC) by (Strigle, 1994)

The diameter must be determined such that the pressure drop is below 1.5 in of H_2O/ft of packed bed height and flooding is avoided (Seader et al., 2011). Accordingly, the maximum capacity parameter *CP* was determined at the highest pressure drop (ΔP = 1.5 in of H_2O/ft) line using the flow parameter as shown in the GPDC correlation.

$$CP = C_S F_P^{0.5} \upsilon^{0.05} \quad \text{Eq. (12)}$$

where, υ is the kinematic viscosity of the liquid, centistokes

υ = dynamic viscosity (centipoises) / liquid density, g/cm^3

Fp is the packing factor, 1/ft

Cs is the *C* factor

The *C* factor (C_S) which is the superficial gas velocity (U_S) corrected for vapor and liquid densities

$$C_S = U_S[{}^{\rho_G}/_{(\rho_L - \rho_G)}]^{0.5} \quad \text{Eq. (13)}$$

The C factor (*Cs*) defines the balance between the vapor momentum force which entrain groups of liquid droplets and the gravity force which resists the upward entrainment. The packed bed column diameter of 5 cm was determined considering 50% of the velocity corresponding to the maximum capacity parameter.

2.2.2 Height of the column

The height of the packed bed column was determined using equilibrium stages and height equivalent to a theoretical plate (HETP).

$$Z = N\ x\ HETP \quad \text{Eq. (14)}$$

where, *Z* is the height of the packed bed column, m

N is the number of equilibrium stages (ideal stages)

HETP is the height equivalent to a theoretical plate, m

An equilibrium stage (theoretical plate) is defined as the hypothetical stage where liquid and gas phase establish equilibrium with each other. Perry et al. (1984) recommended to use a rigorous computational method to perform design calculation of multicomponent system. Therefore, to estimate the equilibrium stages, an equilibrium stage model was developed using the "RadFrac" block in Aspen Plus™ software. The operating conditions (1 atmosphere and 50°C) were selected based on preliminary experiments. The inlet stream of vegetable oil was defined using fatty acids composition as listed in Table 2.1. Non-random two-liquid (NRTL) model was selected as a

thermodynamic model to account for non-idealities in the system. The default values of model parameters, i.e., binary interaction parameters, were used, while the missing binary interaction parameters were estimated using universal quasi chemical (UNIQUAC) functional-group activity coefficients (UNIFAC). A sensitivity analysis of equilibrium stage versus purity of outlet vapor stream was performed to determine the optimum equilibrium stages. Ten equilibrium stages were determined as optimal for the purity of outlet vapor stream over 99%. Another method, i.e., Kremser's method (Perry et al., 1984) which is normally recommended for the dilute system, was also used to determine theoretical number of stages. Kremser formula is given as follows.

$$\frac{Y_1 - Y_2}{Y_1 - mX_2} = \frac{(A^0)^{N+1} - A^0}{(A^0)^{N+1} - 1} \qquad \text{Eq. (15)}$$

For dilute gas,

$$\text{Absorption factor, } A^0 = \frac{L_M^S}{mG_M^0} \text{ and } m \approx K = \frac{y^0}{x} \qquad \text{Eq. (16)}$$

For solute free solvent, $X_2 = 0$, Kremser equation can be reduced to the following:

$$\frac{Y_1 - Y_2}{Y_1} = \frac{(A^0)^{N+1} - A^0}{(A^0)^{N+1} - 1} \qquad \text{Eq. (17)}$$

where, Y_1 is the moles of solute in gas phase per moles of feed gas at the bottom of the column

Y_2 is the moles of solute in gas phase per moles of feed gas at the top of the column

X_2 is the moles of solute per moles of solute-free solvent fed o the top of the column

G_M^0 is moles of rich feed gas to be treated per unit time

L_M^S is moles of solvent per unit time

N is the numbers of equilibrium stages

Theoretical stages calculated through the Kremser's method matched the result of equilibrium stage-based Aspen Plus™ modeling tool.

The height equivalent to a theoretical plate (HETP) includes the packed bed column mass transfer efficiency. Though HETP lacks the fundamental basis, it is widely used method for

estimating the height of the column due to its simplicity in applying to the equilibrium stage calculation. HETP can be predicted by data interpolation, mass-transfer models, and rules of thumb proposed by Kister (1992) and Perry et al. (1984). Kister (1992) stated that the most recommended method of HETP prediction is the data interpolation. In the absence of experimental data, the HETP can be predicted through mass-transfer models such as Billet & Schultes (1999) correlation. However, Billet & Schultes (1999) correlation requires empirical packing specific constants (C_L and C_V). If these constants are not available for the selected packing, HETP can be estimated using predictive methods such as rules of thumb. In this study, the HETP was determined using the rules of thumb.

The rules of thumb for the small columns are given as follows.

$$HETP = 18\, D_P \qquad \text{Eq. (18)}$$

where, D_P is the packing diameter, m

HETP is the height equivalent to a theoretical plate, m

As a result, the predicted height of the packed column used for this research is calculated as 1.1 m, an appropriate height for a laboratory scale set-up.

Kister (1992) provided an alternate rule of thumb in that the HETP should be equivalent to the column diameter (m) for diameters less than 61 cm. Consequently, the height of the packed column used for this research is estimated at 0.5 m. Therefore, in the experimental design as shown in Table 2.4, the packed bed height was varied from 0.5 to 1.1 m and an intermediate value of 0.8 m were used to determine the HETP using experimental data.

The recommended size of the packing is less than $1/8^{th}$ of the column diameter to minimize the liquid maldistribution (Seader et al., 2011). Researchers also reported that metal packings provide better strength and wettability compared to ceramic and plastic packings. For these reasons, metal raschig rings of 6-mm (stainless steel) were selected as the packing materials and purchased from Raschig Jaeger Technologies, Arlington, TX. The characteristics of stainless

steel raschig rings 6 x 6 x 0.3 mm in size, i.e., diameter x length x thickness, purchased from Raschig Jaeger Technologies, Arlington, TX are shown in Table 2.3. The photographic view of raschig rings is shown in Figure 2.2.

Figure 2.2 Photographic view of raschig rings

Table 2.3 Characteristics of raschig rings

Parameters	Values
Size (diameter x length x thickness), mm	6 x 6 x 0.3
Density, kg/m^3	900
Surface area, m^2/m^3	900
Packing factor, 1/m	2297
Void fraction, %	89

2.2.3 Experimental set-up

A wet packed scrubbing system of 0.6 Nm^3/h capacity (as shown in Figure 2.3) was designed, fabricated and installed in the Bioenergy Laboratory at Oklahoma State University, Stillwater, OK. The experimental set-up consists of two major sections: a mixing section to prepare a simulated air containing a mix of tars and an absorption column.

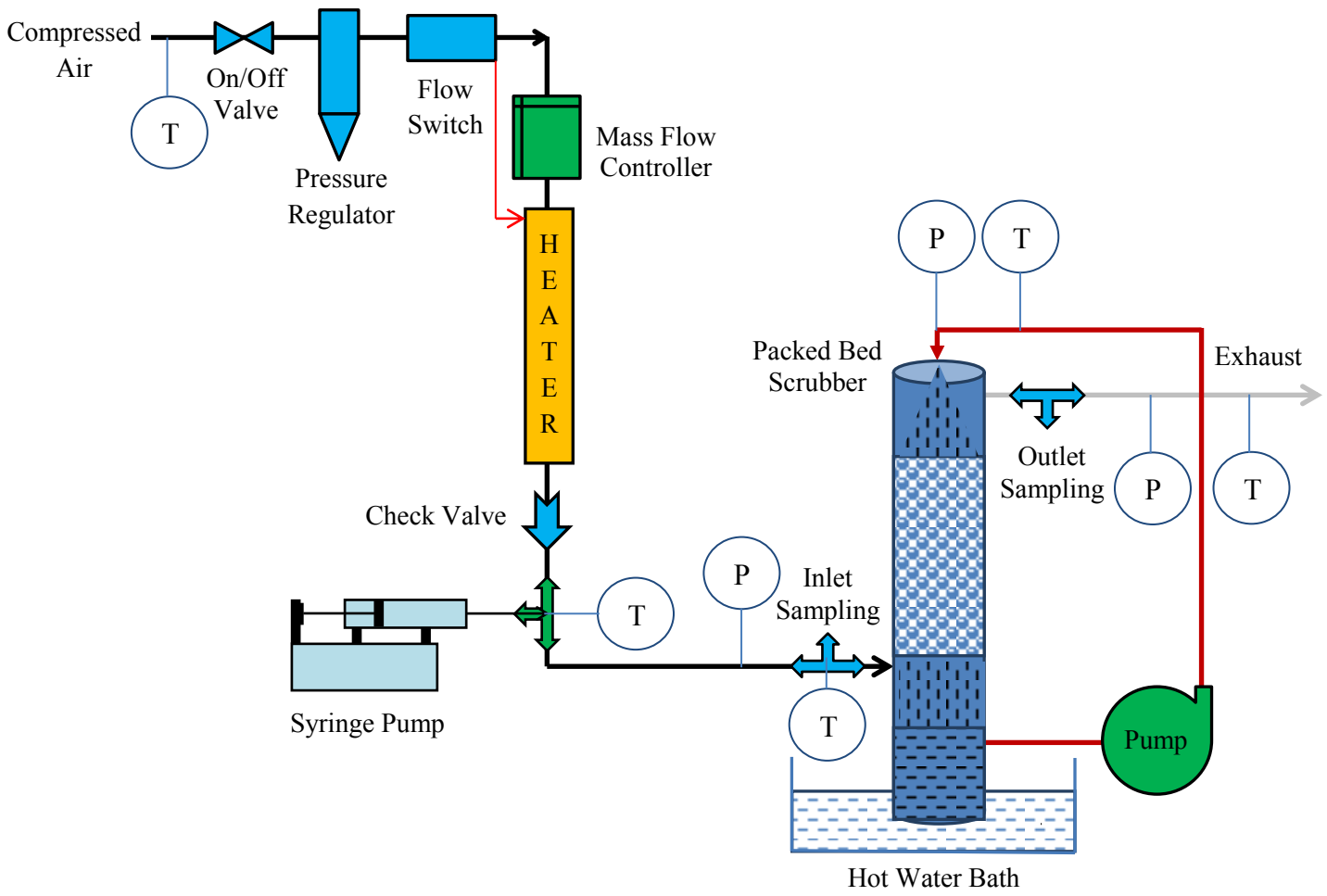

Figure 2.3 Schematic diagram of bench-scale wet scrubbing set-up

P = Pressure, T = Temperature

2.2.3.1 A gas mixing section to prepare a simulated air containing a mix of model tar compounds

A comprehensive review on the preparation of standard gas mixtures was reported by Barratt (1981). He indicated that dynamic methods of standard gas mixtures are preferred over static methods because of several advantages. He also stated that an injection method is a versatile approach for preparing standard gas mixtures, and syringe pumps are the most widely used for the injection method. In this study, a simulated air containing a mix of tars was prepared in a gas mixing section by injecting pure liquid model tar compounds into a stream of hot air (Figure 2.3). The gas mixing section consists of compressed air line, on/off valve, pressure regulator (model 4ZK96, Grainger, Roanoke, TX) with a pressure gauge (model 4FLH6, Grainger, Roanoke, TX), air flow switch (Model FS-926 BR A SCFH-00.50, Gems Sensors Inc., Plainville, CT), mass flow controller (Model GFC37S-VADL2-A0, Aalborg Instruments and Controls, Inc, Orangeburg, NY), heater (Model HT-M-050-100-120-1/8F-1/4F-TF1, Tutco-Farnam Custom Products, Arden, NC) with temperature controller (Model CC-A10, Tutco-Farnam Custom Products, Arden, NC), check valve (Part Number SS-8CPA2-3, Swagelok Oklahoma, Tulsa, OK), syringe pump (Model KDS 280.200, KD Scientific, Holliston, MA), and rupture disc (Part Number 4412T12, McMaster-Carr).

A manual ball valve was provided to start or stop the air supply before the pressure regulator. The pressure regulator controlled the pressure of the inlet air. The air flow switch was installed prior to the heater and sensed air flow. If air flow was present, heat was provided to the inlet air, heating it to 350^{o}C, to ensure the injected liquid tar compounds would vaporize completely. A temperature controller was used to control the air temperature. A check valve was installed between the heater and the injection port of the tar compounds to prevent back-flow of tar vapors. As a safety precaution, the brass rupture disc was installed prior to the absorption column to release excessive pressure if there was a blockage.

The model tar compounds used in this study were benzene, toluene, and ethylbenzene, as procured from Sigma Aldrich. A mixture of tar compounds was prepared by weight distribution, benzene: 50%, toluene: 30%, and ethylbenzene: 20% which are comparable to that measured by Cateni (2007) collected from a fluidized bed gasifier. The prepared mixture was filled in 100-ml gas-tight syringe (Part Number 009760, SGE Analytical Science, Austin, TX) with luer lock needle (Part Number 039827, SGE Analytical Science, Austin, TX). A syringe pump (Model KDS 280.200, KD Scientific, Holliston, MA) was used to inject the model tar compounds mixture into the hot air stream.

The measurement parameters were pressure, temperature, and compositions of the inlet and outlet simulated air stream, air flow rate, solvent temperature, and the pressure drop across the packed bed column. A mass flow controller (Model GFC37S-VADL2-A0, Aalborg Instruments and Controls, Inc, Orangeburg, NY) was used to measure and control the air flow rate. Type-K thermocouples were used to measure the temperature of inlet and outlet air streams, air at tar injection point, and solvent. Temperatures were recorded using a DaqView program (part number OMB-DAQ-55, Omega Engineering, Inc., Stamford, CT, USA). A U-tube manometer (0-20" of H_2O) was installed on the packed bed column to monitor the pressure drop across the column. A differential pressure transducer (Model number GC52, Ashcroft Inc., Stratford, CT) was used to log the pressure drop across the column. The compositions of inlet and outlet gas streams were analyzed using a gas chromatography/mass spectroscopy (GC/MS).

2.2.3.2 Packed bed absorption column

The wet packed bed scrubbing system as shown in Figure 2.4 consists of a stainless steel column fabricated in Biosystems and Agricultural Engineering Laboratory at Oklahoma State University, peristaltic pump (model PC2 70-7002, Harvard Apparatus, Holliston, MA), and water bath heater (model WD28A11B, Grainger, Roanoke, TX). Stainless steel (SS) 304 was selected as the material of construction of the column due to an excellent resistance towards the model tar

compounds used in this study. A design basis of the calculation of the diameter and height of the packed bed absorption column is given in Section 2.2. The column (5 cm internal diameter and 150 cm height) holds the packed bed material (raschig rings) having a height of 50-110 cm. The packing (raschig rings) is supported at the bottom of the column by a corrosion resistant SS 316 woven wire cloth (4x4 mesh, open area of 46.2%).

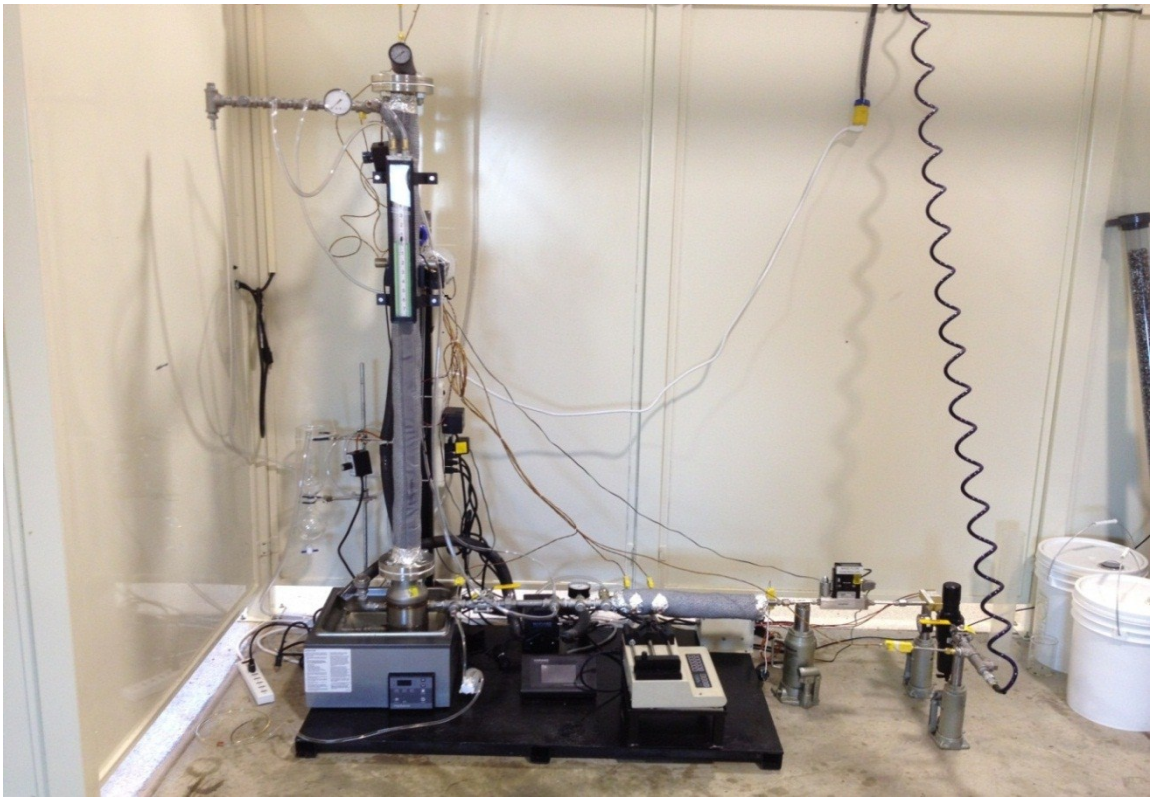

Figure 2.4 Photographic view of bench-scale wet scrubbing set-up

2.2.3.3 Liquid (solvent) distribution

The liquid distribution is the most significant aspect of the wet scrubbing system because it influences the mass transfer efficiency of the packing. An uneven liquid distribution is difficult to compensate due to gravity flow of liquid. Perry et al. (1984) stated that a single spray nozzle can serve the purpose of liquid distribution in a small column. Accordingly, six different types of commercial spray nozzles were tested for the spray distribution of soybean and canola oils. Results showed that all the selected nozzles were not able to adequately spray soybean and canola

oils due to the oils' high viscosities. Other spray nozzle options claiming to handle high viscous liquids were explored; however, these were deemed too expensive. Therefore, it was decided to design and fabricate a liquid distributor to spray vegetable oils uniformly on the top of the packings.

Perry et al. (1984) stated that the orifice liquid distributor is the common types of liquid distributor for an absorption process which was designed based on the head-flow correlation given below.

$$Q = C_D A_h n \sqrt{2 g h} \qquad \text{Eq. (19)}$$

where, Q is the volume flow rate, m^3/s

C_D is the coefficient of discharge = 0.4

A_h is the cross sectional area of a hole, m^2

n is the number of discharge hole of a liquid distributor

g is the gravitational acceleration = 9.8 m/s^2

h is the liquid head above the orifice, m

Using the above head-flow correlation, a liquid distributor was designed considering the diameter of the holes of 0.15 mm, design solvent flow rate of 63 ml/min, pressure head of 20 psig, and coefficient of discharge of 0.4. The number of holes were determined as 9. Perry et al. (1984) recommended at least 40 irrigation points per m^2 with 60-100 per m^2 being ideal. He also stated that a drip point density over 40 showed little difference in packing efficiency at the cost of higher pressure drops and an increase in plugging potential. In this study, a drip point density of 4125 drip points/m^2 was determined considering the liquid distributor consists of 9 holes of 0.15 mm diameter and packed column of 50 mm diameter which is well above the required drip point density. As a comparison, Janzen et al. (2013) distributed water in a 80-mm diameter column using a multipoint source distributor, having a drip point density of 3976 drip points/m^2.

A liquid (solvent) distribution system consists of a multi-point liquid distributor to provide a uniform distribution of solvent (Figure 2.5), a sump, and peristaltic pump (model PC2 70-7002, Harvard Apparatus, Holliston, MA) which is compatible with the selected solvents. The sump (0.8 liter in volume) was placed in the water bath heater to maintain the solvent at the desired temperature.

Figure 2.5 Photographic view of solvent distributor

2.2.4 Experimental design

The range of test conditions is provided in the Table 2.4. Solvents were soybean and canola oils. The three liquid flow rates are based on liquid-to-gas (L/G) ratios of 25%, 50% and 75% higher than the minimum L/G ratio. A 3x3 factorial in a split plot arrangement in a randomized complete block design was used for the bed heights of 0.5, 0.8 and 1.1 m for soybean

oil. Based on the comparison of soybean and canola results at 0.5 m, only the 0.5-m bed height was evaluated for canola oil.

Table 2.4 Test conditions of the wet packed bed scrubber

Variables	Values
Vegetable oils	Soybean, Canola
Packed bed height, m	0.5, 0.8, 1.1
Solvent flow rate, ml/min	53, 63, 73
Solvent temperature, °C	30, 40, 50

A split plot arrangement was adopted to evaluate the wet scrubbing system for the removal of model tar compounds. A split plot approach is frequently applied when there are tough-to-change factors or if there is an economic constraint. In this study, vegetable oil type and packed bed height were considered as a block and 3x3 (solvent temperature x solvent flow rate) randomized block design was applied for each block.

2.2.5 Test procedure and measurement

Initially, the sump was filled with 800 ml of vegetable oil. The water bath heater was started to maintain the desired solvent temperature. Then, air was supplied and maintained at 0.65 m^3/h with the operating pressure set at 20 psig measured using a pressure regulator. Once the air flow rate was confirmed through the mass flow controller, the heater was started to heat the incoming air to 350°C which was maintained using the temperature controller. After about 30 minutes of operation when the sump temperature reached the desired temperature, the solvent circulation pump was started. After about 10 minutes after starting the solvent circulation pump, the heater on the solvent pipe was started to maintain the required solvent temperature. Solvent temperature was continuously monitored on the DaqView output display. Once the system reached equilibrium condition (about 60 minutes), a mixture of model tar compounds was injected continuously at 40 ml/h into the hot air stream using a syringe pump (Model KDS 200,

KD Scientific Inc., Holliston, MA). Tar-laden air entered the bottom of the packed bed column at 70°C. The exiting stream of air was channeled through a dry ice condenser trap (part number Z422347, Sigma-Aldrich, USA) before exiting to the exhaust. The first sample of the exiting air was taken 1 minute after tar injection was initiated and then every six minutes thereafter.

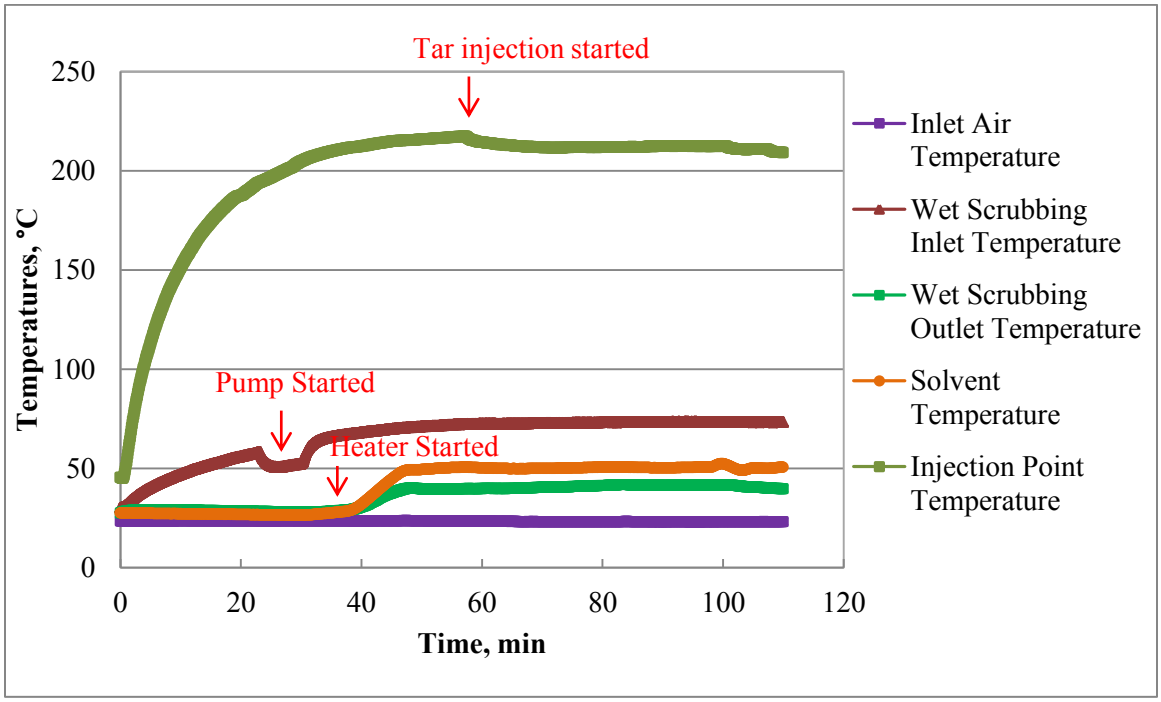

Figure 2.6 A typical temperature profile at the bed height of 1.1 m, solvent flow rate of 73 ml/min and solvent temperature of 50°C

A typical temperature profile of an experiment is shown in Figure 2.6. First, the air heater was started to heat the inlet air stream. Initially, the temperature of tar injection point increases exponentially. Once the system was thermally stable, it remains constant. After about 30 minutes, the solvent circulation pump was started. A sudden rise in the inlet air temperature was observed due to the restriction in the air flow path which increases the residence time of the inlet air stream before the column. After about 40 minutes, the heater on the solvent pipe was started to maintain the selected solvent temperature. All temperatures stabilized after about 60 minutes of operation. When the temperatures were stabilized, model tar compounds were injected into the inlet hot air

stream through a syringe pump at the rate of 40 ml/h resulting in a slight decrease in the tar injection point temperature. Similar temperature profiles were observed for all other experiments. Figure 2.7 shows a typical pressure drop across the column for one of the experiments. Initially, the pressure drop across the column was in the range of 6.5 to 7.5 mm of water column (WC) when only air was flowing through the packed bed column. Once the solvent circulation pump started, the pressure drop across the column immediately increased from 7.5 to 18 mm of W.C. After heater started, the pressure drop across the column gradually decreased because of the reduction in solvent density and the viscosity. After stabilization, pressure drop across the column remained constant at 16.6 +/- 0.2 mm of WC. A small variation (+/- 0.2 mm of WC) in the pressure drop across the column was due to a small variation in the inlet air flow rate, i.e., +/- 0.01 l/min (Figure 2.8). A typical air flow rate profile of one of the experiments is shown in Figure 2.8. The inlet air flow rate of 10.84 +/- 0.01 l/min remained constant throughout the experimental run.

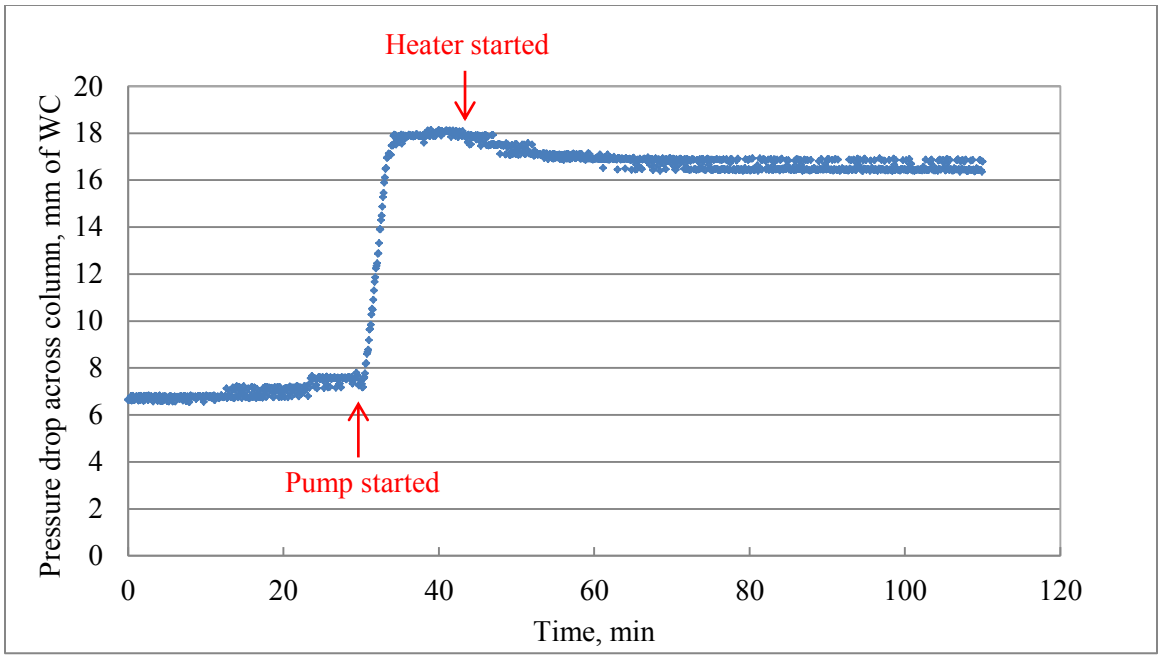

Figure 2.7 A pressure drop across the column profile at the bed height of 1.1 m, solvent flow rate of 73 ml/min and solvent temperature of 50°C

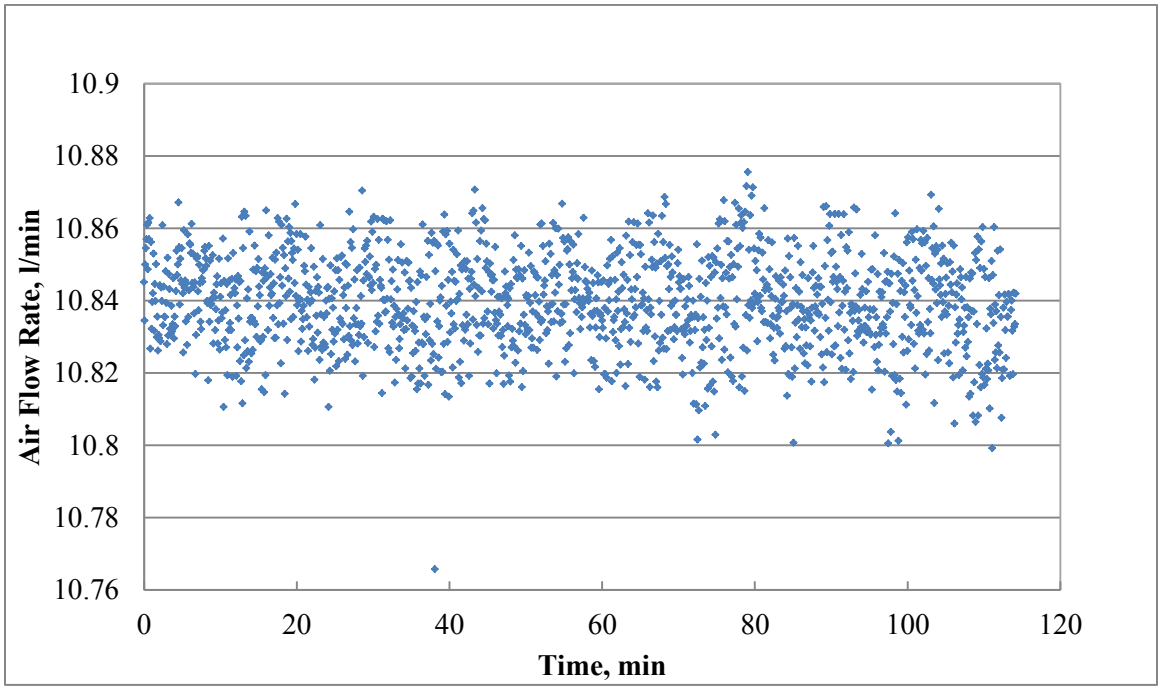

Figure 2.8 A typical air flow rate profile at the bed height of 1.1 m, solvent flow rate of 73 ml/min and solvent temperature of 50°C

2.2.6 Prediction of pressure drop across the column

A proper choice of the packing material is important for the optimum performance of the counter-current packed bed absorption column. The pressure drop is one of the decisive criteria for the selection of packing materials. Most of the pressure drop correlations found in the literature is either empirical or semi-empirical. The pressure drop correlations developed by Stichlmair et al. (1989) and Billet & Schultes (1999) are fundamental in nature which includes hydrodynamics of packed bed column.

Stichlmair et al. (1989) stated that the hydrodynamics of a packed bed column is described by two major approaches: channel model and particle model. In the channel model, it is assumed that the empty space, i.e., void fraction of the dumped or arranged packing, can be replaced by numerous vertical flow channels. The liquid flows down the wall of the channels having some characteristic dimensions which reduces the cross sectional area available for the gas flowing upward inside the channels; thus causing increased pressure drop. In the particle model, it is assumed that the gas flow around the packing particle has a characteristic dimension and liquid flowing down increases the dimension of the particle by its adherence to the surface of the packing particles. The void fraction of packed bed also reduces due to presence of the liquid.

2.2.6.1 Stichlmair et al. (1989) pressure drop correlation

Stichlmair et al. (1989) pressure drop correlation given below (equation 20) uses a particle model. Two major constraints must be considered to use this model were: first, “the number of correlating constants should be minimized” and second, “the fundamental geometric properties of the packings, such as surface area and void fraction should suffice in most cases to account for differences in packing behavior”. Using these two constraints, Stichlmair et al. (1989) provided following correlation for predicting pressure drop across the column.

$$\frac{\Delta P_{irr}}{\Delta P_{dry}} = \left\{ \left[1 - \varepsilon\left(1 - \frac{h}{\varepsilon}\right)\right] \Big/ (1 - \varepsilon) \right\}^{(2+c)/3} \left(1 - h/\varepsilon\right)^{-4.65} \quad \text{Eq. (20)}$$

where, ΔP_{irr} is the irrigated pressure drop, N/m^2

ΔP_{dry} is the dry pressure drop, N/m^2

ε is the bed void fraction (porosity), m^3/m^3

h is the liquid holdup, m^3/m^3

c is the exponent for irrigated pressure drop

Stichlmair et al. (1989) liquid holdup (h) correlation below the loading point is given as follows.

$$h = 0.555\, Fr_L^{1/3} \quad \text{Eq. (21)}$$

where, Fr_L is the Froude number for liquid

h is the liquid holdup below loading point, m^3/m^3

Stichlmair et al. (1989) used Froude number which is a function of liquid loading for the given packing is provided below.

$$Fr_L = \frac{U_L^2 a}{g\, \varepsilon^{4.65}} \quad \text{Eq. (22)}$$

where, U_L is the superficial liquid velocity through a packed bed, m/s

a is the specific surface area of packing, m^2/m^3

g is the gravitational constant, m/s^2

ε is the bed void fraction (porosity), m^3/m^3

The prediction of Stichlmair et al. (1989) liquid holdup (equation 21) did not fitted well with the experimental values of the present system, i.e., air-vegetable oil system, because the Stichlmair et al. (1989) holdup correlation was validated only for air-water system. Therefore, the liquid holdup experimental data given in Table 2.5 of this research study was correlated by the following equation which was used in the subsequent calculations.

$$h = 4.05\, Fr_L^{1/3}$$ Eq. (23)

Stichlmair et al. (1989) used following exponent c for irrigated pressure drop.

$$c = \frac{-\frac{C_1}{Re_g} - \frac{C_2}{2\, Re_g^{1/2}}}{f_0}$$ Eq. (24)

where, C_1 and C_2 are the packing specific constants

Re_g is the Reynolds number for the gas

f_0 is the friction factor for flow past a single particle

The friction factor for flow past a single particle provided by Stichlmair et al. (1989) is given below.

$$f_0 = \frac{C_1}{Re_g} + \frac{C_2}{Re_g^{1/2}} + C_3$$ Eq. (25)

$$Re_g = \frac{d_p\, U_g\, \rho_g}{\mu_g}$$ Eq. (26)

where, C_1, C_2, and C_3 are the packing specific constants

Re_g is the Reynolds number for the gas

d_p is the particle diameter, m

U_g is the superficial gas velocity through a packed bed, m/s

ρ_g is the density of the gas, kg/m^3

μ_g is the absolute viscosity of gas, kg/m-s

Stichlmair et al. (1989) used following equation 27 to determine the equivalent diameter (d_P) of the particle.

$$d_p = \frac{6(1-\varepsilon)}{a}$$ Eq. (27)

where, ε is the bed void fraction (porosity), m^3/m^3

a is the specific surface area of packing, m^2/m^3

d_p is the particle diameter, m

C_1, C_2, and C_3 were not available for the raschig rings of 6 mm in size. Therefore, the optimum value of an exponent c was determined using experimental wet and dry pressure drop data for all the operating conditions of this research study and using equation 20. A trial and error method was adopted to determine the optimum value of the exponent c for each of the twenty seven experimental conditions, and then an average value of exponent c of the twenty seven conditions was determined, which was used to predict the theoretical pressure drop across the column. Finally, predicted pressure drop was validated using experimental data.

2.2.6.2 Billet & Schultes (1999) pressure drop correlation

Billet & Schultes (1999) pressure drop correlation used a channel model in which the void space of dumped or arranged packings is assumed to be replaced by vertical flow channels through which the liquid flows downwards while the gas flows upward inside the channels counter currently. However, in real applications, flow channels deviate from the vertical and are finally determined by the shape of the random packings. Billet & Schultes (1999) assume the deviation of real flows of the phases from vertical channels can be expressed by packing specific parameters which were determined using equation 28 and experimental data from this research project.

The irrigated pressure drop ($\Delta P/H$) correlation of Billet & Schultes (1999) is

$$\frac{\Delta P_O}{H} = \psi_L \frac{a}{(\varepsilon - h_L)^3} \frac{F_v^2}{2} \frac{1}{K} \qquad \text{Eq. (28)}$$

where, ψ_L is the liquid resistance coefficient

a is the specified surface area of the dumped packing, m^2/m^3

ε is the void fraction, m^3/m^3

h_L is the column holdup, m^3/m^3

F_v is the gas or vapor capacity factor, $\sqrt{Pa}$

K is the wall factor

Billet & Schultes (1999) used following correlation to determine theoretical holdup.

$$h_L = \left(12 \frac{1}{g} \frac{\eta_L}{\rho_L} u_L a^2\right)^{1/3} \quad \text{Eq. (29)}$$

Billet & Schultes (1999) theoretical holdup is based on the channel model which assumes the void volume of random or structured packing by vertical flow channels as discussed above. However, in real applications, the flow of phases deviates due to the shape of random or structured packing and the surface of packing often partially covered by liquid. Therefore, theoretical liquid holdup prediction by equation 29 deviates from the real column holdup. Billet & Schultes (1999) stated that the deviation of real holdup from theoretical can be conveyed by considering hydraulic surface area of the packing. Accordingly, the real holdup of the column can be predicted by following equation provided by (Billet & Schultes, 1999).

$$h_{LS} = \left(12 \frac{1}{g} \frac{\eta_L}{\rho_L} u_L a^2\right)^{1/3} \left(\frac{a_h}{a}\right)^{2/3} \quad \text{Eq. (30)}$$

The hydraulic surface area (a_h) equation described by (Billet & Schultes, 1999) is given as follows.

$$Re_L = \frac{u_L \rho_L}{a\, \eta_L} < 5 : \frac{a_h}{a} = C_h \left(\frac{u_L \rho_L}{a\, \eta_L}\right)^{0.15} \left(\frac{u_L{}^2 a}{g}\right)^{0.1} \quad \text{Eq. (31)}$$

$$Re_L = \frac{u_L \rho_L}{a\, \eta_L} \geq 5 : \frac{a_h}{a} = C_h 0.85 \left(\frac{u_L \rho_L}{a\, \eta_L}\right)^{0.25} \left(\frac{u_L{}^2 a}{g}\right)^{0.1} \quad \text{Eq. (32)}$$

where, C_h is the hydraulic constant

h_L is the column holdup, m^3/m^3

h_{LS} is the loading point column holdup, m^3/m^3 (Loading point is defined as the point from where the liquid holdup increases as the gas velocity increases for the constant liquid loading.)

The hydraulic constant (C_h) depends on packing material geometry and must be determined empirically. Billet & Schultes (1999) provided hydraulic constants for various packings; however, it is not available for the raschig rings of 6-mm size. Therefore, the hydraulic constant

(C_h) was determined using experimental data of the column holdup of this research study (Table 2.5) and equations 30-32. The average value of C_h = 2.52, determined experimentally, was used to predict the liquid holdup in the subsequent calculation.

The gas or vapor capacity factor (F_V) provided by (Billet & Schultes, 1999) was determined using gas density and velocity from the following equation 33.

$$F_V = u_V\sqrt{\rho_V} \qquad \text{Eq. (33)}$$

where, u_v is the gas velocity, m/s

ρ_v is the density of gas or vapor, kg/m^3

Billet & Schultes (1999) stated that in the real packed bed column, the local void fraction (ε) differs from the theoretical value due to free space available at the wall of the column depending on the column diameter (d_S). The wall factor (K) given by (Billet & Schultes, 1999) was determined using following equation 34 which considers the increased void fraction at the column wall.

$$\frac{1}{K} = 1 + \frac{2}{3}\frac{1}{1-\varepsilon}\frac{d_p}{d_s} \qquad \text{Eq. (34)}$$

where, K is the wall factor

ε is the void fraction, m^3/m^3

d_p is the particle diameter, m

d_s is the column diameter, m

The particle diameter (equation 35) described by (Billet & Schultes, 1999) is the ratio of volume of packing (V_P) to its total area (A_P).

$$d_p = 6\frac{V_P}{A_P} = 6\frac{(1-\varepsilon)}{a} \qquad \text{Eq. (35)}$$

where, d_p is the particle diameter, m

V_P is the volume of the packing, m^3

A_P is the area of the packing, m^2

ε is the void fraction, m^3/m^3

a is the specified surface area of the dumped packing, m^2/m^3

Billet & Schultes (1999) stated that in the irrigated column, the free cross-sectional area available for the gas is reduced due to column holdup, and the surface structure of the packing changes due to coating of liquid film over packing surface. Thus, the liquid resistance coefficient (ψ_L) described by (Billet & Schultes, 1999) must be considered in the prediction of wet pressure drop across the column.

$$\psi_L = C_{P,O}\left(\frac{64}{Re_v} + \frac{1.8}{Re_v^{0.08}}\right)\left(\frac{\varepsilon - h_L}{\varepsilon}\right)^{1.5}\left(\frac{h_L}{h_{L,S}}\right)^{0.3}\exp\left(C_1\sqrt{Fr_L}\right) \quad \text{Eq. (36)}$$

$$C_1 = \frac{13300}{a^{3/2}} \quad \text{Eq. (37)}$$

$$Fr_L = \frac{u_L^2 a}{g} \quad \text{Eq. (38)}$$

$$Re_v = \frac{u_v d_p}{(1-\varepsilon)\upsilon_v} K \quad \text{Eq. (39)}$$

where, C_l is the constant

a is the specified surface area of the dumped packing, m^2/m^3

Fr_L is the Froude number for liquid

u_L is the velocity of liquid with reference to the free column cross-section, m/s

g is the gravitational constant, m/s^2

h_L is the column holdup, m^3/m^3

η_L is the dynamic viscosity of liquid, kg m/s

ρ_L is the density of liquid, kg/m^3

ρ_V is the density of gas or vapor, kg/m^3

$h_{L,S}$ is the column holdup at loading point, m^3/m^3

u_V is the velocity of gas or vapor with reference to the free column cross-section, m/s

The constant ($C_{P,0}$) describes the geometry and surface properties of packing and, therefore, is specific to the selected type of packings. Billet & Schultes (1999) provided packing specific constant ($C_{P,0}$) for various types of packings; however, C_{P0} of raschig rings of 6-mm size is not available. Moreover, the packing specific constants provided by Billet and Schultes (1999) were validated for only an air-water system. The present research project uses vegetable oil-air system. Therefore, $C_{P,0}$ was determined using experimental pressure drop data of all twenty seven conditions (3 bed heights x 3 solvent temperatures x 3 solvent flow rates) of this research project and equations 28 and 36. The $C_{P,0}$ was determined using trial and error method and the average values of $C_{P,0}$ = 2.93 and Ch = 2.52 were used for the prediction of pressure drop determination for all twenty seven conditions. Finally, the predicted pressure drop across the column was compared with the experimental data.

2.2.7 Determination of Billet & Schultes (1999) packing specific constants for prediction of height equivalent to a theoretical plate (HETP)

Perry et al. (1984) stated that the height equivalent to a theoretical plate (HETP) which applies to design dilute absorption and stripping or distillation columns is given below.

$$HETP = \frac{\ln \lambda}{\lambda - 1} HTU_{OV} \quad \text{Eq. (40)}$$

$$\lambda = \frac{m_{yx}}{L/V} \quad \text{Eq. (41)}$$

where, $HETP$ is the height equivalent to a theoretical plate, m

λ is the stripping factor

m_{yx} is the slope of the equilibrium curve, kmol/kmol

L is the molar flow of the liquid, kmol/h

V is the molar flow of the gas or vapor, kmol/h

HTU_{OV} is the overall height of a gas-phase mass transfer unit, m

The overall height of a gas-phase mass transfer unit (HTU_{OV}) depends on the height of a gas-phase mass transfer unit (HTU_V) and height of a liquid-phase mass transfer unit (HTU_L). The overall height of a gas-phase mass transfer unit (HTU_{OV}) correlation provided by Billet & Schultes (1999) is given below.

$$HTU_{OV} = HTU_V + \lambda\, HTU_L = \frac{u_V}{\beta_V a_{ph}} + \frac{m_{yx}}{L/V}\frac{u_L}{\beta_L a_{ph}} \quad \text{Eq. (42)}$$

$$\beta_L a_{ph} = C_L 12^{1/6} u'^{-1/2}_L \left(\frac{D_L}{d_h}\right)^{1/2} a\left(\frac{a_{ph}}{a}\right) \quad \text{Eq. (43)}$$

$$\beta_V a_{ph} = C_V \frac{1}{(\varepsilon - h_L)^{1/2}} \frac{a^{3/2}}{a_h^{1/2}} D_V \left(\frac{u_V}{a\upsilon_V}\right)^{3/4} \left(\frac{\upsilon_V}{D_V}\right)^{1/3} \left(\frac{a_{ph}}{a}\right) \quad \text{Eq. (44)}$$

$$u'_L = \frac{u_L}{h_L} \quad \text{Eq. (45)}$$

$$\frac{a_{ph}}{a} = 1.5\,(a d_h)^{-0.5} \left(\frac{u_L\, d_h}{\upsilon_L}\right)^{-0.2} \left(\frac{u_L^2\, \rho_L\, d_h}{\sigma_L}\right)^{0.75} \left(\frac{u_L^2}{g d_h}\right)^{-0.45} \quad \text{Eq. (46)}$$

$$d_h = 4\frac{\varepsilon}{a} \quad \text{Eq. (47)}$$

where, u_V is the velocity of gas or vapor with reference to free column cross section, m/s

u_L is the velocity of liquid with reference to free column cross section, m/s

$\beta_V a_{ph}$ is the gas phase volumetric mass transfer coefficient, 1/s

$\beta_L a_{ph}$ is the liquid phase volumetric mass transfer coefficient, 1/s

C_L is the packing specific constant for liquid phase

C_V is the packing specific constant for gas or vapor phase

u'_L is the mean effective velocity of liquid, m/s

h_L is the column liquid holdup, m^3/m^3

ε is the void fraction, m^3/m^3

a is the specified surface area of the dumped packing, m^2/m^3

a_{ph} is the specific interface area between the phases, m^2/m^3

d_h is the hydraulic diameter of the dumped packing, m

υ_L is the kinematic viscosity of liquid, m^2/s

υ_V is the kinematic viscosity of gas or vapor, m^2/s

D_V is the diffusion coefficient of solute in gas or vapor, m^2/s

D_L is the diffusion coefficient of solute in liquid, m^2/s

The column liquid holdup was determined using Billet & Schultes (1999) correlation given in equation 30. The prediction of the overall height of a gas-phase mass transfer unit (HTU_{OV}) requires empirical packing specific constants (C_V and C_L). Billet & Schultes (1999) provided these constants for various packings which were validated for an air-water system. However, these constants are not available for the raschig rings of 6 mm size used in this research. Therefore, constants C_V =0.80 and C_L = 2.40 were determined using Billet & Schultes (1999) mass transfer correlations as mentioned above and using the experimental HETP data of this research.

Table 2.5 Experimental liquid holdup for the given bed height, solvent temperature and solvent flow rate

Bed height	Temperature	Flow rate	Liquid holdup, ml	
m	°C	ml/min	Mean	S.E.*
0.5	30	53	145	21
0.5	30	63	168	18
0.5	30	73	190	14
0.5	40	53	135	7
0.5	40	63	140	0
0.5	40	73	165	7
0.5	50	53	110	14
0.5	50	63	120	14
0.5	50	73	135	7
0.8	30	53	270	14
0.8	30	63	290	0
0.8	30	73	315	7
0.8	40	53	240	0
0.8	40	63	260	0
0.8	40	73	280	0
0.8	50	53	215	7
0.8	50	63	225	7
0.8	50	73	243	4
1.1	30	53	385	7
1.1	30	63	425	7
1.1	30	73	455	7
1.1	40	53	360	14
1.1	40	63	375	21
1.1	40	73	390	28
1.1	50	53	330	0
1.1	50	63	345	7
1.1	50	73	360	14

*Standard error

2.2.8 Analysis of model tar compounds

2.2.8.1 GC/MS method

Samples of air containing model tar compounds exiting the scrubber were analyzed using gas chromatography (Model 7890A, Serial Number CN10937094, Agilent Technologies, Inc.) / mass spectroscopy (Product Number G1701EA, Agilent Technologies, Inc.). The GC/MS is equipped with HP-5MS 30 m x 250 μm x 0.25 μm film capillary column (Product Number 19091S-433, Agilent Technologies, Inc., New Castle, DE, USA). Ultra-high purity helium was used as the carrier gas. The GC oven started at 50°C for 1 minute, ramped 15°C/min to 100°C and was held at 100°C for 4.33 minutes. The operating temperatures of the injector, column and detector were maintained at 250, 100 and 250°C, respectively. A split ratio of 50:1 was used for the analysis. The sample size of 200 μl was used for the calibration as well as analysis of actual samples.

2.2.8.2 Standard gas mixtures preparation for GC/MS Calibration

Model tar compounds-air standard mixtures were prepared using pure liquid tar compounds and ultra-high purity air as diluting gas. Commercial standard gas mixtures of model tar compounds in low ppm level were deemed too expensive. In addition, commercial standard gas mixtures in higher ppm are not possible due to high pressure of the compressed gas cylinder. Barratt (1981) described several techniques to develop standard gas mixtures. These techniques involve the addition of known masses or volumes of volatile liquid compounds into diluting gas filled container of known and fixed volume (Barratt, 1981). US-EPA Method 18 (EPA, 1987) uses Tedlar bags for the “measurement of gaseous organic compounds emission by gas chromatography”. In this study, Tedlar bag of 1 liter capacity (Product Number 232-01, SKC Gulf Coast, Inc., Houston, TX, USA) was used to contain the mixtures. To prepare the calibration mixtures, an ultra-high purity air (Stillwater Steel and Supply, Stillwater, OK) of 1L metered

through the air sampling pump (Product Number 222-2301, SKC Gulf Coast, Inc., Houston, TX, USA) and filled a Tedlar bag. The required amount of liquid tar compounds for the desired concentration of tar compounds in the air mixture was calculated using following equation (Ozturk & Yilmaz, 2006).

$$V_L = \frac{P\ V_{TB}\ C\ MW}{\rho_L R\ T\ 1000} \quad \text{Eq. (48)}$$

where, V_L is the volume of liquid tar compounds, µl

P is the inside pressure of Tedlar bag, atm

V_{TB} is the volume of Tedlar bag, L

C is the intended tar compound concentration, ppmv

MW is the molecular weight of the tar compound, g/mole

ρ_L is the density of liquid tar compound, g/ml

R is the universal gas constant, L atm/mol °K

T is the temperature, °K

A calibration curve was prepared by plotting the concentration versus the area under the peak obtained for each tar compounds. The concentration varies in the range of 27-9500 ppm, 50-4800 ppm and 50-2400 ppm for benzene, toluene and ethylbenzene, respectively. The calibration charts of benzene, toluene and ethylbenzene are given in Appendix A.

2.2.8.3 Statistical analysis

For the statistical analysis, slopes of the response of model tar compounds (benzene, toluene and ethylbenzene) to time were calculated with least square regression for each combination of replication, solvent type, bed height, solvent temperature and solvent flow rate. Differences in slopes were determined using analysis of variance (ANOVA) procedure considering a split plot model. For example, in the statistical analysis of vegetable oil types, oil (solvent) was the main unit factor, the solvent temperature and flow rates were considered as split

unit factors and replication is the blocking factor. Similarly, the statistical analysis of bed height was conducted considering the packed bed height as a main unit factor, solvent temperature and flow rates were considered as split unit factors and replication is the blocking factor. In this statistical analysis, simple effects were compared because all interactions were significant.

2.3 Equilibrium based process modeling

Absorption of tars is carried out in a counter-current (gas flows upward while liquid flows downward) wet packed bed scrubbing column. The contact of gas and liquid is increased using 6-mm raschig rings. The model tar compounds are transferred from gas phase to liquid phase. The traditional approach of modeling absorption columns is using equilibrium stages. One equilibrium stage is calculated assuming the equilibrium between model tar compounds concentration in the gas and liquid leaving the stage.

2.3.1 Selection of chemical compounds

Aspen Plus™ possesses a large database of chemical components that are typically used in industry. The built-in database mainly contains organic, inorganic, aqueous, electrolytic and salt compounds. In this study, the chemical compounds selected from the in-built database include air, model tar compounds (benzene, toluene and ethylbenzene) and vegetable oils (derived from palmitic, steric, linoleic, linolenic and oleic acids).

2.3.2 Selection of thermodynamic property models

Thermodynamic properties of chemical components, such as density, enthalpy, entropy, Gibbs free energy, K-values, and vapor liquid equilibrium (VLE), are predicted through various thermodynamic property models. Aspen Plus™ database contains many of these models. The selection of the property model significantly influences the modeling results (S. Gebreyohannes, 2011). A detailed discussion on the selection of thermodynamic model is given in Carlson (1996).

Mateescu et al. (2011) stated that the vapor-liquid equilibrium (VLE) of volatile organic compounds (VOCs) in biodiesel fuels (methyl palmitate, methyl oleate, methyl lenolenate, ethyl stearate) was predicted reliably through UNIQUAC functional-group activiti coefficients (UNIFAC) method. Kuramochi et al. (2009) reported that the VLE of methanol-soybean based biodiesel and methanol-glycerin systems is predicted accurately by UNIFAC and Dortmund-UNIFAC models. Carlson (1996) and Ravindranath et al. (2007) reported that non-random two-liquid (NRTL) and universal quasi chemical (UNIQUAC) activity coefficient models provide better VLE property predictions than the UNIFAC model for highly non-ideal system. Seethamraju et al. (2013) also used NRTL property model for modeling tars absorption in vegetable oil and the missing binary interaction parameters were estimated by UNIFAC method. However, the accuracy of NRTL model prediction highly depends on VLE prediction that depends on the regressed binary interation parameters based on experimental VLE data for the selected system (Ravindranath et al., 2007).

The present system consists of hydrocarbons (toluene, benzene and ethylbenzene), air and vegatable oils. Experimental VLE data of model tar compounds in vegetable oils are not found in the literature. This study uses the NRTL model to simulate the wet scrubbing process as explained in Section 1.5 of Chapter 1; and the missing interation binary parameters were estimated using UNIFAC method.

2.3.3 Equilibrium stage-based Aspen Plus™ packed bed scrubbing system model

A process model of the wet packed bed scrubbing system was developed using an equilibrium stage based "RadFrac" model of Aspen Plus™ software. "RadFrac" is a rigrous model that is used to perform rigrous rating and design calculations of wide range of processes such as absorption, stripping, and distillation.

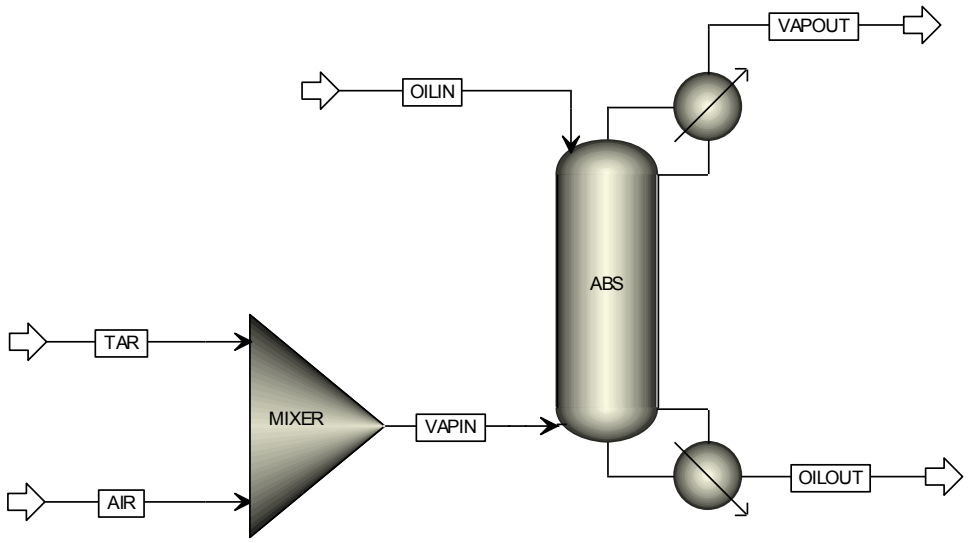

Figure 2.9 Equilibrium stage based Aspen Plus™ process model of wet packed bed scrubbing system

A process flow diagram of an equilibrium stage-based steady state model is shown in Figure 2.9. A "MIXER" block was used to mix the model tar compounds and an inlet air stream to formulate a simulated air stream. The simulated air stream is introduced at the bottom of the packed bed column, i.e., at the tenth stage which was named as "VAPIN" stream. "VAPOUT" stream denotes a partly clean simulated air stream after the absorption of model tar compounds. "OILIN" signifies a solvent inlet stream which is introdued at the top of the column, i.e., first stage of the column. "OILOUT" is the waste vegetable oil stream containing traces of absorbed model tar compounds.

A split approach (φ/γ) is used for the estimation of phase behavior. Nonrandom two-liquid (NRTL) model for the estimation of liquid phase activity coefficient (γ) and Peng-Robinson (PENG-ROB) equation of state for the estimation of vapor phase fugacity coefficient (φ) were used. A thermodynamic data of binary intercation parameters for NRTL model is very important for an accurate prediction of thermodynamic properties. The thermodynamic data matrix for the present compounds is shown in Figure 2.10. The experimental values of the

interaction parameters for binary pairs of benzene, toluene, and ethylbenzene highlighted with green blocks in the Figure 2.10 are available in the DECHEMA database which were regressed and used in the model. The present system also includes supercritical gases (oxygen and nitrogen); however, the Henry's constant of oxygen and nitrogen in vegetable oil compositions are not available, and therefore, Henry's constant were not considered in the model. The missing interaction parameters were estimated using UNIFAC methods.

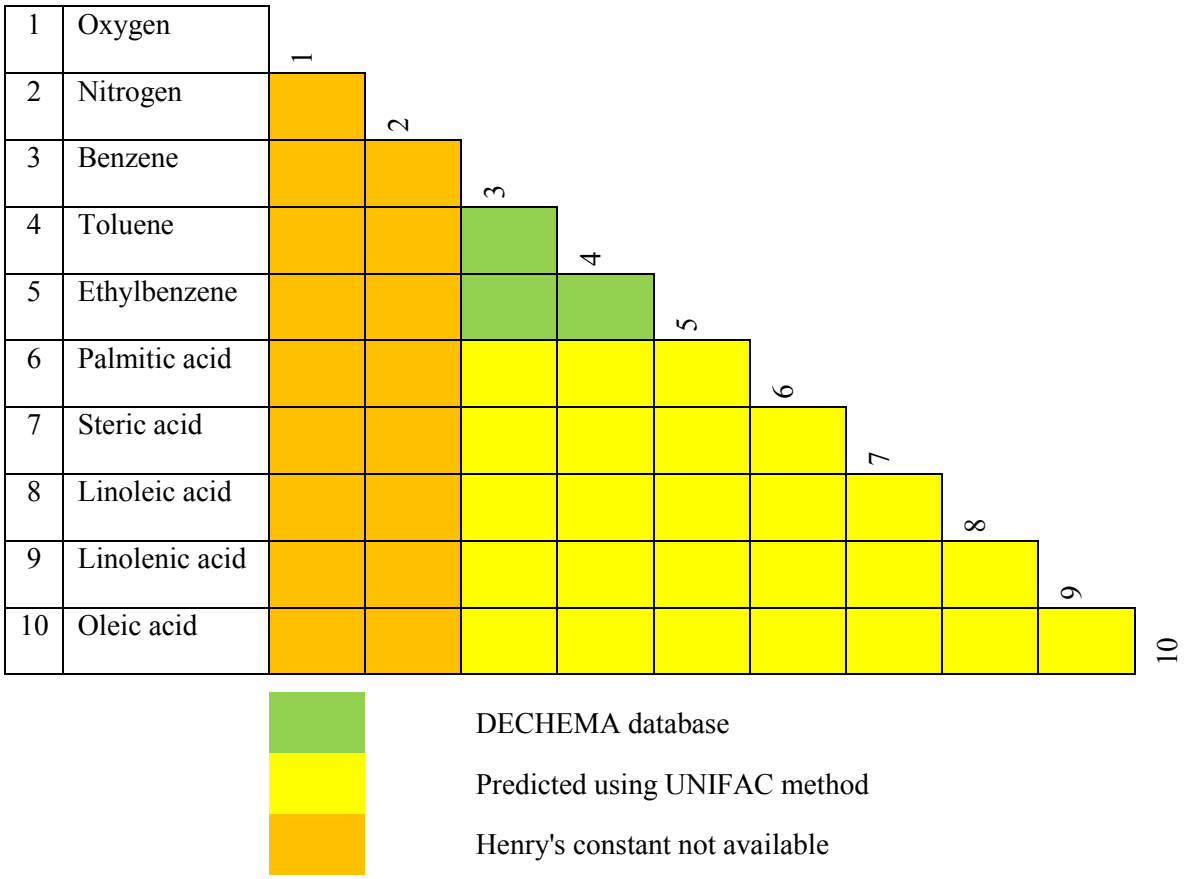

Figure 2.10 Thermodynamic data matrix of binary pairs

The simulation was performed in a packed column of 50 mm diameter and 0.5 and 1.1 m of packing bed height. Stainless steel raschig rings of 6 mm in size used as the packing media were specified using supplier's specification (Table 2.3). Air flow was set at 10.8 l/min. The concentration of model tar compounds in the inlet simulated air stream is given in Table 2.6. Vegetable oil is represented using supplier's composition of fatty acids (palmitic, steric, linoleic,

linolenic and oleic acids) as given in Table 2.1. The simulated air inlet stream pressure, temperature and concentration levels of tar compounds were indicated using values measured during the physical experiments.

Table 2.6 Maximum concentration of tar compounds

Tar compounds	Concentration, ppm
Benzene	8355
Toluene	4206
Ethyl benzene	2439

A simplified approach was adopted to generate a dynamic process model. In this approach, a mass balance was carried out to determined the amount of model tar compounds absorbed in vegetable oil by integrating the absorbed concentration of model tar compounds in parts per million by volume (ppmv) over the experimental time period. The concentration of model tar compounds in the inlet vegetable oil stream, i.e., OILIN, were determined by dividing the absorbed model tar compounds to the total volume of vegetable oils used during experimental tests, i.e., sump volume. The calculated model tar compounds' concentrations at every time period were entered as an input in "OILIN" stream of the the steady state model as shown in Figure 2.9 and the concentration of model tar compounds were predicted in "VAPOUT" stream to determined the predicted tar removal efficiency. A similar approach was adopted to determined predicted tar removal efficiency at the other process conditions.

CHAPTER III

RESULTS AND DISCUSSION

This chapter provides experimental and modeling results for the absorption of model tar compounds in vegetable oils using a bench scale wet packed bed scrubbing unit. Model tar compounds were benzene, toluene and ethylbenzene. The experimental results are presented in terms of removal efficiencies of tar compounds and reported as a function of the wet scrubbing system design and operating parameters, i.e., packed bed height, solvent temperature, and solvent flow rate, over the range listed in the Table 2.4. Tar removal efficiency (η) was calculated using following equations:

$$\eta, \% = \frac{C_{in} - C_{out}}{C_{in}} \quad \text{Eq. (49)}$$

Where, C_{in} = concentration of tar compounds (benzene, toluene and ethylbenzene) at the inlet of the column, ppmv

C_{out} = concentration of tar compounds (benzene, toluene and ethylbenzene) at the outlet of the column, ppmv

Inlet and outlet tar concentrations were determined by analyzing samples using gas chromatography/mass spectrometry (GC/MS). Pressure drop across the absorption column was measured using a differential pressure transducer and recorded through DaqView program every five seconds. Experimental results of pressure drop are reported as a function of solvent temperature, flow rate, and packed bed height.

3.1 Effect of type of vegetable oil

Vegetable oils are composed of triglycerides formed through reaction of long chain fatty acids with glycerin. A detailed list of fatty acids compositions of the selected vegetable oils is provided in Table 2.1. Soybean and canola oils were selected as solvents to study the variability of fatty acids on the removal efficiency of model tar compounds. The effect of vegetable oil type was analyzed at the lowest bed height of 0.5 m, three levels of solvent temperature and three levels of solvent flow rate (Figures 3.1-3.6). Both soybean and canola oils follow the same trend for all the conditions of solvent temperatures and flow rates. Statistical analysis showed that there is no significant difference ($p>0.05$) between the soybean and canola oils as a solvent for the removal of benzene, toluene and ethylbenzene except for the toluene and ethylbenzene removal efficiency at 50°C and solvent flow rate of 73 ml/min (Tables 3.1-3.3). It was determined that the solvent temperature controller at 50°C was unable to maintain solvent temperature after about 36 minutes of operation which resulted in a perceptible deviation in tar removal efficiencies. Therefore, in Figures 3.1-3.6, the removal efficiency of tar compounds after 36 minutes is not included.

Based on these results, it was concluded that soybean and canola oils were not statistically different in removal efficiencies of benzene, toluene and ethylbenzene. Accordingly, further evaluation of effect of bed height on the removal of model tar compounds was performed for only the soybean oil as a solvent as discussed in Sections 3.2 to 3.4. The selection of soybean oil was based on the availability in large quantities and the relative low cost of soybean oil compared to canola oil.

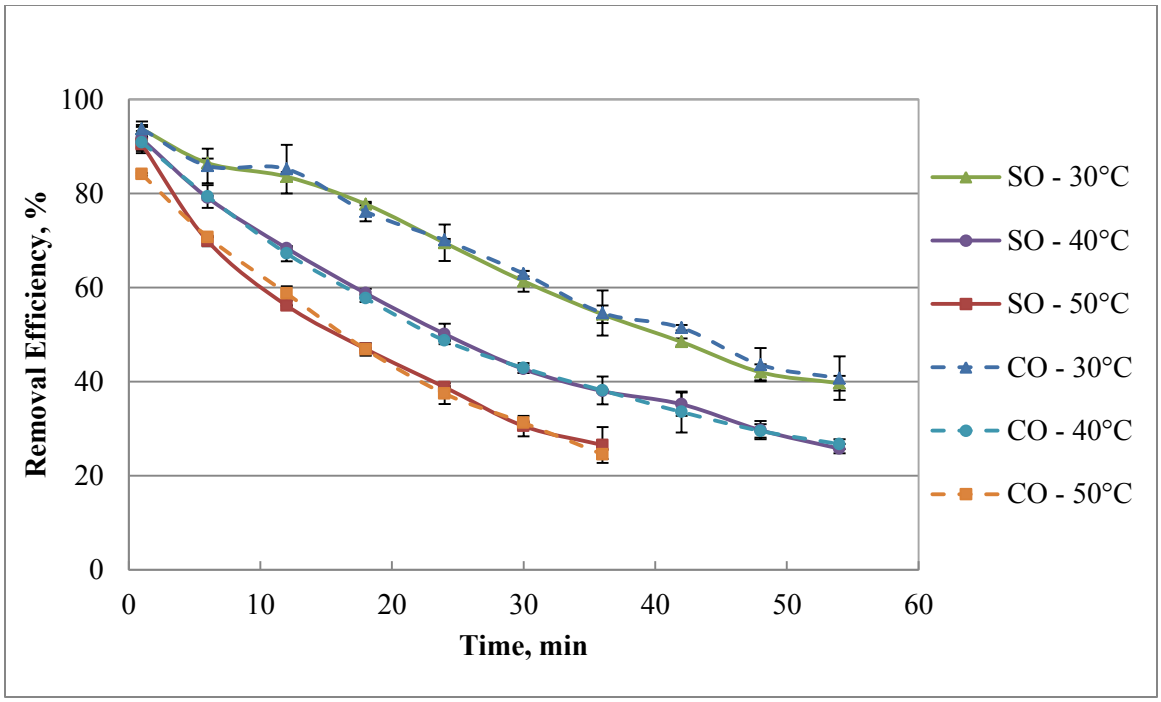

Figure 3.1 Effect of solvent type on the removal efficiency of benzene at a bed height of 0.5 m, solvent temperatures of 30, 40 and 50°C, and solvent flow rate of 53 ml/min [SO: soybean oil, CO: canola oil]

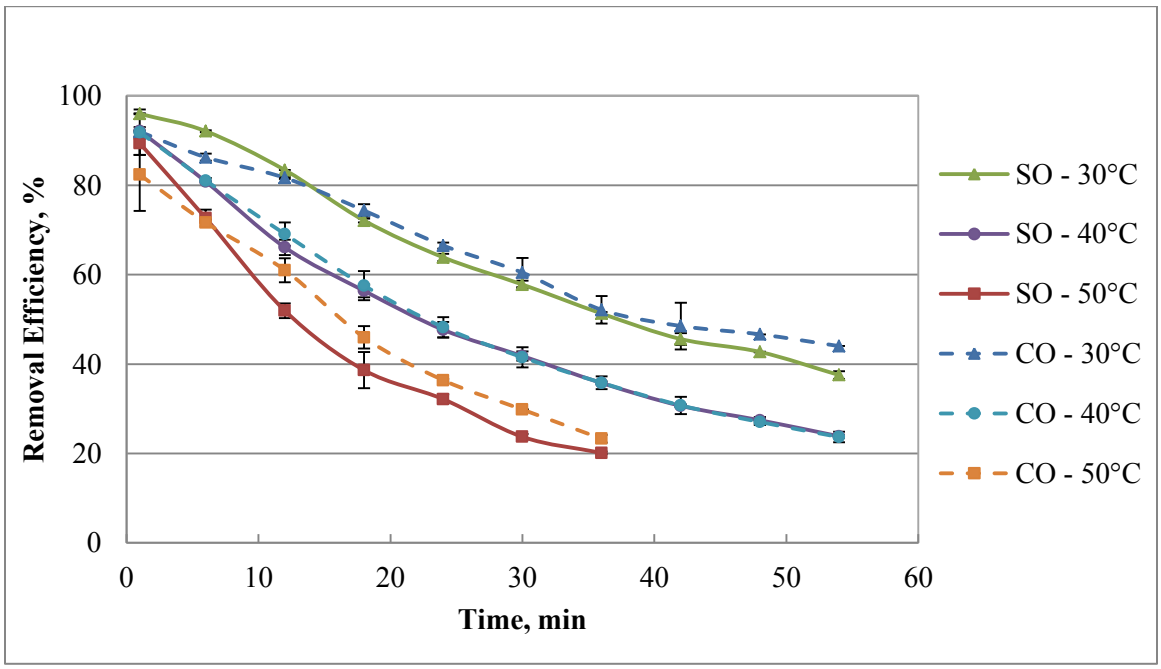

Figure 3.2 Effect of solvent type on the removal efficiency of benzene at a bed height of 0.5 m, solvent temperatures of 30, 40 and 50°C, and solvent flow rate of 73 ml/min [SO: soybean oil, CO: canola oil]

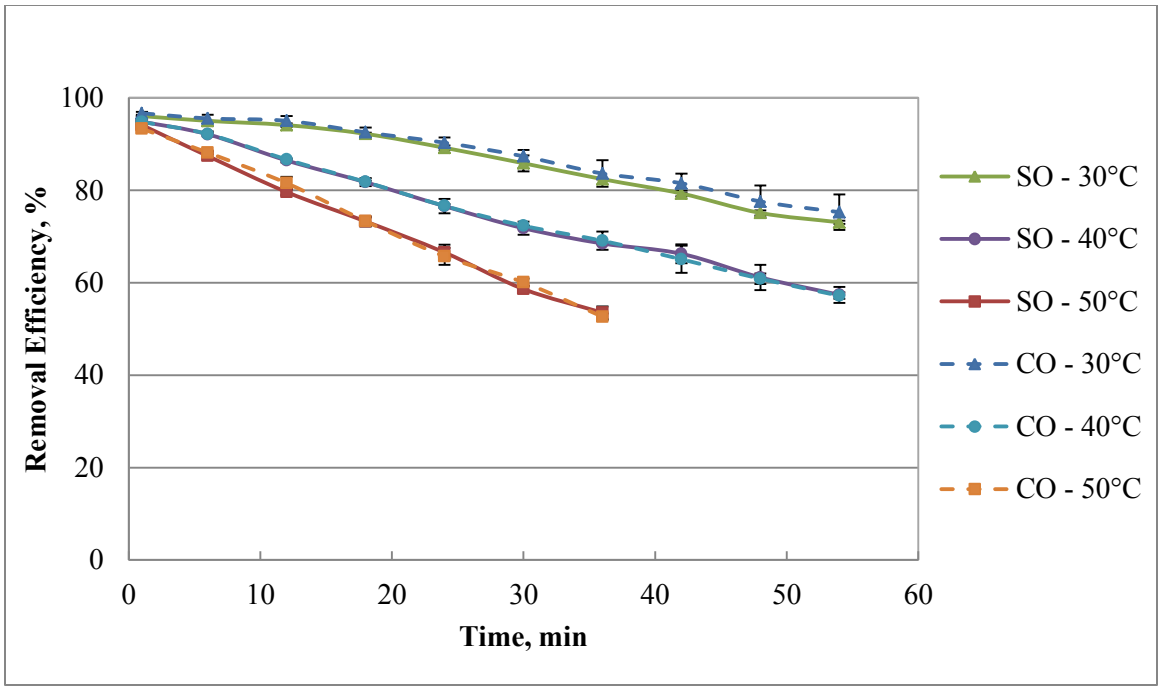

Figure 3.3 Effect of solvent type on the removal efficiency of toluene at a bed height of 0.5 m, solvent temperatures of 30, 40 and 50°C, and solvent flow rate of 53 ml/min [SO: soybean oil, CO: canola oil]

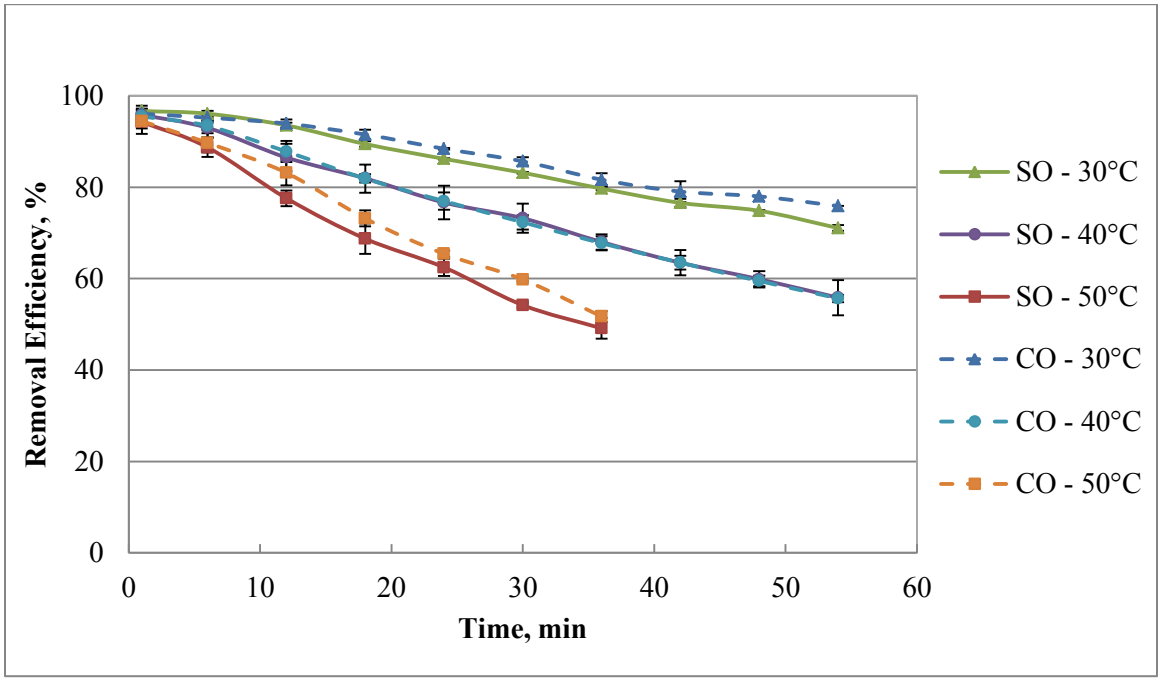

Figure 3.4 Effect of solvent type on the removal efficiency of toluene at a bed height of 0.5 m, solvent temperatures of 30, 40 and 50°C, and solvent flow rate of 73 ml/min [SO: soybean oil, CO: canola oil]

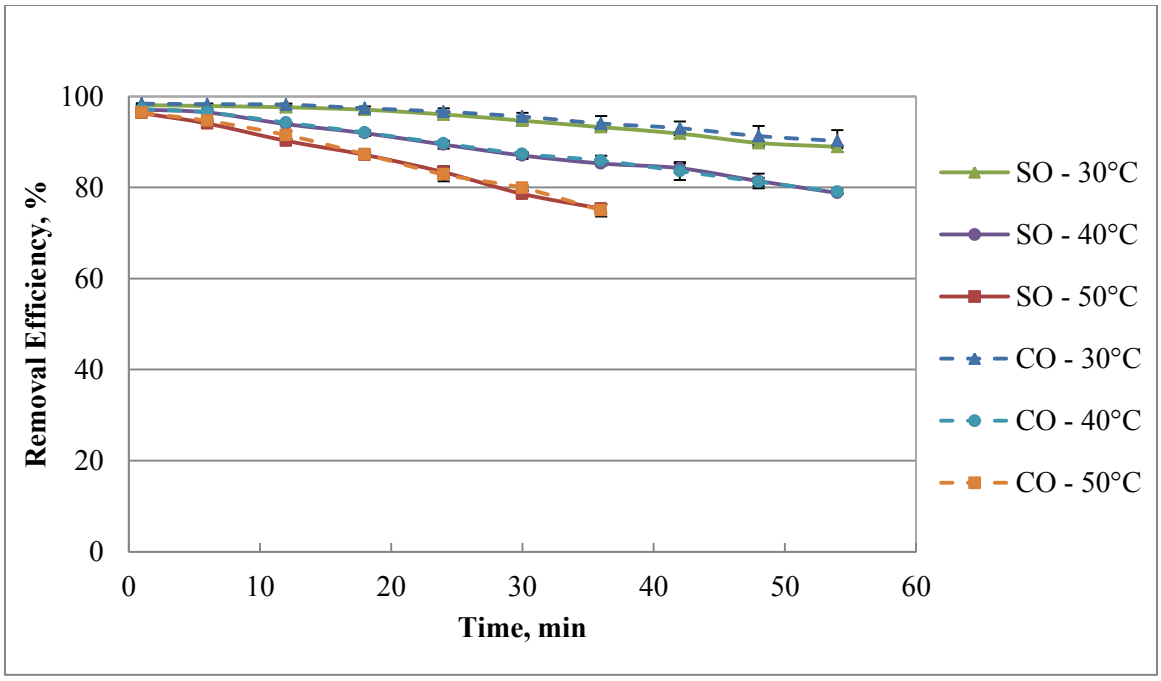

Figure 3.5 Effect of solvent type on the removal efficiency of ethylbenzene at a bed height of 0.5 m, solvent temperatures of 30, 40 and 50°C, and solvent flow rate of 53 ml/min [SO: soybean oil, CO: canola oil]

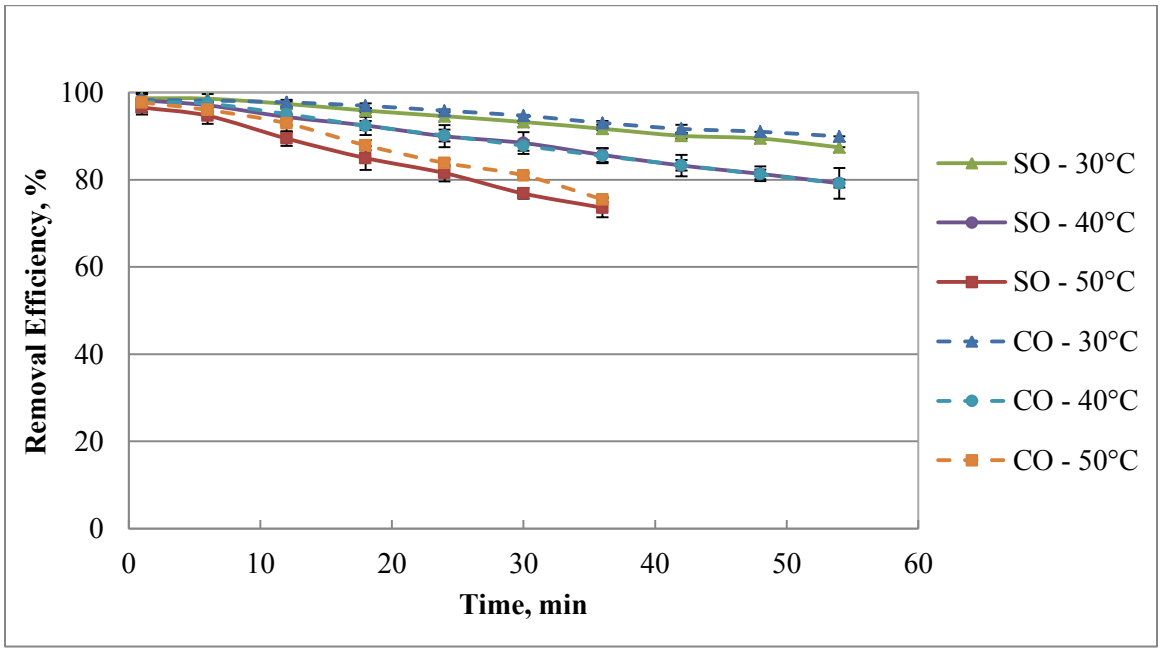

Figure 3.6 Effect of solvent type on the removal efficiency of ethylbenzene at a bed height of 0.5 m, solvent temperatures of 30, 40 and 50°C, and solvent flow rate of 73 ml/min [SO: soybean oil, CO: canola oil]

Table 3.1 Statistical analysis of the effect of solvent type on the benzene removal efficiency at a bed height of 0.5 m for the given solvent temperature and flow rate

Temperature	Flow rate	Solvent	Benzene slope		*p* value
°C	ml/min		Mean	S.E.*	
30	53	Canola	-1.033	0.104	0.643
30	53	Soybean	-1.072	0.023	
30	63	Canola	-1.138	0.037	0.933
30	63	Soybean	-1.131	0.065	
30	73	Canola	-1.060	0.116	0.287
30	73	Soybean	-1.150	0.003	
40	53	Canola	-1.179	0.062	0.858
40	53	Soybean	-1.194	0.001	
40	63	Canola	-1.225	0.060	0.711
40	63	Soybean	-1.226	0.036	
40	73	Canola	-1.277	0.031	0.784
40	73	Soybean	-1.254	0.005	
50	53	Canola	-1.233	0.003	0.860
50	53	Soybean	-1.247	0.075	
50	63	Canola	-1.280	0.021	0.831
50	63	Soybean	-1.297	0.085	
50	73	Canola	-1.331	0.064	0.324
50	73	Soybean	-1.248	0.053	

*Standard error

Table 3.2 Statistical analysis of the effect of solvent type on the toluene removal efficiency at a bed height of 0.5 m for the given solvent temperature and flow rate

Temperature	Flow rate	Solvent	Toluene slope		*p* value
°C	ml/min		Mean	S.E.*	
30	53	Canola	-0.424	0.064	0.426
30	53	Soybean	-0.462	0.003	
30	63	Canola	-0.481	0.001	0.543
30	63	Soybean	-0.510	0.028	
30	73	Canola	-0.439	0.046	0.171
30	73	Soybean	-0.506	0.009	
40	53	Canola	-0.722	0.030	0.849
40	53	Soybean	-0.713	0.024	
40	63	Canola	-0.742	0.020	0.846
40	63	Soybean	-0.751	0.032	
40	73	Canola	-0.780	0.010	0.790
40	73	Soybean	-0.767	0.011	
50	53	Canola	-1.028	0.022	0.614
50	53	Soybean	-1.052	0.043	
50	63	Canola	-1.110	0.010	0.600
50	63	Soybean	-1.135	0.013	
50	73	Canola	-1.173	0.048	0.001
50	73	Soybean	-0.990	0.069	

*Standard error

Table 3.3 Statistical analysis of the effect of solvent type on the ethylbenzene removal efficiency at a bed height of 0.5 m for the given solvent temperature and flow rate

Temperature	Flow rate	Solvent	Ethylbenzene slope		*p* value
°C	ml/min		Mean	S.E.*	
30	53	Canola	-0.163	0.037	0.489
30	53	Soybean	-0.185	0.002	
30	63	Canola	-0.190	0.003	0.409
30	63	Soybean	-0.216	0.011	
30	73	Canola	-0.174	0.014	0.147
30	73	Soybean	-0.220	0.009	
40	53	Canola	-0.351	0.018	0.746
40	53	Soybean	-0.341	0.015	
40	63	Canola	-0.340	0.006	0.715
40	63	Soybean	-0.351	0.022	
40	73	Canola	-0.371	0.002	0.870
40	73	Soybean	-0.366	0.017	
50	53	Canola	-0.602	0.021	0.642
50	53	Soybean	-0.616	0.025	
50	63	Canola	-0.658	0.020	0.668
50	63	Soybean	-0.671	0.026	
50	73	Canola	-0.671	0.040	0.001
50	73	Soybean	-0.546	0.040	

*Standard error

Canola oil was tested at the highest bed height and flow rate (Figures 3.7-3.9) to confirm the hypothesis that the tar removal efficiencies of soybean and canola oils were not statistically different. Statistical analysis (Table 3.4) showed that the removal efficiencies of benzene, toluene and ethylbenzene through soybean and canola oil were not statistically (p >0.05) different. In addition, as shown in Figures 3.7-3.9, the removal efficiency of benzene, toluene and ethylbenzene at the solvent temperature of 50°C is not included after 30 minutes of operation due to fault in the temperature controller.

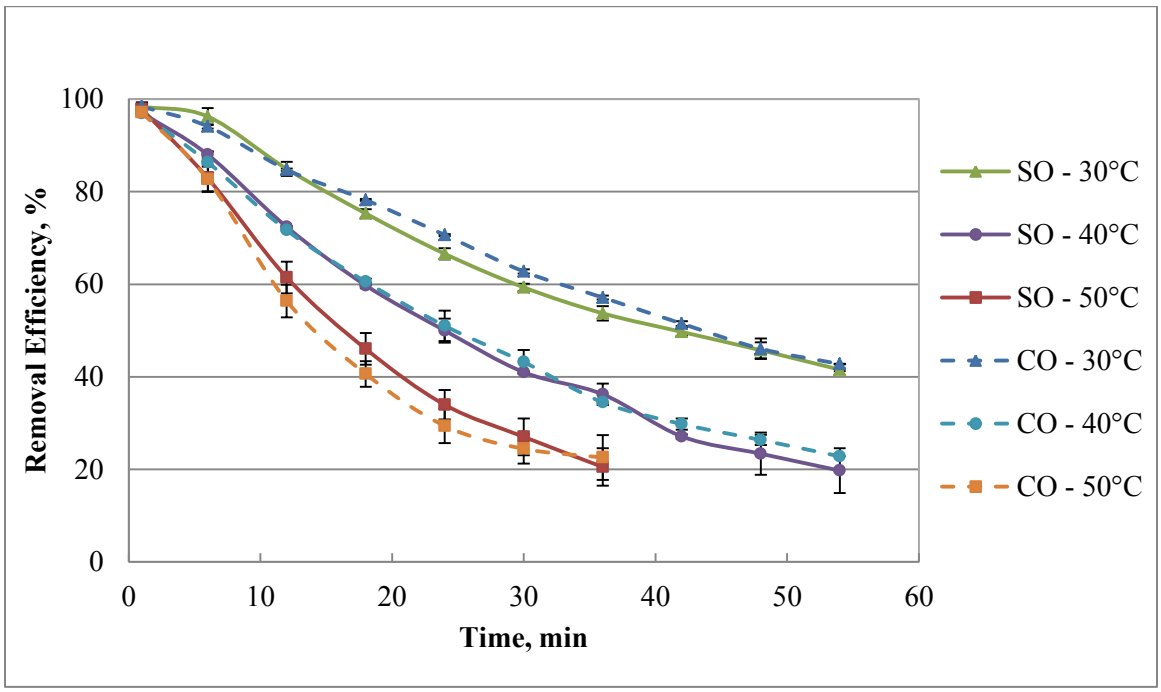

Figure 3.7 Effect of solvent type on the removal efficiency of benzene at a bed height of 1.1 m, solvent temperatures of 30, 40 and 50°C, and solvent flow rate of 73 ml/min [SO: soybean oil, CO: canola oil]

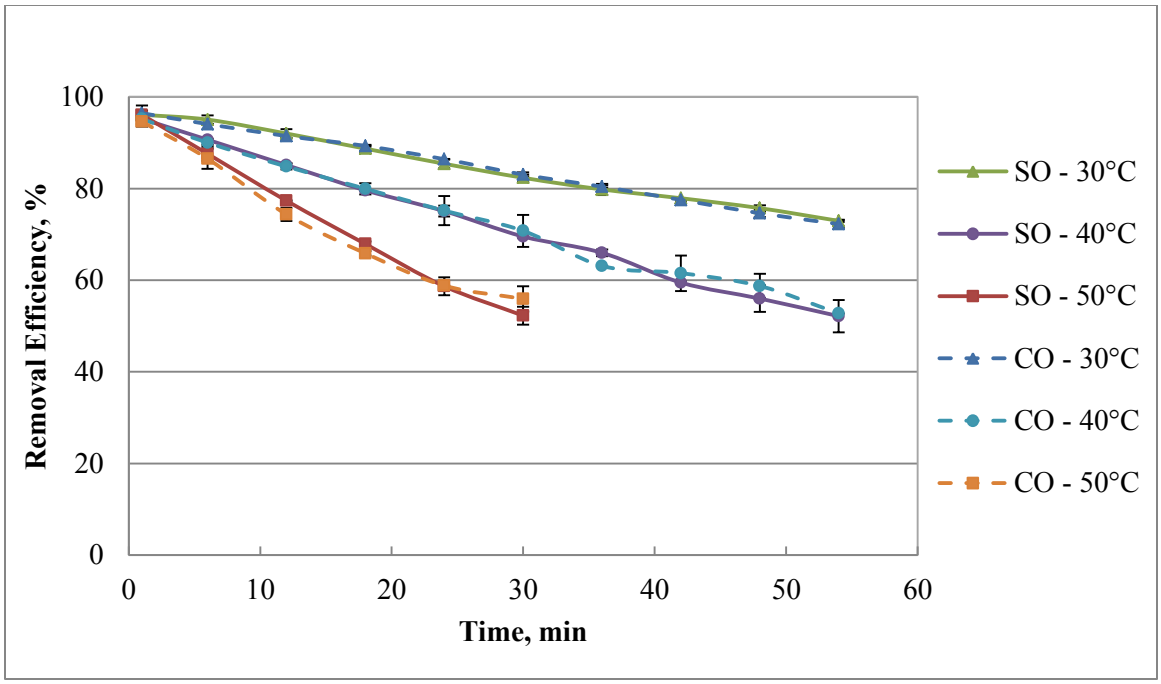

Figure 3.8 Effect of solvent type on the removal efficiency of toluene at a bed height of 1.1 m, solvent temperatures of 30, 40 and 50°C, and solvent flow rate of 73 ml/min [SO: soybean oil, CO: canola oil]

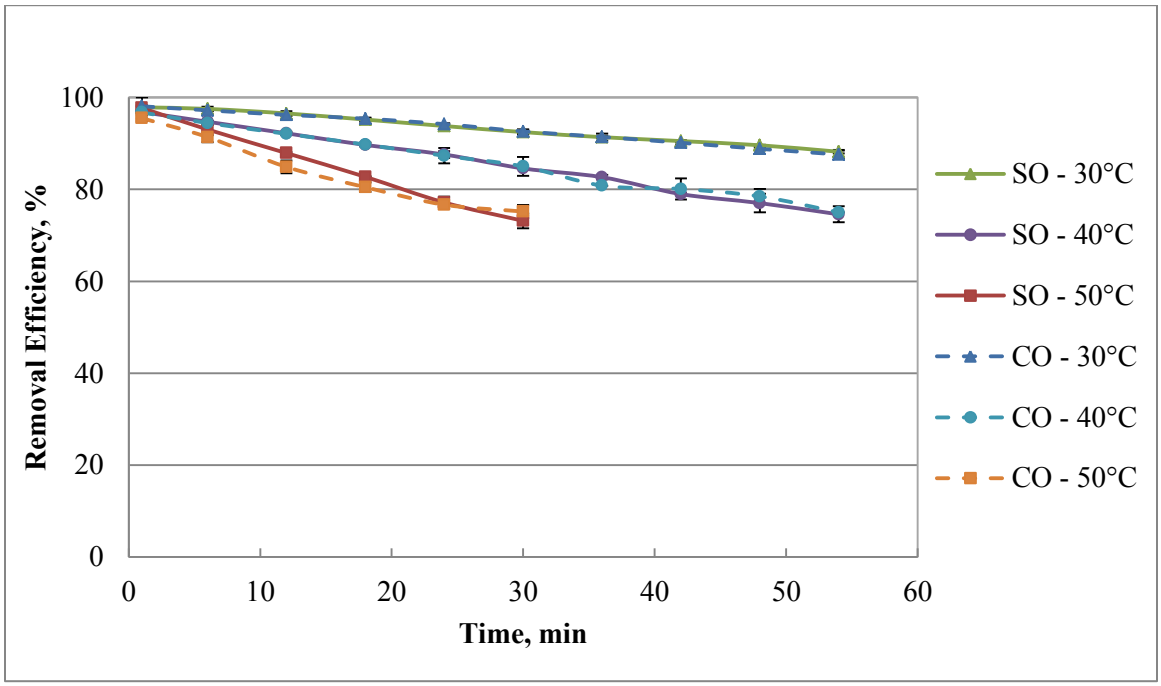

Figure 3.9 Effect of solvent type on the removal efficiency of ethylbenzene at a bed height of 1.1 m, solvent temperatures of 30, 40 and 50°C, and solvent flow rate of 73 ml/min [SO: soybean oil, CO: canola oil]

Table 3.4 Statistical analysis of the effect of solvent type on benzene (A), toluene (B) and ethylbenzene (C) removal efficiency for the given solvent temperature at the bed height of 1.1 m and solvent flow rate of 73 ml/min

(Table 3.4-A)

Temperature	Solvent	Benzene slope		*p* value
°C		Mean	S.E.*	
30	Canola	-1.095	0.005	0.690
30	Soybean	-1.134	0.028	
40	Canola	-1.450	0.039	0.761
40	Soybean	-1.480	0.062	
50	Canola	-1.399	0.136	0.765
50	Soybean	-1.370	0.032	

*Standard error

(Table 3.4-B)

Temperature	Solvent	Toluene slope		*p* value
°C		Mean	S.E.*	
30	Canola	-0.463	0.008	0.876
30	Soybean	-0.453	0.012	
40	Canola	-0.764	0.044	0.399
40	Soybean	-0.820	0.040	
50	Canola	-0.815	0.073	0.477
50	Soybean	-0.862	0.048	

*Standard error

(Table 3.4-C)

Temperature	Solvent	Ethylbenzene slope		*p* value
°C		Mean	S.E.*	
30	Canola	-0.201	0.008	0.783
30	Soybean	-0.189	0.003	
40	Canola	-0.387	0.034	0.427
40	Soybean	-0.422	0.023	
50	Canola	-0.435	0.044	0.336
50	Soybean	-0.478	0.037	

*Standard error

3.2 Effect of solvent temperature

3.2.1 Removal efficiency of model tar compounds

Solvent temperature had a prominent influence on the mass transfer of model tar compounds and resulting removal efficiencies. The effect of solvent temperature on the removal efficiency of tar compounds with time is shown in Figures 3.10-3.15. As shown, the trends of the effect of solvent temperature on removal efficiencies of benzene, toluene and ethylbenzene are similar. The sequence of the maximum removal efficiencies of model tar compounds are ethylbenzene, toluene and benzene (Figure 3.16) because the equilibrium ratio, i.e., K-value of ethylbenzene < K-value of toluene < K-value of benzene for the specific pressure and temperature. The lower the K-value, the higher the driving force for the mass transfer of model tar compounds resulting the higher removal efficiency.

As shown in Figures 3.10, 3.12 and 3.14 and Table 3.5, as the solvent temperature increased from 30 to 50°C at the bed height of 1.1 m and solvent flow rate of 53 ml/min, the slope of removal efficiencies of benzene, toluene and ethylbenzene decreased from -1.38 to -1.75, -0.54 to -1.22 and -0.24 to -0.75, respectively. An increase in the removal efficiencies of benzene with the reduction in the solvent temperature is due to an increase in solubility of model tar compounds, i.e., decrease in equilibrium ratio (K-value). In addition, decrease in the solvent temperature leads to an increase in density and viscosity of vegetable oil that increases the available interfacial mass transfer area. This increase in interfacial mass transfer area increases the mass transfer of tar compounds resulting high tar removal efficiencies. Also, solvent temperature influences the surface tension of solvent significantly. The surface tension of solvent, i.e., vegetable oils, reduces as the solvent temperature decreases which enhances the wettability and increases the effective interfacial area which leads to a high mass transfer of the tar compounds.

It was also observed that the rate of removal efficiency appears linear in case of toluene and ethylbenzene while it is polynomial for the benzene because the equilibrium ratios of toluene and ethylbenzene are much lower than benzene which enhances absorption capacity. As a result, the rate of absorption of toluene and ethylbenzene appears as linear for the 54-minute experiments.

As shown in Figures 3.10 and 3.11, an increase in the removal efficiency with a decrease in the solvent temperature increases as the solvent flow rates increases. Thus, the overall absorption of tar compounds increases as the solvent flow rate increases for the given solvent temperature and at a packed height of 1.1 m. This occurs because higher solvent flow rate increases wetted surface resulting higher interfacial area for mass transfer of tar compounds. However, as the bed height reduced from 1.1 m to 0.8 and 0.5 m, the effect of solvent flow rate was not significant (p>0.05). This occurs due to reduced contact between gas and liquid and short residence time.

Results of statistical analysis are presented in Table 3.5. As shown, the effect of solvent temperature on the benzene removal efficiencies for the bed height of 0.5 m was not significant for all solvent flow rates. For bed heights of 0.8 and 1.1 m, the effect of solvent temperature on benzene removal efficiency is highly significant ($p < 0.0001$) for all solvent flow rates (53, 63 and 73 ml/min). The effect of solvent temperature on benzene removal efficiency is not significant because a malfunction of solvent temperature controller affected slopes of benzene removal efficiency resulting in statistically no difference in slopes at solvent temperature of 40 and 50°C. For example, as shown in Figure 3.11, the trend of benzene removal efficiency at the solvent temperature of 50°C was expected follow in a similar way the benzene removal efficiencies followed at the solvent temperature of 30 and 40°C. However, due to a malfunction in solvent temperature controller, the trend of benzene removal efficiency deviated after 36 minutes of operation resulting in statistically different slopes of benzene removal efficiency.

Therefore, as shown in Figures 3.10-3.15, the removal efficiency of benzene, toluene and ethylbenzene were not included after 36 minutes of experimental run at the highest solvent temperature of 50°C and the packed bed height of 1.1 m. While in case of toluene and ethylbenzene, the effects of malfunction of temperature controller on the removal efficiency curve were not as evident, resulting in significantly different slopes of removal efficiency. Therefore, a statistical analysis of effects of solvent temperature on toluene and ethylbenzene removal efficiencies is highly significant ($p < 0.0001$) for all bed heights and all solvent flow rates.

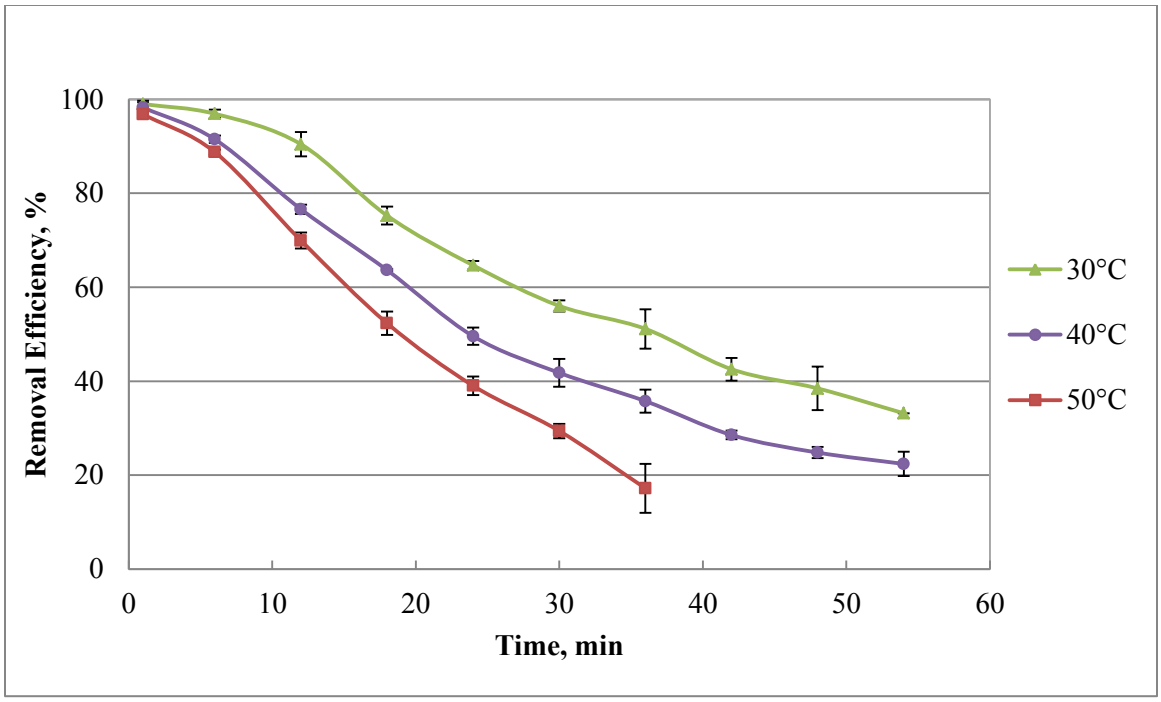

Figure 3.10 Effect of solvent temperature on the removal efficiency of benzene at a bed height of 1.1 m, solvent flow rate of 53 ml/min, and using soybean oil as a solvent

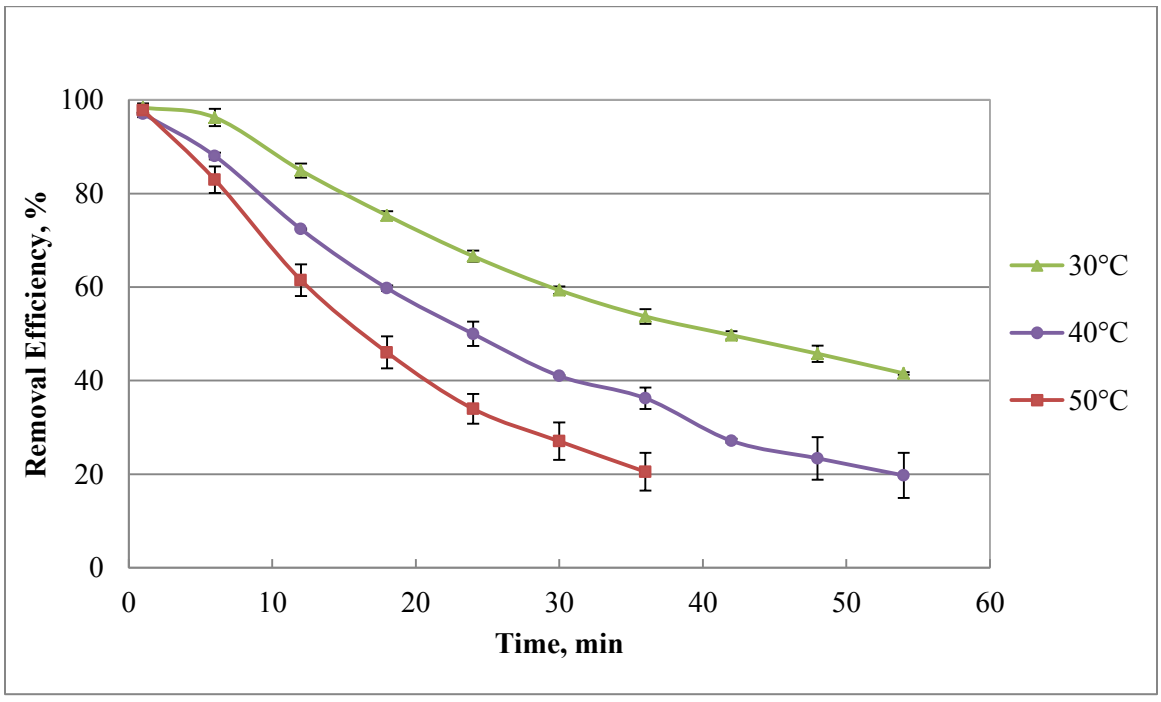

Figure 3.11 Effect of solvent temperature on the removal efficiency of benzene at a bed height of 1.1 m, solvent flow rate of 73 ml/min, and using soybean oil as a solvent

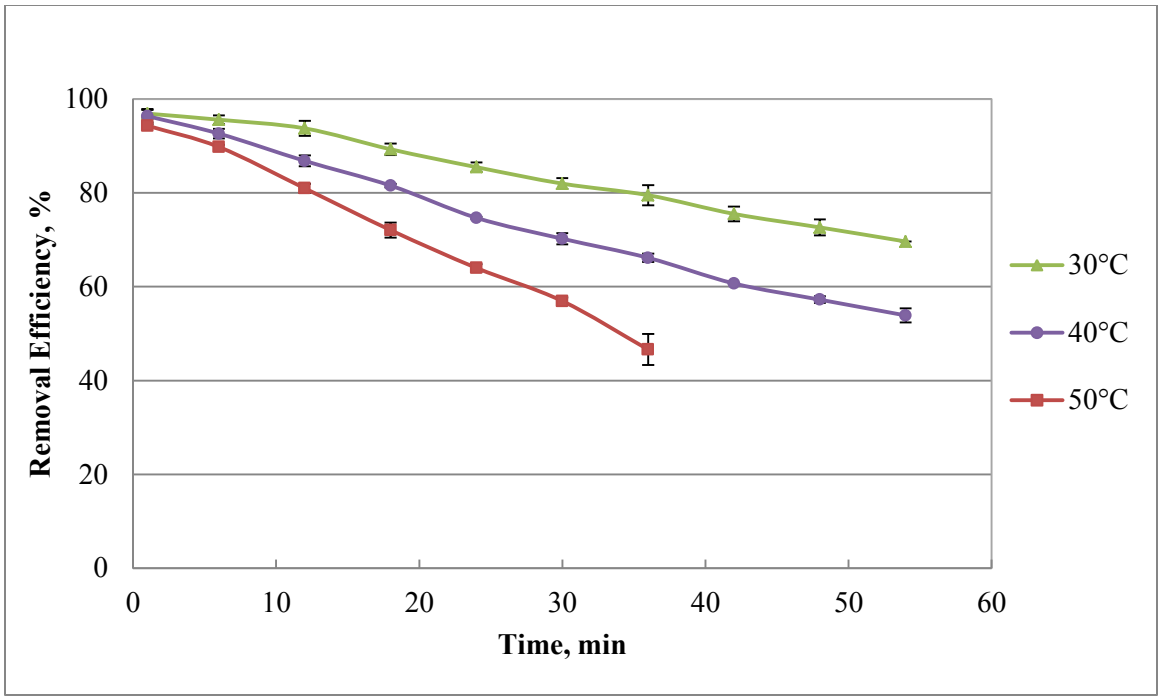

Figure 3.12 Effect of solvent temperature on the removal efficiency of toluene at a bed height of 1.1 m, solvent flow rate of 53 ml/min, and using soybean oil as a solvent

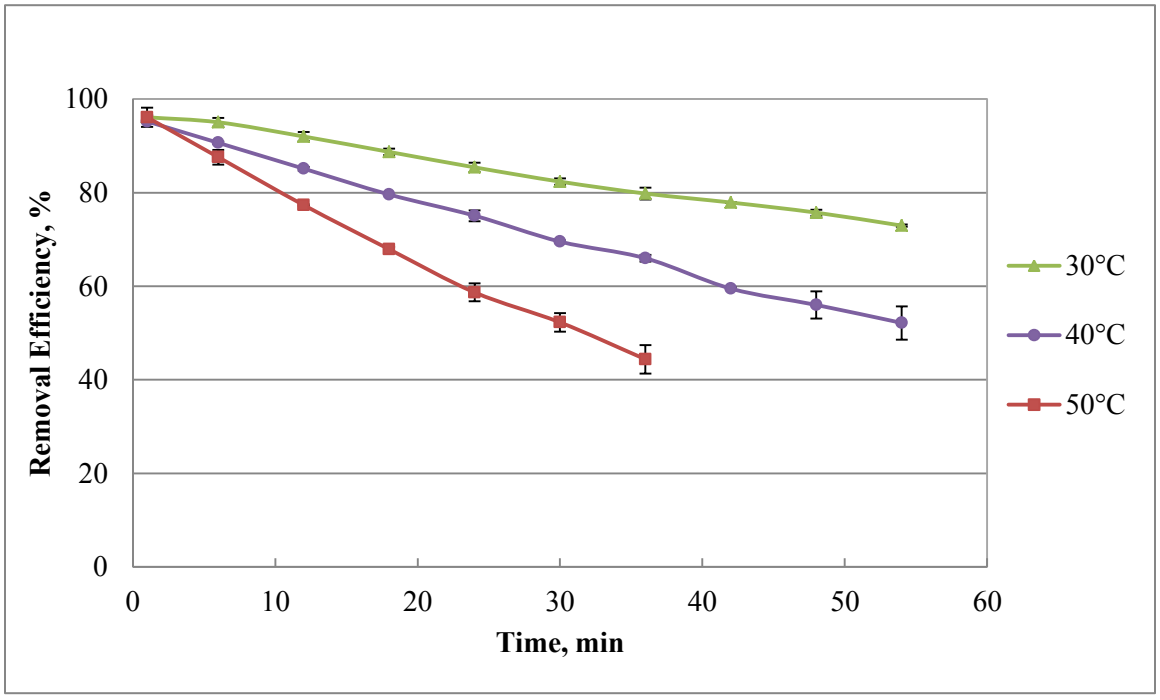

Figure 3.13 Effect of solvent temperature on the removal efficiency of toluene at a bed height of 1.1 m, solvent flow rate of 73 ml/min, and using soybean oil as a solvent

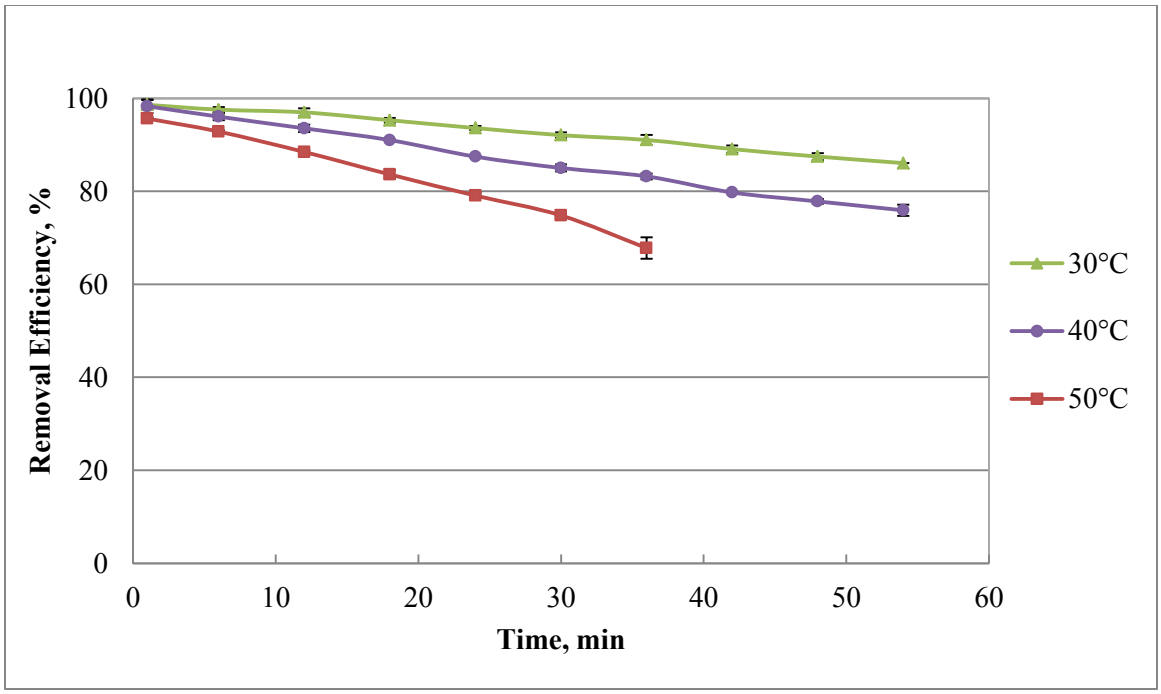

Figure 3.14 Effect of solvent temperature on the removal efficiency of ethylbenzene at a bed height of 1.1 m, solvent flow rate of 53 ml/min, and using soybean oil as a solvent

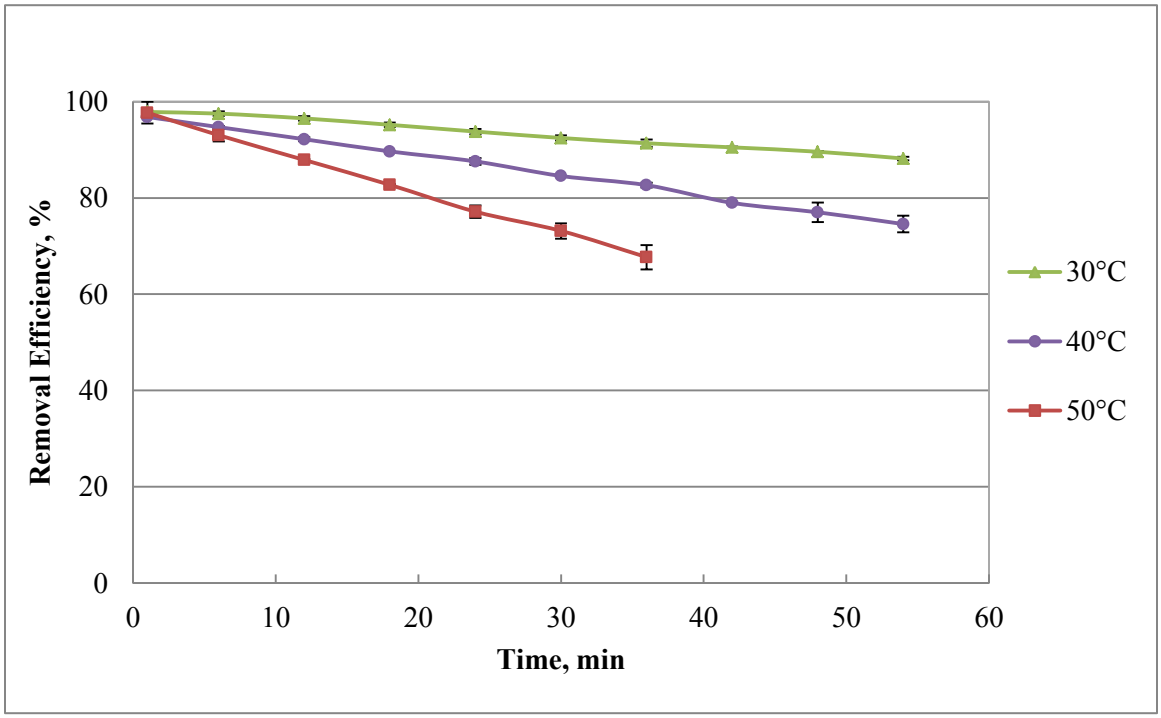

Figure 3.15 Effect of solvent temperature on the removal efficiency of ethylbenzene at a bed height of 1.1 m, solvent flow rate of 73 ml/min, and using soybean oil as a solvent

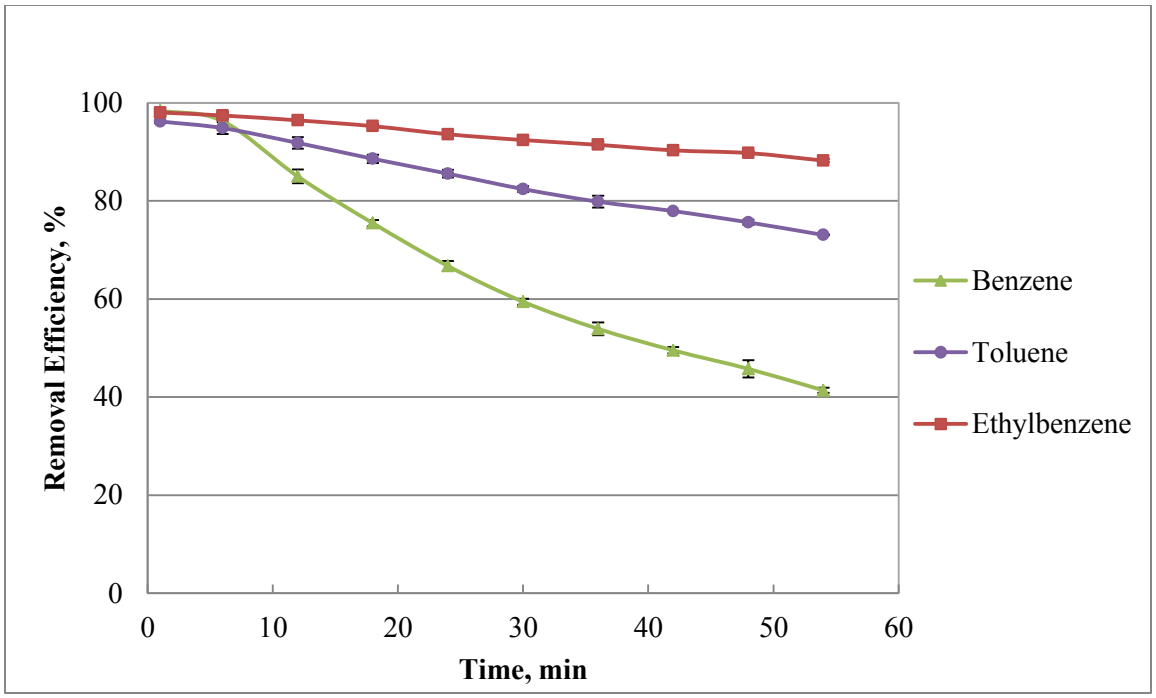

Figure 3.16 Removal efficiency of benzene, toluene, and ethylbenzene at a bed height of 1.1 m, solvent temperature of 30°C, solvent flow rate of 73 ml/min and using soybean oil as a solvent

Table 3.5 Statistical analysis of the effect of solvent temperature on benzene, toluene, and ethylbenzene removal efficiency for the given bed height and solvent flow rate

Bed height	Flow rate	Temp.	Benzene slope		Toluene slope		Ethylbenzene slope	
m	ml/min	°C	Mean*	S.E.**	Mean*	S.E.**	Mean*	S.E.**
0.5	53	30	-1.071 a	0.023	-0.462 a	0.003	-0.184 a	0.002
0.5	53	40	-1.193 a	0.001	-0.712 b	0.024	-0.340 b	0.015
0.5	53	50	-1.247 a	0.075	-1.051 c	0.043	-0.616 c	0.025
0.5	63	30	-1.131 a	0.065	-0.510 a	0.028	-0.216 a	0.011
0.5	63	40	-1.255 a	0.036	-0.751 b	0.032	-0.351 b	0.022
0.5	63	50	-1.297 a	0.085	-1.134 c	0.013	-0.671 c	0.026
0.5	73	30	-1.150 a	0.003	-0.506 a	0.009	-0.220 a	0.009
0.5	73	40	-1.254 a	0.005	-0.766 b	0.011	-0.365 b	0.017
0.5	73	50	-1.247 a	0.053	-0.989 c	0.069	-0.546 c	0.040
0.8	53	30	-1.145 a	0.005	-0.445 a	0.004	-0.184 a	0.000
0.8	53	40	-1.442 b	0.046	-0.799 b	0.031	-0.420 b	0.016
0.8	53	50	-1.574 b	0.021	-1.158 c	0.001	-0.704 c	0.012
0.8	63	30	-1.113 a	0.041	-0.436 a	0.009	-0.183 a	0.008
0.8	63	40	-1.448 b	0.109	-0.810 b	0.070	-0.408 b	0.047
0.8	63	50	-1.426 b	0.048	-1.075 c	0.034	-0.630 c	0.028
0.8	73	30	-1.183 a	0.027	-0.482 a	0.001	-0.209 a	0.001
0.8	73	40	-1.360 b	0.021	-0.785 b	0.013	-0.400 b	0.008
0.8	73	50	-1.479 b	0.115	-1.033 c	0.105	-0.581 c	0.060
1.1	53	30	-1.380 a	0.005	-0.542 a	0.016	-0.240 a	0.013
1.1	53	40	-1.507 a	0.046	-0.826 b	0.035	-0.432 b	0.029
1.1	53	50	-1.753 b	0.039	-1.229 c	0.032	-0.757 c	0.033
1.1	63	30	-1.259 a	0.029	-0.511 a	0.010	-0.225 a	0.005
1.1	63	40	-1.872 c	0.118	-0.975 b	0.001	-0.522 b	0.013
1.1	63	50	-1.611 b	0.062	-1.174 c	0.007	-0.732 c	0.009
1.1	73	30	-1.134 a	0.028	-0.452 a	0.012	-0.189 a	0.003
1.1	73	40	-1.480 b	0.062	-0.820 b	0.040	-0.422 b	0.023
1.1	73	50	-1.369 b	0.032	-0.861 b	0.048	-0.478 b	0.037

*Means followed by same letter within a column at the same bed height and solvent flow rate are not significantly different ($p>0.05$)

**Standard error

3.2.2 Pressure drop across the column

The effect of solvent temperature on the pressure drop across the column for two column bed heights is shown in Figures 3.17 and 3.18. For the 0.5 m packed bed height, it was observed that as the solvent temperature increased from 30 to 50°C, the pressure drop across the column decreased from 7.33 to 6.74, 8.01 to 7.27 and 8.74 to 7.68 mm of WC for the solvent flow rate of 53, 63 and 73 ml/min, respectively (Figure 3.17). The statistical analysis given in Table 3.6 showed that the solvent temperature had a highly significant (p<0.0001) effect on the pressure drop across the column for all solvent flow rates and bed heights. The reduction in the pressure drop was due to reduction in the density and viscosity of the solvent causing a reduction in the liquid holdup as the solvent temperature increased from 30 to 50°C. A statistical analysis of effect of solvent temperature on liquid holdup is shown in Table 3.8. As shown, the solvent temperature had a highly significant (p<0.01) effect on the liquid holdup for the given solvent flow rate and bed height. The void fraction of the bed increases as the liquid holdup reduces, consequently a lower frictional drop as the solvent temperature increases.

It was also observed that the reduction in the pressure drop across the column with an increase in the solvent temperature increases as the packed bed height increases (Figures 3.17 and 3.18). This occurs due to a higher liquid holdup at the higher bed height compared to a lower bed height. The higher the liquid holdup, the higher the gas-liquid contact. The higher gas-liquid contact leads to a higher frictional pressure drop across the column. Similarly, it was found that the reduction in the pressure drop across the column with an increase in the solvent temperature increases as the solvent flow rate increases. In this case, the increased liquid holdup with an increase in the solvent flow rate was again the reason for an increase in the pressure drop.

The pressure drop across the column was predicted using Stichlmair et al. (1989) and Billet & Schultes (1999) pressure drop correlations as given in the Section 2.2.6. It was observed that the predicted pressure drop using Stichlmair et al. (1989) correlation deviated a maximum of

15% from the experimental data because of two major reasons. First, Stichlmair et al. (1989) liquid holdup correlation is a function of only the liquid rate. Second, correlations were validated only for an air-water system while the present study involves an air-vegetable oil system. Conversely, Billet & Schultes (1999) liquid holdup correlation is a function of kinematic viscosity of liquid (i.e., ratio of dynamic viscosity and density) and the liquid rate. In addition, liquid holdup is a function of the hydraulic surface area (a_h) which takes in to account of deviation of flow channels and partial coverage of packing surface. Therefore, Billet & Schultes (1999) pressure drop correlation was considered to predict the pressure drop across the column. In Billet & Schultes (1999) pressure drop correlation, packing specific constants (i.e., C_h and $C_{P,0}$) are not available for 6-mm metal raschig rings. Therefore, packing specific constants were determined using experimental data of all twenty seven test conditions. Average values of C_h and C_{P0} were determined as 2.52 and 2.93, respectively. A predicted versus experimental pressure drop across the column is given in Table 3.7 and Figure 3.19. It was observed that predicted pressure drop data using the above mentioned packing specific constants showed a very good fit with the experimental data as the average deviation is 4.3% (Figure 3.19).

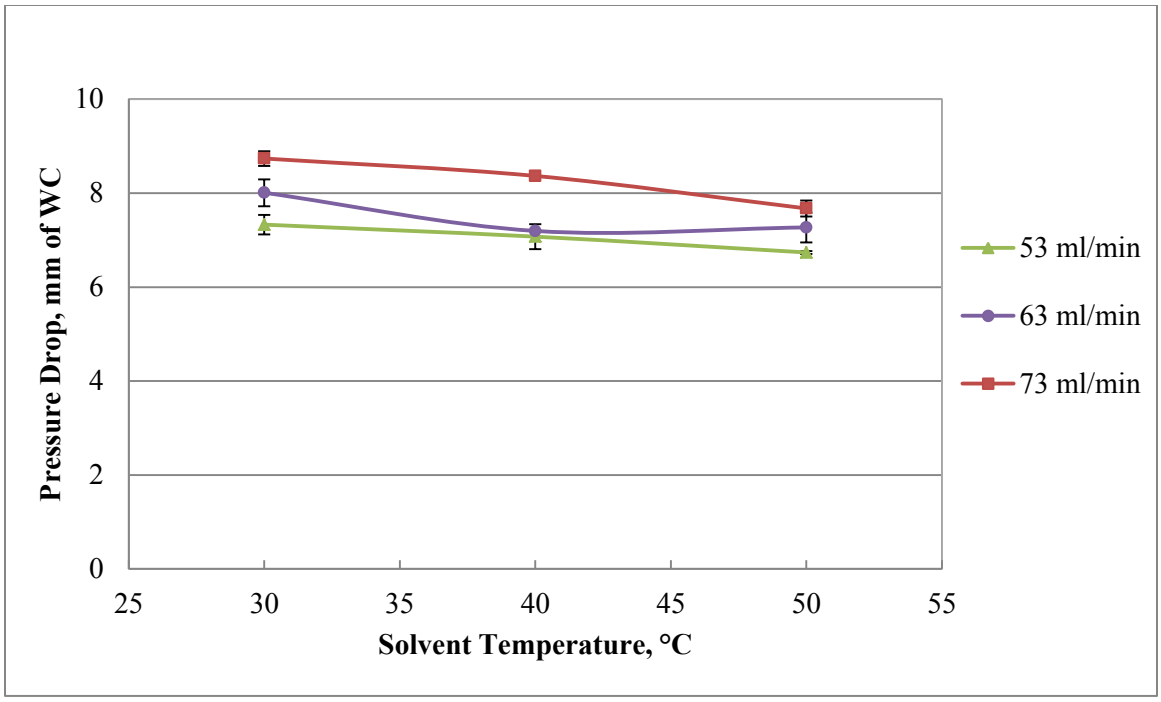

Figure 3.17 Effect of solvent temperature on the pressure drop across the column at a bed height of 0.5 m and using soybean oil as a solvent

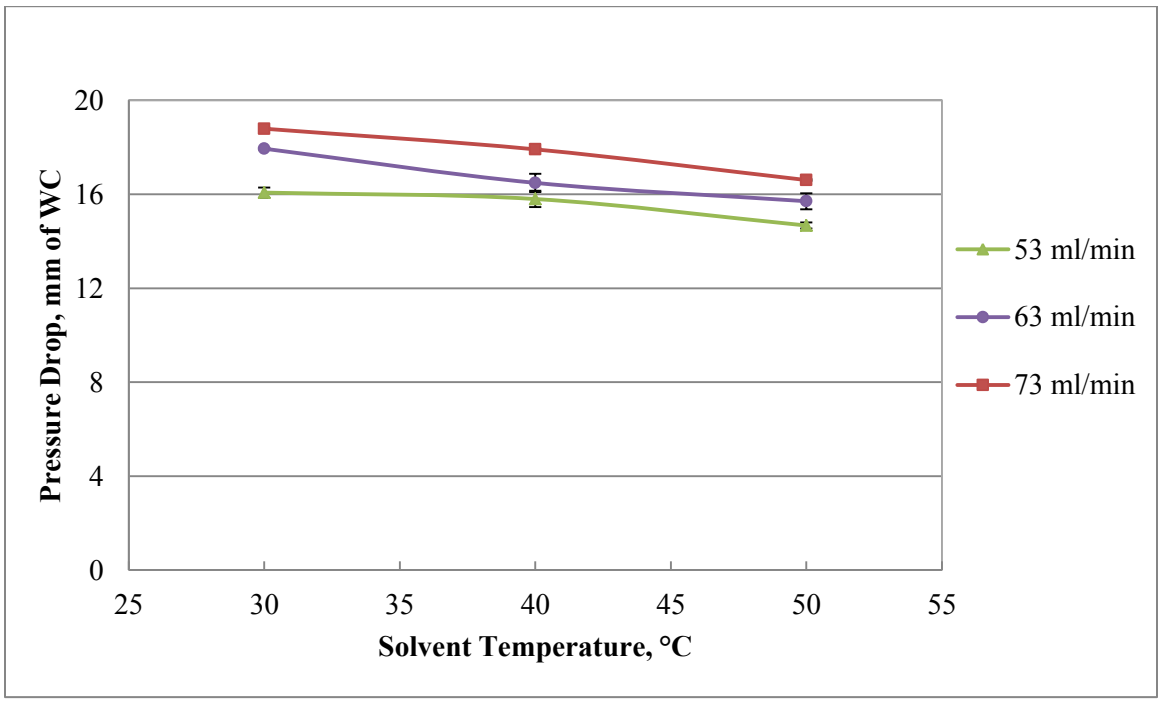

Figure 3.18 Effect of solvent temperature on the pressure drop across the column at a bed height of 1.1 m and using soybean oil as a solvent

Table 3.6 Statistical analysis of the effect of solvent temperature on pressure drop across the column for the given bed height and solvent flow rate

Bed height	Flow rate	Temperature	Pressure drop across the column, mm of WC	
m	ml/min	°C	Mean*	S.E.**
0.5	53	30	7.330 a	0.148
0.5	53	40	7.074 ab	0.187
0.5	53	50	6.737 a	0.022
0.5	63	30	8.009 a	0.202
0.5	63	40	7.196 b	0.004
0.5	63	50	7.046 b	
0.5	73	30	8.738 a	0.111
0.5	73	40	8.367 a	
0.5	73	50	7.675 b	0.119
0.8	53	30	12.381 a	0.012
0.8	53	40	11.611 b	0.111
0.8	53	50	10.853 c	0.019
0.8	63	30	13.377 a	0.242
0.8	63	40	12.572 b	0.175
0.8	63	50	11.442 c	0.008
0.8	73	30	15.123 a	0.041
0.8	73	40	13.717 b	0.264
0.8	73	50	12.338 c	0.047
1.1	53	30	16.072 a	0.155
1.1	53	40	15.798 a	0.247
1.1	53	50	14.670 b	0.093
1.1	63	30	17.942 a	0.025
1.1	63	40	16.486 b	0.277
1.1	63	50	15.706 c	0.239
1.1	73	30	18.792 a	0.029
1.1	73	40	17.913 b	0.025
1.1	73	50	16.606 c	0.022

*Means followed by same letter within a column at the same bed height and solvent flow rate are not significantly different ($p>0.05$)

**Standard error

Table 3.7 Model prediction versus experimental results of the pressure drop across the column for the given bed height, solvent temperature, and solvent flow rate

Bed height m	Temperature °C	Flow rate ml/min	Pressure drop, mm of WC: Billet and Schultes model prediction	Pressure drop, mm of WC: Experimental data	S.E.*
0.5	30	53	8.1	7.3	0.21
0.5	30	63	8.3	8.0	0.29
0.5	30	73	8.5	8.7	0.16
0.5	40	53	7.4	7.1	0.27
0.5	40	63	7.6	7.2	-
0.5	40	73	7.8	8.4	-
0.5	50	53	7.0	6.7	0.03
0.5	50	63	7.1	7.0	-
0.5	50	73	7.2	7.7	0.2
0.8	30	53	12.9	12.4	0.02
0.8	30	63	13.3	13.4	0.34
0.8	30	73	13.6	15.1	0.06
0.8	40	53	11.9	11.6	0.16
0.8	40	63	12.2	12.6	0.25
0.8	40	73	12.4	13.7	0.37
0.8	50	53	11.2	10.9	0.03
0.8	50	63	11.4	11.4	0.01
0.8	50	73	11.6	12.3	0.07
1.1	30	53	17.7	16.1	0.22
1.1	30	63	18.2	17.9	0.04
1.1	30	73	18.7	18.8	0.04
1.1	40	53	16.4	15.8	0.35
1.1	40	63	16.7	16.5	0.39
1.1	40	73	17.1	17.9	0.04
1.1	50	53	15.3	14.7	0.13
1.1	50	63	15.6	15.7	0.34
1.1	50	73	15.9	16.6	0.03

*Standard error

Table 3.8 Statistical analysis of the effect of solvent temperature on liquid holdup for the given bed height and solvent flow rate

Bed height	Flow rate	Temperature	Liquid holdup, ml	
m	ml/min	°C	Mean*	S.E.**
0.5	53	30	145 a	15
0.5	53	40	135 a	5
0.5	53	50	110 b	10
0.5	63	30	167 a	12
0.5	63	40	140 b	0
0.5	63	50	120 b	10
0.5	73	30	190 a	10
0.5	73	40	165 b	5
0.5	73	50	135 c	5
0.8	53	30	270 a	10
0.8	53	40	240 b	0
0.8	53	50	215 c	5
0.8	63	30	290 a	0
0.8	63	40	260 b	0
0.8	63	50	225 c	5
0.8	73	30	315 a	5
0.8	73	40	280 b	0
0.8	73	50	242 c	2
1.1	53	30	385 a	5
1.1	53	40	360 b	10
1.1	53	50	330 c	0
1.1	63	30	425 a	5
1.1	63	40	375 b	15
1.1	63	50	345 c	5
1.1	73	30	455 a	5
1.1	73	40	390 b	20
1.1	73	50	360 c	10

*Means followed by same letter within a column at the same bed height and solvent flow rate are not significantly different (p>0.05)

**Standard error

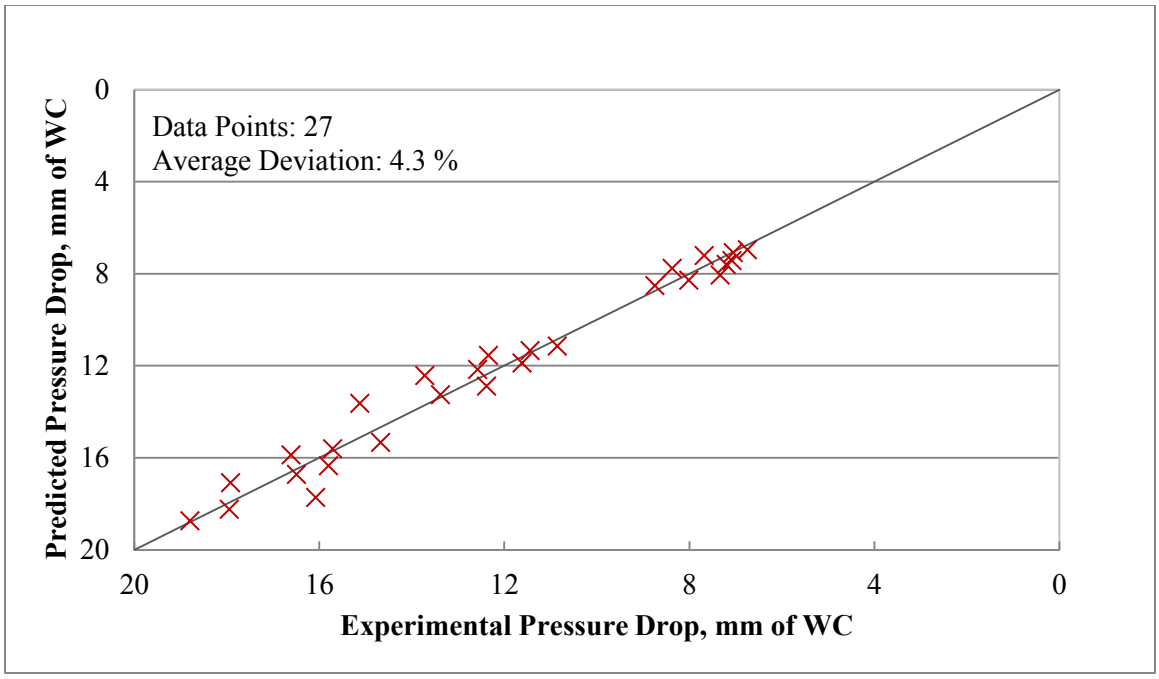

Figure 3.19 Experimental versus predicted pressure drop

3.3 Effect of bed height

3.3.1 Removal efficiency of model tar compounds

The packed bed height had a significant effect on the removal efficiency of the model tar compounds. The removal efficiencies of benzene, toluene and ethylbenzene with time and as a function of the bed height are shown in Figures 3.20-3.26. As shown in Figure 3.20, as the bed height increased from 0.5 to 1.1 m, the removal efficiency of benzene increased from 90% to over 96% at the start of the experiment. The trend of increasing the removal efficiency of benzene as the bed height increases was observed until 24-30 minutes of operation at which time the trend reversed due to saturation of solvent that occurs earlier at the highest bed height (Figure 3.20). The tar removal efficiency increased with an increase in packed bed height because the mass transfer area of model tar compounds is directly proportional to the bed height for the given packing materials. In addition, an increased bed height also increases liquid holdup which reduces a cross sectional area of the column which in turn increases gas and liquid velocity and, as a result, mass transfer of tar compounds increases. In addition, theoretical number of stages also

increases as the bed height increases which has a significant impact on the absorption of model tar compounds.

An increase in the removal efficiency decreases as the packed bed height increased from 0.8 to 1.1 m compared to bed height increased from 0.5 to 0.8 m (Figures 3.20-3.22). This occurs due to reduction in the gradient for the mass transfer of model tar compounds for the packed bed height above 0.8 m at the solvent temperature of 50°C and solvent flow rates of 53, 63 and 73 ml/min (Figures 3.20-3.22). An increase in packed bed height beyond 1.1 m will increase the cost of packing materials and the pressure drop across the column with marginal improvement in the removal efficiency of model tar compounds. The effective bed height is defined as the bed height beyond which an increase in bed height has a minimal effect on the removal efficiency. In this study, the effective bed height was determined at 1.1 m.

It was also observed that an increase in the removal efficiency of benzene with an increase in the packed bed height reduces as the solvent flow rate increased from 53 ml/min to 73 ml/min (Figures 3.21 and 3.22) due mainly to a decrease in the theoretical number of stages as the solvent flow rate increases. For toluene and ethylbenzene, it was observed that the difference in an increase of removal efficiencies with bed height is far less compared to benzene due to low equilibrium ratio (Figures 3.23-3.26) and therefore it requires much fewer (less than four) theoretical stages than benzene.

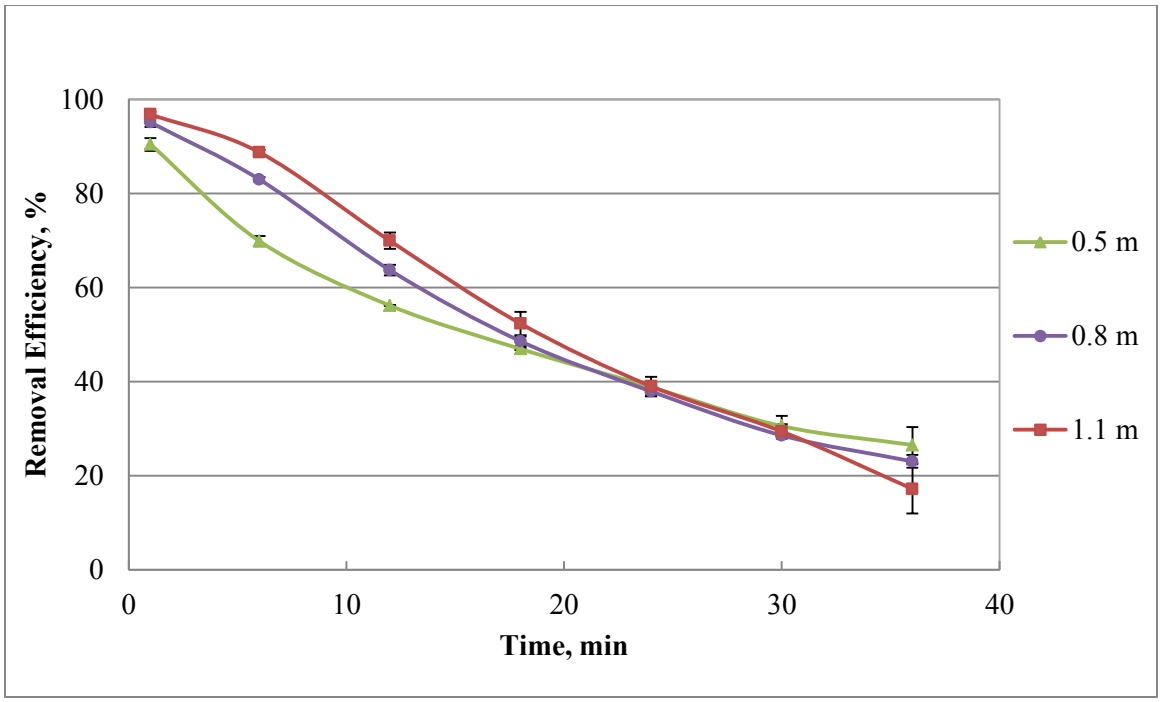

Figure 3.20 Effect of bed height on the removal efficiency of benzene at a solvent temperature of 50°C, solvent flow rate of 53 ml/min, and using soybean oil as a solvent

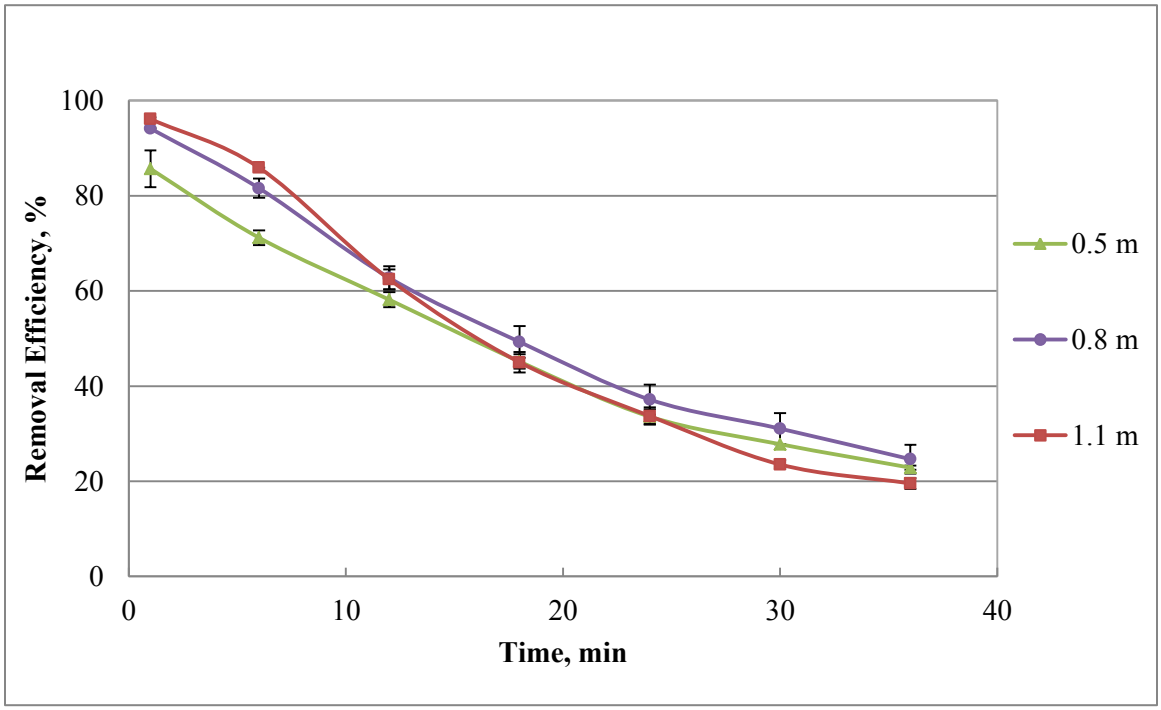

Figure 3.21 Effect of bed height on the removal efficiency of benzene at a solvent temperature of 50°C, solvent flow rate of 63 ml/min, and using soybean oil as a solvent

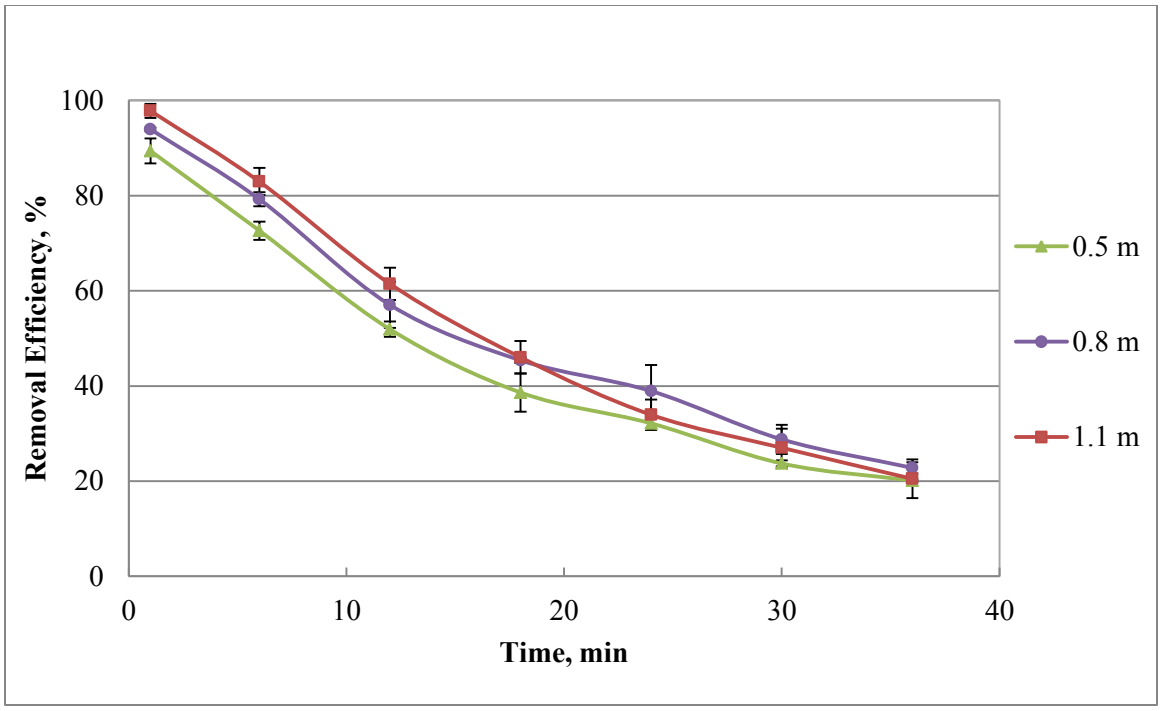

Figure 3.22 Effect of bed height on the removal efficiency of benzene at a solvent temperature of 50°C, solvent flow rate of 73 ml/min, and using soybean oil as a solvent

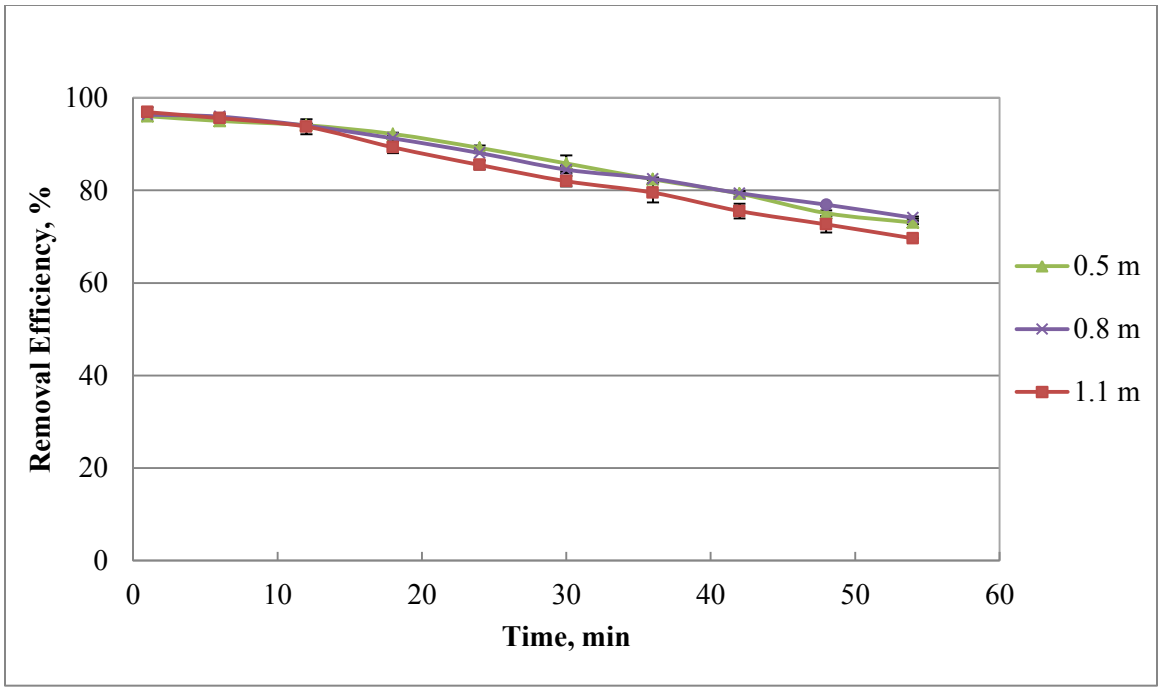

Figure 3.23 Effect of bed height on the removal efficiency of toluene at a solvent temperature of 30°C, solvent flow rate of 53 ml/min, and using soybean oil as a solvent

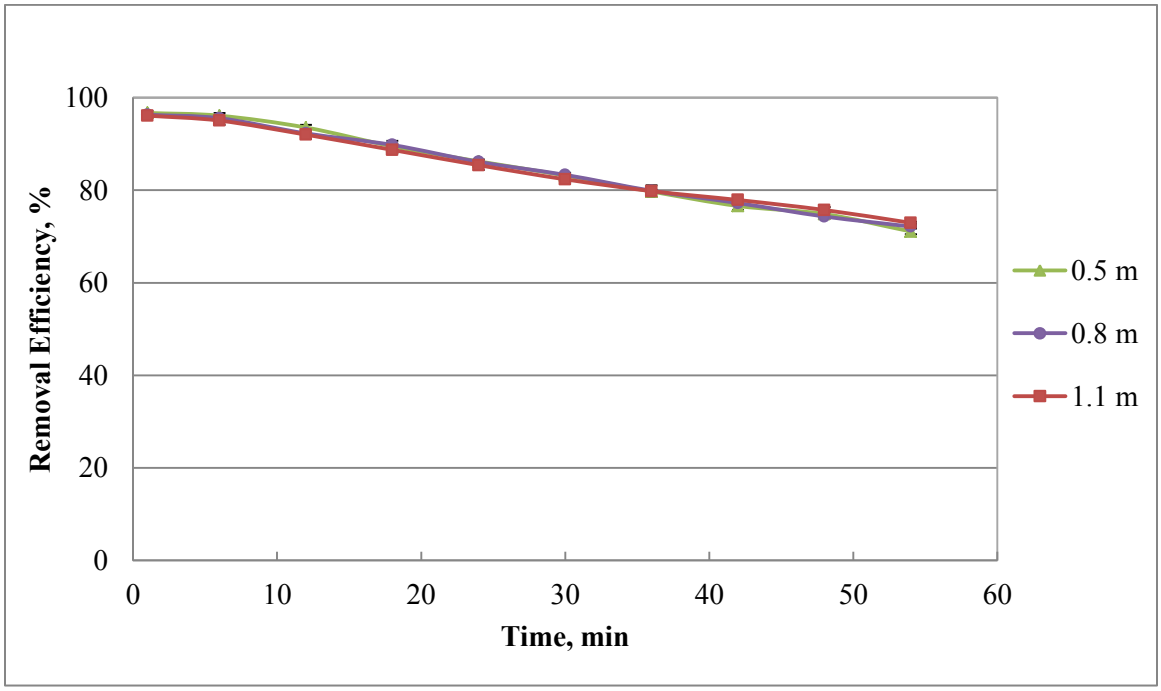

Figure 3.24 Effect of bed height on the removal efficiency of toluene at a solvent temperature of 30°C, solvent flow rate of 73 ml/min, and using soybean oil as a solvent

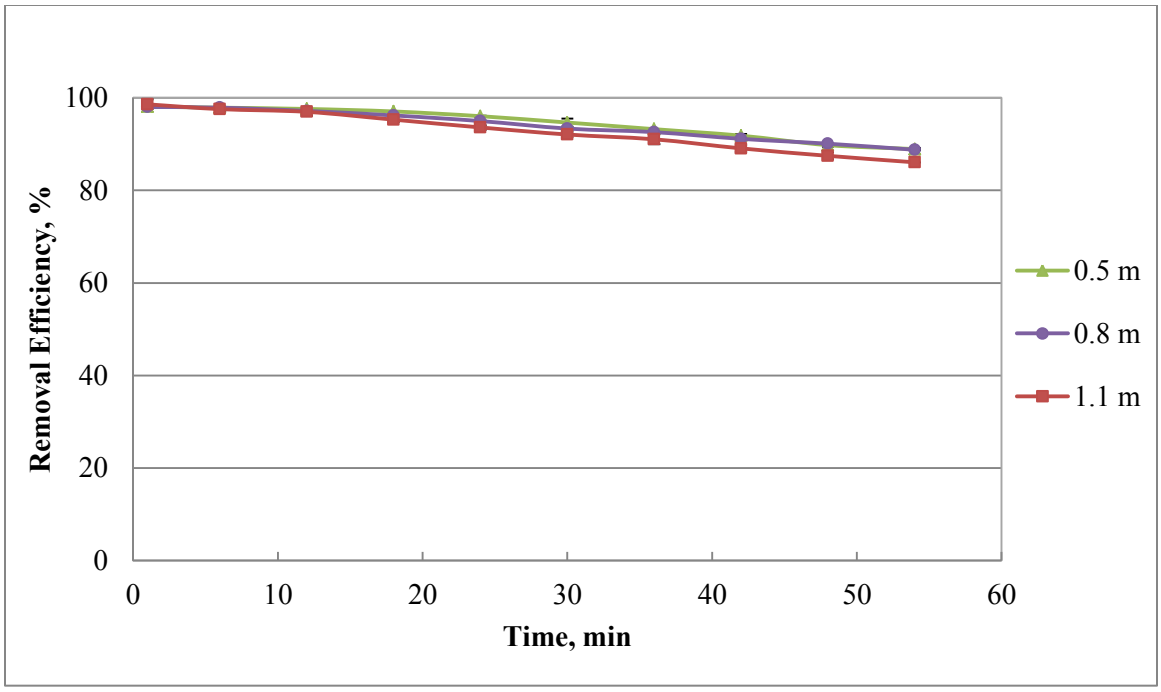

Figure 3.25 Effect of bed height on the removal efficiency of ethylbenzene at a solvent temperature of 30°C, solvent flow rate of 53 ml/min, and using soybean oil as a solvent

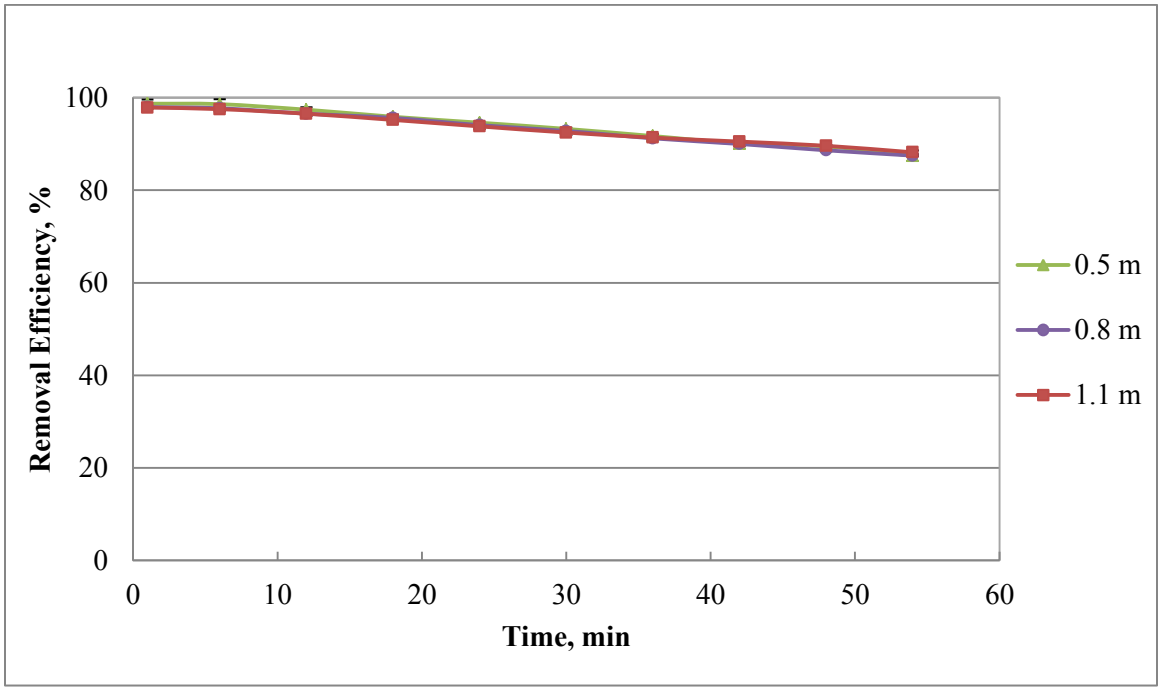

Figure 3.26 Effect of bed height on the removal efficiency of ethylbenzene at a solvent temperature of 30°C, solvent flow rate of 73 ml/min, and using soybean oil as a solvent

The packed bed height highly significantly ($p < 0.0001$) effected benzene removal efficiency at the solvent temperatures of 40 and 50°C and at solvent flow rates of 53, 63 and 73 ml/min for each solvent temperature (Table 3.9). The effect of bed height was not significant at the lowest solvent temperature of 30°C and at the higher solvent flow rates of 63 and 73 ml/min. This occurs because at low solvent temperature and high solvent flow rates the driving force for the mass transfer is the maximum, resulting in the higher absorption efficiency. For toluene, the effect of bed height is significant only at the solvent temperature of 40°C and solvent flow rate of 63 ml/min and at solvent temperature of 50°C and solvent flow rate of 73 ml/min. In case of ethylbenzene, the effect of bed height is highly significant at the highest solvent temperature of 50°C and all solvent flow rates (53, 63 and 73 ml/min) and at the solvent temperature of 40°C and solvent flow rates of 53 and 63 ml/min (Table 3.9). It was expected that the effect of bed height would not be significant for the toluene and ethylbenzene as the driving force for the ethylbenzene and toluene is much higher than that of benzene. However, the experimental results showed a significant effect for some conditions due mainly to contamination remaining after a previous experimental run. In addition, the malfunction of temperature controller at 50^{o}C could be the other reason.

Table 3.9 Statistical analysis of the effect of packed bed height on benzene, toluene, and ethylbenzene removal efficiency for the given solvent temperature and flow rate

Temp.	Flow rate	Bed height	Benzene slope		Toluene slope		Ethylbenzene slope	
°C	ml/min	m	Mean*	S.E.**	Mean*	S.E.**	Mean*	S.E.**
30	53	0.5	-1.071 a	0.023	-0.462 a	0.003	-0.184 a	0.002
30	53	0.8	-1.145 a	0.005	-0.445 a	0.004	-0.184 a	0.000
30	53	1.1	-1.380 b	0.005	-0.542 a	0.016	-0.240 a	0.013
30	63	0.5	-1.131 a	0.065	-0.510 a	0.028	-0.216 a	0.011
30	63	0.8	-1.113 a	0.041	-0.436 a	0.009	-0.183 a	0.008
30	63	1.1	-1.259 a	0.029	-0.511 a	0.010	-0.225 a	0.005
30	73	0.5	-1.150 a	0.003	-0.506 a	0.009	-0.220 a	0.009
30	73	0.8	-1.183 a	0.027	-0.482 a	0.001	-0.209 a	0.001
30	73	1.1	-1.134 a	0.028	-0.452 a	0.012	-0.189 a	0.003
40	53	0.5	-1.193 a	0.001	-0.712 a	0.024	-0.340 a	0.015
40	53	0.8	-1.442 b	0.046	-0.799 a	0.031	-0.420 b	0.016
40	53	1.1	-1.507 b	0.046	-0.826 a	0.035	-0.432 b	0.029
40	63	0.5	-1.255 a	0.036	-0.751 a	0.032	-0.351 a	0.022
40	63	0.8	-1.448 b	0.109	-0.810 a	0.070	-0.408 a	0.047
40	63	1.1	-1.872 c	0.118	-0.975 b	0.001	-0.522 b	0.013
40	73	0.5	-1.254 a	0.005	-0.766 a	0.011	-0.365 a	0.017
40	73	0.8	-1.360 ab	0.021	-0.785 a	0.013	-0.400 a	0.008
40	73	1.1	-1.480 b	0.062	-0.820 a	0.040	-0.422 a	0.023
50	53	0.5	-1.247 a	0.075	-1.051 a	0.043	-0.616 a	0.025
50	53	0.8	-1.574 b	0.021	-1.158 b	0.001	-0.704 b	0.012
50	53	1.1	-1.753 c	0.039	-1.229 b	0.032	-0.757 b	0.033
50	63	0.5	-1.297 a	0.085	-1.134 a	0.013	-0.671 ab	0.026
50	63	0.8	-1.426 a	0.048	-1.075 a	0.034	-0.630 a	0.028
50	63	1.1	-1.611 b	0.062	-1.174 a	0.007	-0.732 a	0.009
50	73	0.5	-1.247 a	0.053	-0.989 b	0.069	-0.546 ab	0.040
50	73	0.8	-1.479 b	0.115	-1.033 b	0.105	-0.581 b	0.060
50	73	1.1	-1.369 a	0.032	-0.861 a	0.048	-0.478 a	0.037

*Means followed by same letter within a column at the same solvent temperature and solvent flow rate are not significantly different (p>0.05)

**Standard error

3.3.2 Pressure drop across the column

Even though the packing material provides a large interfacial area for the mass transfer of model tar compounds, it increases pressure drop across the column due to friction between fluid streams and the packing surface. For the given packings, solvent flow rate, solvent temperature and the simulated air flow rate, the pressure drop across the column increases as the bed height increases due mainly to the higher packing surface area which enhances friction between fluid streams and packing surface. A high mass transfer and a low pressure drop resulting in low energy consumption are very important for the performance of wet packed bed absorption column. The pressure drop across the column as a function of bed height for two solvent temperatures is shown in Figure 3.27. For the solvent temperature of 30°C, as the bed height increased from 0.5 to 1.1 m the pressure drop across the column increased by over 100% from 7.33 to 16.07, 8.01 to 17.94 and 8.74 to 18.79 mm of WC for the solvent flow rate of 53, 63, and 73 ml/min, respectively (Figure 3.27).

A statistical analysis of the effect of bed height on the pressure drop across the column is given in Table 3.10. Bed height had a highly significant (p<0.0001) effect on the pressure drop across the column for all solvent temperatures and solvent flow rates. The pressure drop across the column increased as the packed bed height increases due primarily to an increased area of the packing materials. In addition, an increase in packed bed height had a direct correlation with the liquid holdup. A statistical analysis of effect of bed height on liquid holdup is shown in Table 3.11. As shown, the bed height had a highly significant (p<0.01) effect on the liquid holdup for the given solvent temperature and solvent flow rate. An increase in liquid holdup with an increase in column bed height decreases the cross sectional area of the column. The reduction in the column area leads to an increase in the gas and liquid velocities which enhances the friction between fluid streams and packing surfaces and thus the pressure drop across the column increases.

An increase in the pressure drop across the column with an increase in bed height reduces as the solvent temperature increases (Figure 3.27). This occurs because of reduction in density and the viscosity of the solvent with an increase in temperature reduces liquid holdup which increases the void space of the packed column, i.e., reduction in frictional pressure drop. Conversely, an increase in the pressure drop across the column with an increase in the bed height increases as the solvent flow rate increases. This occurs due to increase in liquid holdup with an increase in liquid flow rate which greatly reduces the cross sectional area of the column, i.e., high frictional pressure drop.

A pressure drop across the bed was also predicted using Billet & Schultes (1999) pressure drop correlation and the comparison of predicted vs experimental pressure drop data are given in Table 3.7 and Figure 3.19. The differences in the predicted and experimental values are due mainly to variation in the measured liquid hold volumes as shown in Table 3.11.

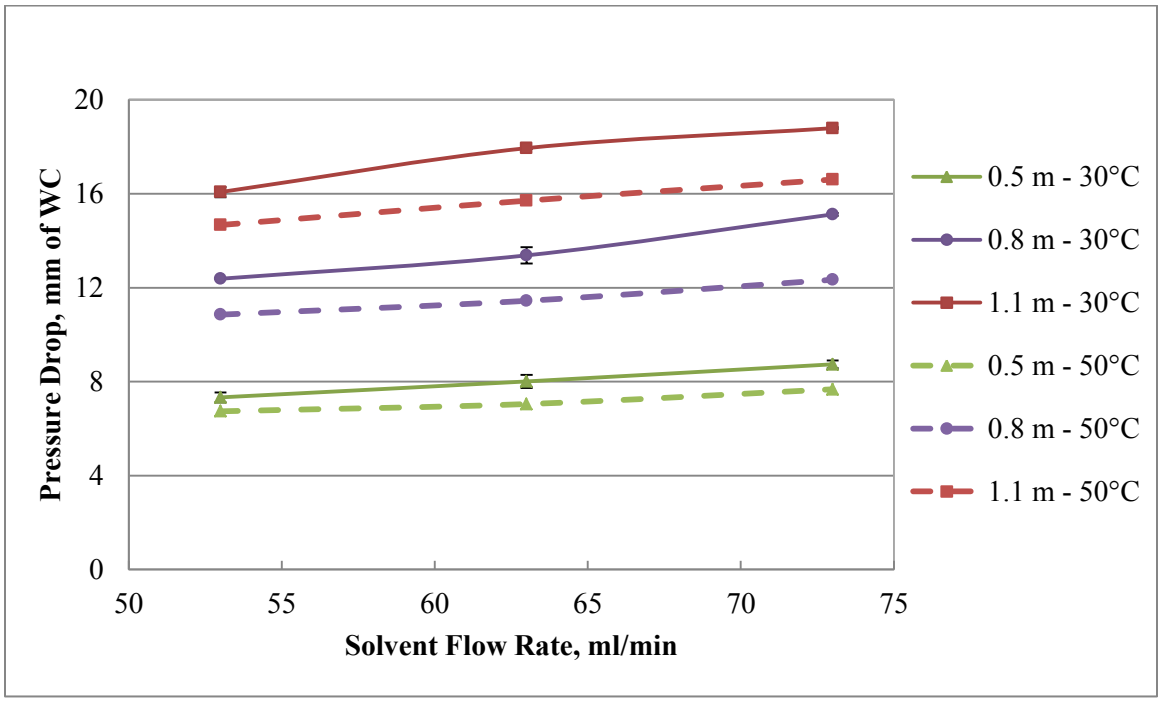

Figure 3.27 Effect of bed height on the pressure drop across the column at solvent temperatures of 30 and 50°C and using soybean oil as a solvent

Table 3.10 Statistical analysis of the effect of bed height on the pressure drop across the column for the given solvent flow rate and temperature

Flow rate	Temperature	Bed height	Pressure drop across the column, mm of W.C.	
ml/min	°C	m	Mean*	S.E.**
53	30	0.5	7.330 a	0.148
53	30	0.8	12.381 b	0.013
53	30	1.1	16.072 c	0.156
53	40	0.5	7.074 a	0.187
53	40	0.8	11.611 b	0.111
53	40	1.1	15.798 c	0.247
53	50	0.5	6.737 a	0.022
53	50	0.8	10.853 b	0.019
53	50	1.1	14.670 c	0.094
63	30	0.5	8.009 a	0.202
63	30	0.8	13.377 b	0.243
63	30	1.1	17.942 c	0.026
63	40	0.5	7.196 a	0.004
63	40	0.8	12.572 b	0.175
63	40	1.1	16.486 c	0.277
63	50	0.5	7.046 a	
63	50	0.8	11.442 b	0.008
63	50	1.1	15.706 c	0.240
73	30	0.5	8.738 a	0.112
73	30	0.8	15.123 b	0.042
73	30	1.1	18.792 c	0.030
73	40	0.5	8.367 a	
73	40	0.8	13.717 b	0.265
73	40	1.1	17.913 c	0.025
73	50	0.5	7.675 a	0.120
73	50	0.8	12.338 b	0.048
73	50	1.1	16.606 c	0.022

*Means followed by same letter within a column at the same solvent temperature and solvent flow rate are not significantly different ($p>0.05$)

**Standard error

Table 3.11 Statistical analysis of the effect of bed height on the liquid holdup for the given solvent flow rate and temperature

Flow rate	Temperature	Bed height	Liquid holdup, ml	
ml/min	°C	m	Mean*	S.E.**
53	30	0.5	145 a	15
53	30	0.8	270 b	10
53	30	1.1	385 c	5
53	40	0.5	135 a	5
53	40	0.8	240 b	0
53	40	1.1	360 c	10
53	50	0.5	110 a	10
53	50	0.8	215 b	5
53	50	1.1	330 c	0
63	30	0.5	167 a	12
63	30	0.8	290 b	0
63	30	1.1	425 c	5
63	40	0.5	140 a	0
63	40	0.8	260 b	0
63	40	1.1	375 c	15
63	50	0.5	120 a	10
63	50	0.8	225 b	5
63	50	1.1	345 c	5
73	30	0.5	190 a	10
73	30	0.8	315 b	5
73	30	1.1	455 c	5
73	40	0.5	165 a	5
73	40	0.8	280 b	0
73	40	1.1	390 c	20
73	50	0.5	135 a	5
73	50	0.8	242 b	2
73	50	1.1	360 c	10

*Means followed by same letter within a column at the same solvent temperature and solvent flow rate are not significantly different (p>0.05)

**Standard error

3.4 Effect of solvent flow rate

3.4.1 Removal efficiency of model tar compounds

Figures 3.28-3.33 show the response of solvent flow rates on the removal efficiencies of benzene, toluene and ethylbenzene. Solvent flow rate did not have a significant effect ($p>0.05$) on the removal efficiencies of model tar compounds of the test random packings (Table 3.12). Statistical analysis as provided in Table 3.12 disclosed that the solvent flow rates had significant ($p < 0.05$) effects on the removal efficiency of benzene only at the solvent temperature of 50°C and packed bed height of 1.1 m. This occurred due to malfunction of temperature controller at high solvent temperature. It was expected to have a significant effect of solvent flow rate on the removal efficiency because the driving force for the mass transfer of model tar compounds greatly improved as the solvent flow rate increases from 53 to 73 ml/min. However, as the solvent flow rate increases, the liquid film thickness also increases which leads to higher mass transfer resistance on the liquid side. In addition, an increase in solvent flow rate increases liquid holdup which reduces the cross sectional area of the column; thus, gas velocity increases which reduces the residence time of the gas-liquid contact. Therefore, the effect of increased solvent flow rate is balanced by increased mass transfer resistance and reduced residence time.

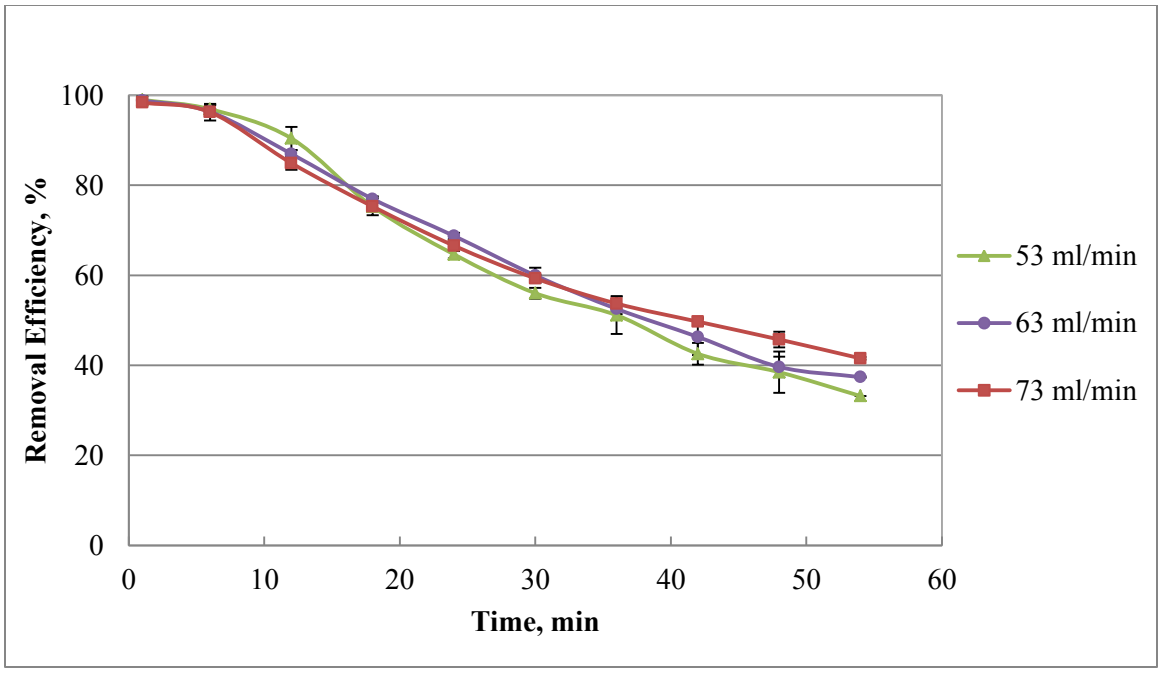

Figure 3.28 Effect of solvent flow rate on the removal efficiency of benzene at a bed height of 1.1 m, solvent temperature of 30°C, and using soybean oil as a solvent

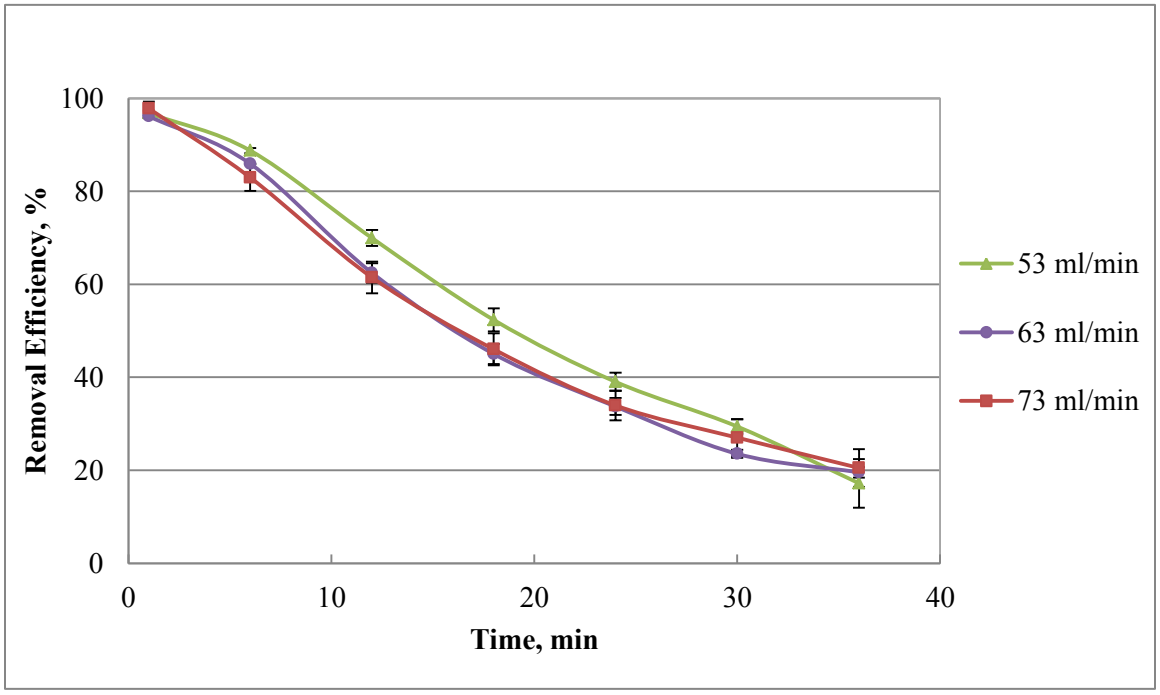

Figure 3.29 Effect of solvent flow rate on the removal efficiency of benzene at a bed height of 1.1 m, solvent temperature of 50°C, and using soybean oil as a solvent

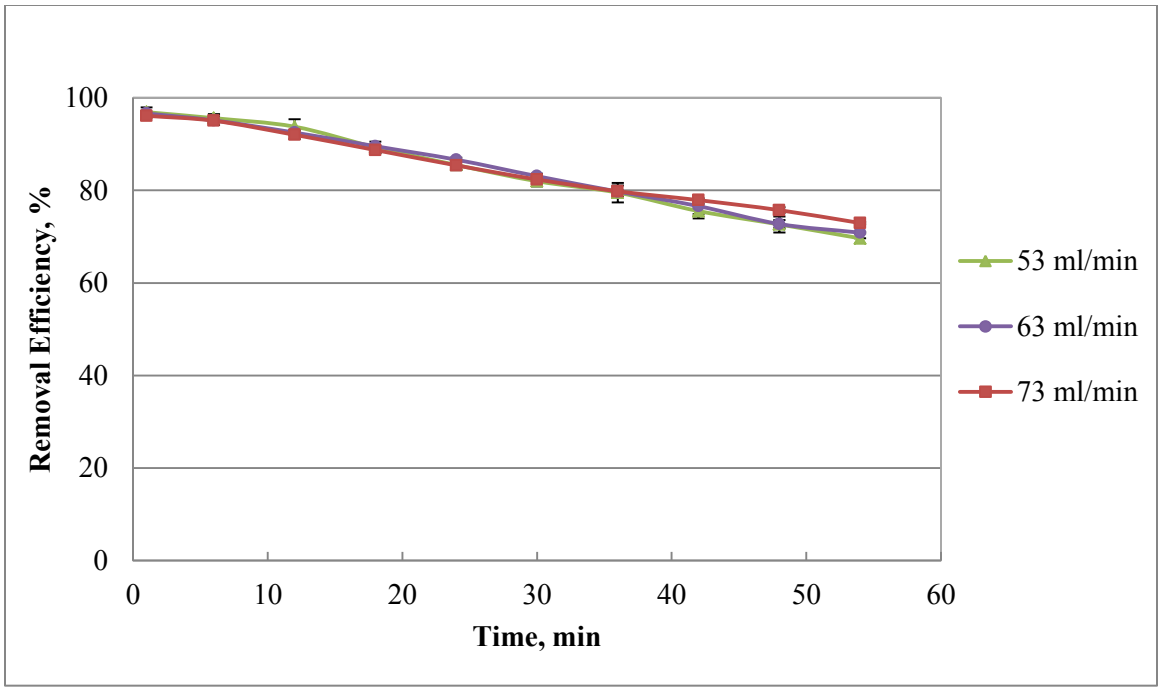

Figure 3.30 Effect of solvent flow rate on the removal efficiency of toluene at a bed height of 1.1 m, solvent temperature of 30°C, and using soybean oil as a solvent

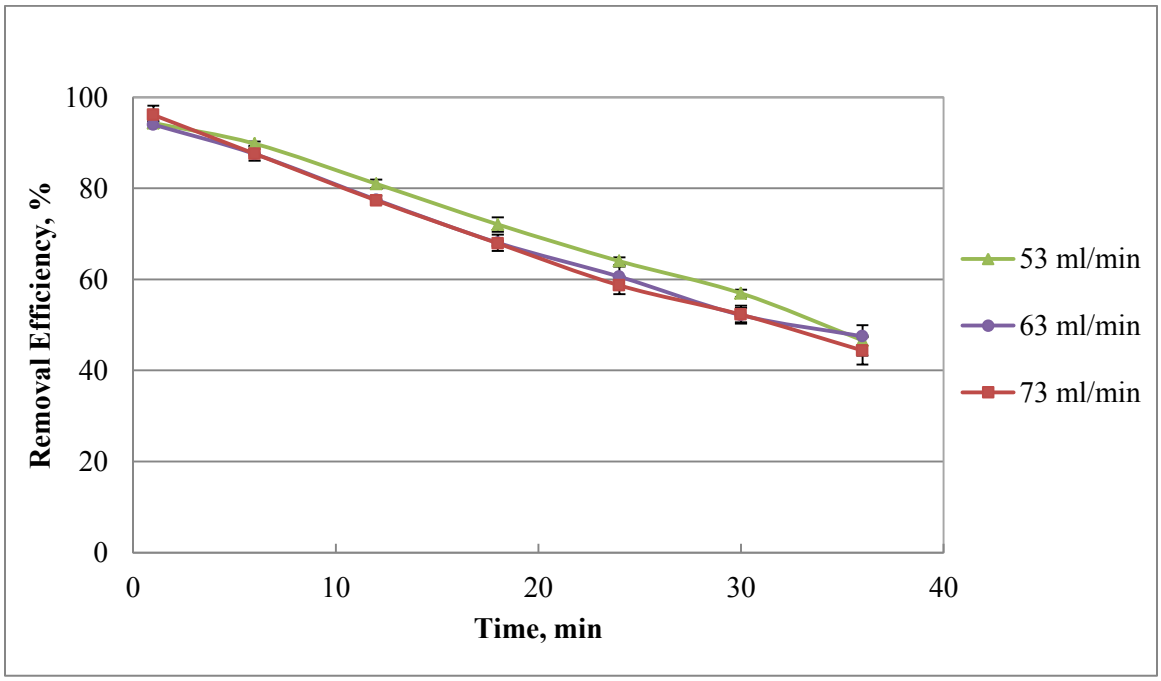

Figure 3.31 Effect of solvent flow rate on the removal efficiency of toluene at a bed height of 1.1 m, solvent temperature of 50°C, and using soybean oil as a solvent

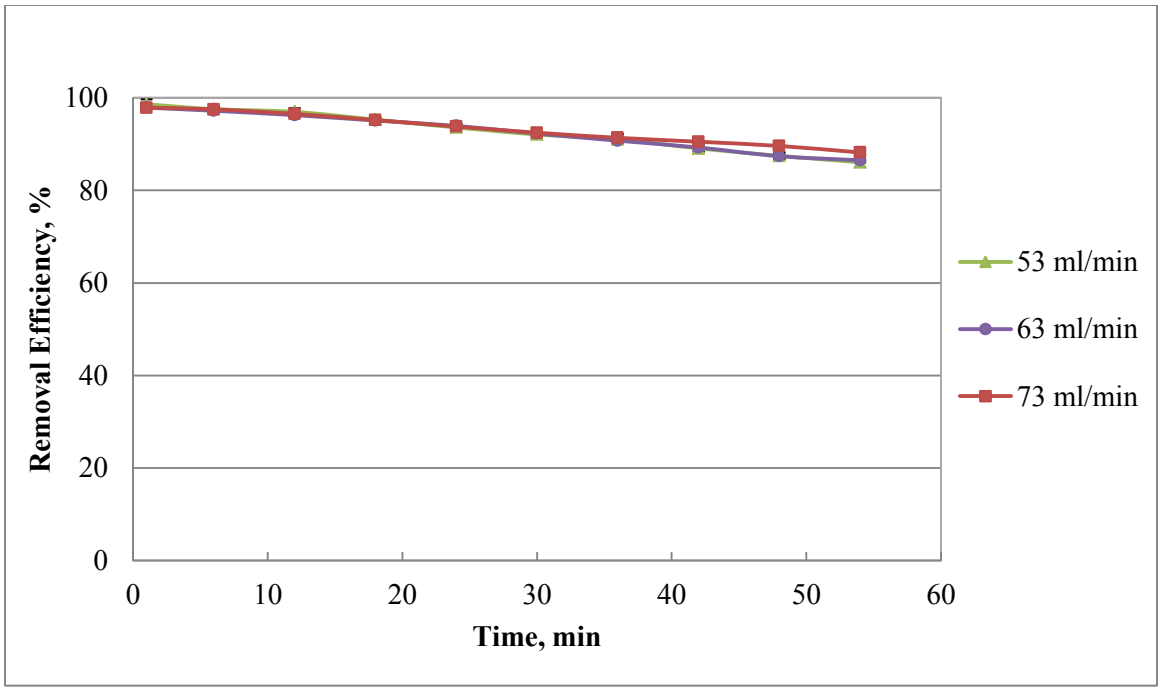

Figure 3.32 Effect of solvent flow rate on the removal efficiency of ethylbenzene at a bed height of 1.1 m, solvent temperature of 30°C, and using soybean oil as a solvent

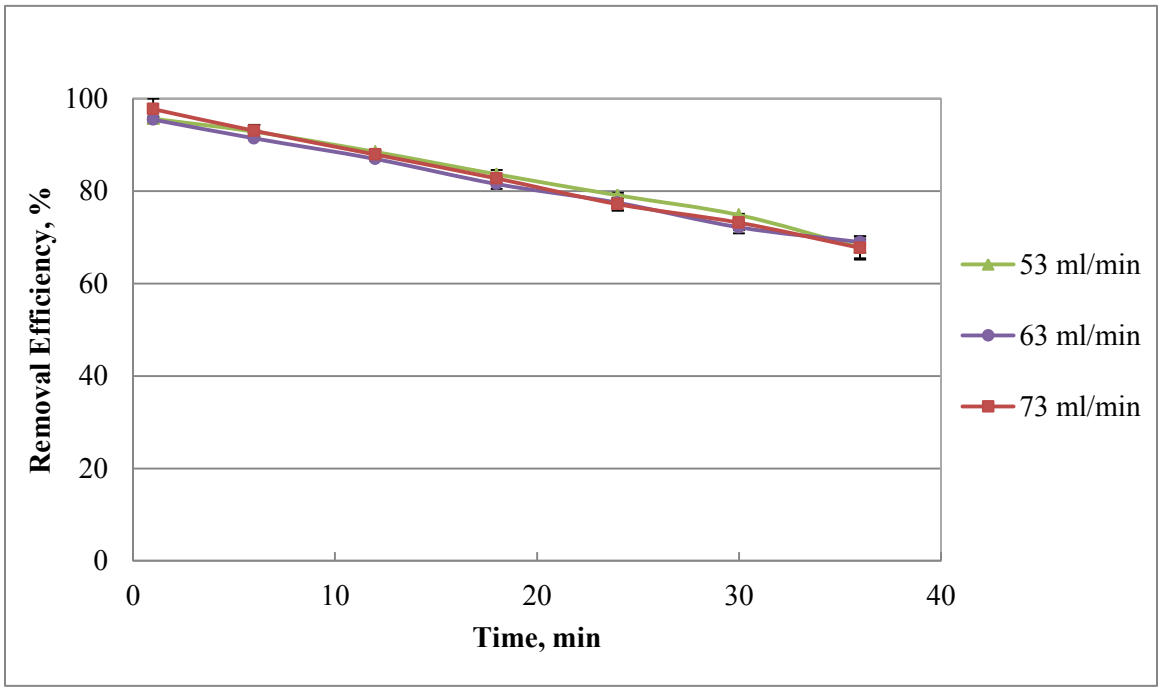

Figure 3.33 Effect of solvent flow rate on the removal efficiency of ethylbenzene at a bed height of 1.1 m, solvent temperature of 50°C, and using soybean oil as a solvent

Table 3.12 Statistical analysis of the effect of solvent flow rate on benzene, toluene and ethylbenzene removal efficiency for the given bed height and solvent temperature

Bed height	Temp.	Flow rate	Benzene slope		Toluene slope		Ethylbenzene slope	
m	°C	ml/min	Mean*	S.E.**	Mean*	S.E.**	Mean*	S.E.**
0.5	30	53	-1.071 a	0.023	-0.462 a	0.003	-0.184 a	0.002
0.5	30	63	-1.131 a	0.065	-0.510 a	0.028	-0.216 a	0.011
0.5	30	73	-1.150 a	0.003	-0.506 a	0.009	-0.220 a	0.009
0.5	40	53	-1.193 a	0.001	-0.712 a	0.024	-0.340 a	0.015
0.5	40	63	-1.255 a	0.036	-0.751 a	0.032	-0.351 a	0.022
0.5	40	73	-1.254 a	0.005	-0.766 a	0.011	-0.365 a	0.017
0.5	50	53	-1.247 a	0.075	-1.051 ab	0.043	-0.616 b	0.025
0.5	50	63	-1.297 a	0.085	-1.134 b	0.013	-0.671 b	0.026
0.5	50	73	-1.247 a	0.053	-0.989 a	0.069	-0.546 a	0.040
0.8	30	53	-1.145 a	0.005	-0.445 a	0.004	-0.184 a	0.000
0.8	30	63	-1.113 a	0.041	-0.436 a	0.009	-0.183 a	0.008
0.8	30	73	-1.183 a	0.027	-0.482 a	0.001	-0.209 a	0.001
0.8	40	53	-1.442 a	0.046	-0.799 a	0.031	-0.420 a	0.016
0.8	40	63	-1.448 a	0.109	-0.810 a	0.070	-0.408 a	0.047
0.8	40	73	-1.360 a	0.021	-0.785 a	0.013	-0.400 a	0.008
0.8	50	53	-1.574 a	0.021	-1.158 a	0.001	-0.704 b	0.012
0.8	50	63	-1.426 a	0.048	-1.075 a	0.034	-0.630 a	0.028
0.8	50	73	-1.479 a	0.011	-1.033 a	0.105	-0.581 a	0.060
1.1	30	53	-1.380 a	0.005	-0.542 a	0.016	-0.240 a	0.013
1.1	30	63	-1.259 a	0.029	-0.511 a	0.010	-0.225 a	0.005
1.1	30	73	-1.134 a	0.028	-0.452 a	0.012	-0.189 a	0.003
1.1	40	53	-1.507 a	0.046	-0.826 a	0.035	-0.432 a	0.029
1.1	40	63	-1.872 b	0.118	-0.975 b	0.001	-0.522 b	0.013
1.1	40	73	-1.480 a	0.062	-0.820 a	0.040	-0.422 a	0.023
1.1	50	53	-1.753 b	0.039	-1.229 b	0.032	-1.757 b	0.033
1.1	50	63	-1.611 b	0.062	-1.174 b	0.007	-1.732 b	0.009
1.1	50	73	-1.369 a	0.032	-0.861 a	0.048	-0.478 a	0.037

*Means followed by same letter within a column at the same bed height and solvent temperature are not significantly different (p>0.05)

**Standard error

3.4.2 Pressure drop across the column

Solvent flow rate had a significant effect on the pressure drop across the column. Figures 3.34 and 3.35 present the effects of solvent flow rates on the pressure drop across the column at the solvent temperatures of 30, 40 and 50°C for column bed heights of 0.5 and 1.1 m. As shown in Figure 3.34, as the solvent flow rate increased from 53 to 73 ml/min for the 0.5 m bed height, the pressure drop across the column increased from 7.33 to 8.74 mm of WC, 7.07 to 8.37 mm of WC and 6.74 to 7.68 mm of WC for the solvent temperature of 30, 40 and 50°C, respectively. Similar trends were observed at the higher bed heights of 0.8 and 1.1 m (Figure 3.35).

A statistical analysis of the effect of solvent flow rate on the pressure drop across the column is given in Table 3.13. The analysis showed that the solvent flow rate had a highly significant ($p<0.0001$) effect on the pressure drop across the column for all solvent temperatures and bed heights. The increased pressure drop across the column with an increase in solvent flow rate was due primarily to increased liquid holdup. A statistical analysis of effect of solvent flow rate on liquid holdup is shown in Table 3.14. As shown, the solvent flow rate had a significant ($p<0.05$) effect on the liquid holdup for the given solvent temperature except for the solvent temperature of 50°C and bed height of 0.5, 0.8 and 1.1 m. At 50°C, the effect of solvent flow rate is not significant because at higher solvent temperatures the viscosity and density of solvent reduces and the surface tension of solvent increases. As the liquid holdup increased with an increase in solvent flow rate, the cross sectional area of the column was reduced which leads to an increase in gas and liquid velocity, thus a frictional pressure drop increases as the solvent flow rate increased from 53 to 73 ml/min.

An increase in the pressure drop across column with an increase in solvent flow rate increased nearly 100% as the bed height increased from 0.5 to 1.1 m. This occurs due mainly to increased contact area of the fluid phases and packing surface, gas velocity and liquid velocity as the packed bed height increases. It was also observed that an increase in the pressure drop across

the column with an increase in solvent flow rate reduces as the solvent temperature increased from 30 to 50°C. This occurs due to reduction in the density and the viscosity of the solvent which greatly reduced a liquid holdup and consequently gas and liquid velocities reduces. A reduction in the velocities has a significant impact on the frictional pressure drop across the column.

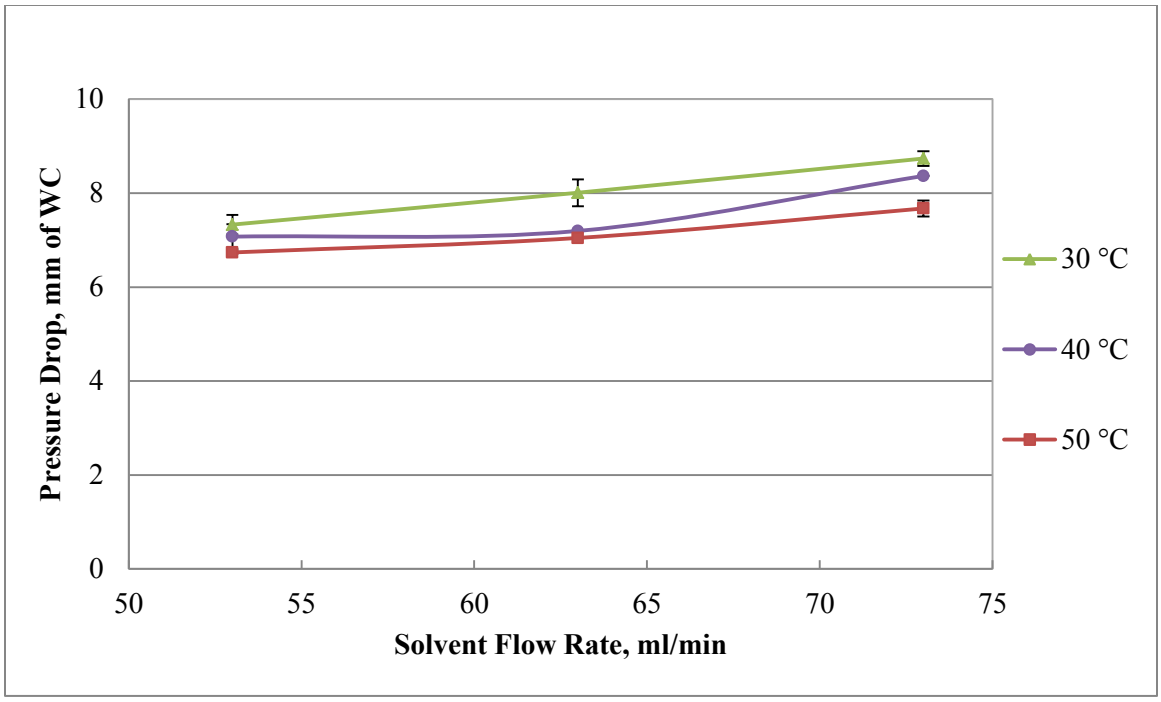

Figure 3.34 Effect of solvent flow rate on the pressure drop across the column at a bed height of 0.5 m, solvent temperatures of 30, 40, and 50°C and using soybean oil as a solvent

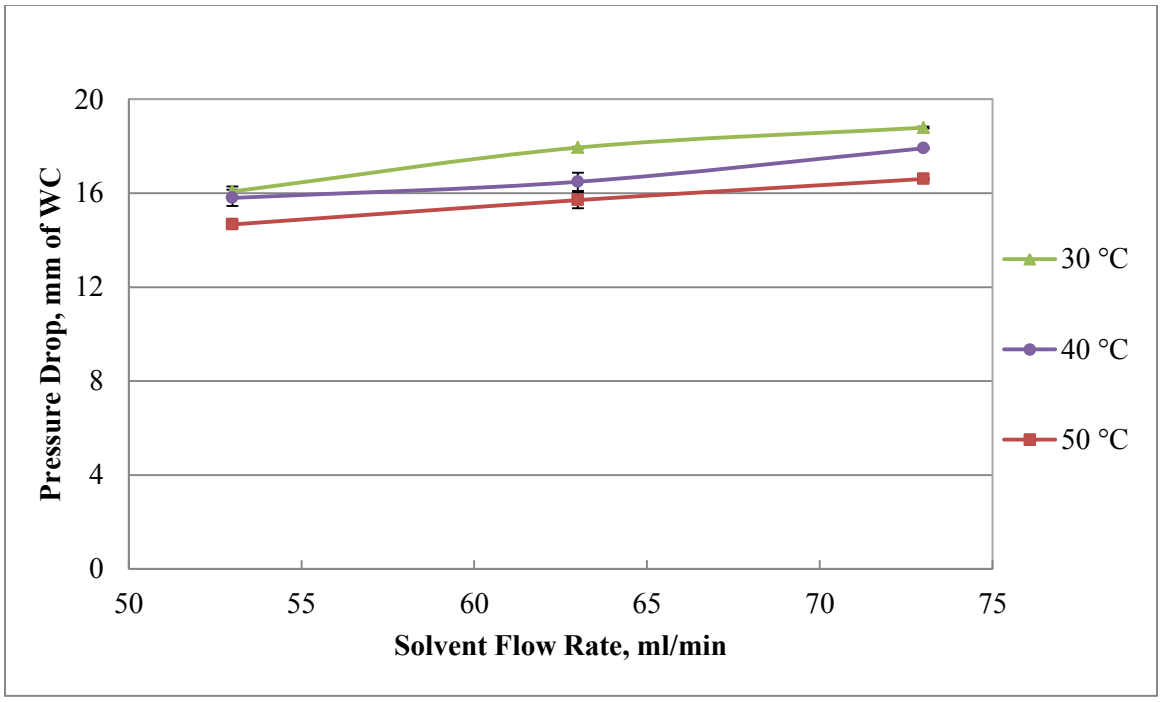

Figure 3.35 Effect of solvent flow rate on the pressure drop across the column at a bed height of 1.1 m, solvent temperatures of 30, 40, and 50°C and using soybean oil as a solvent

Table 3.13 Statistical analysis of the effect of solvent flow rate on the pressure drop across the column for the given bed height and solvent temperature

Bed height	Temperature	Flow rate	Pressure drop across the column, mm of W.C.	
m	°C	ml/min	Mean*	S.E.**
0.5	30	53	7.330 a	0.148
0.5	30	63	8.009 b	0.202
0.5	30	73	8.738 c	0.112
0.5	40	53	7.074 a	0.187
0.5	40	63	7.196 a	0.003
0.5	40	73	8.367 b	
0.5	50	53	6.737 a	0.022
0.5	50	63	7.046 a	
0.5	50	73	7.675 b	0.119
0.8	30	53	12.381 a	0.012
0.8	30	63	13.377 b	0.242
0.8	30	73	15.123 c	0.041
0.8	40	53	11.611 a	0.111
0.8	40	63	12.572 b	0.175
0.8	40	73	13.717 c	0.264
0.8	50	53	10.853 a	0.019
0.8	50	63	11.442 b	0.008
0.8	50	73	12.338 c	0.047
1.1	30	53	16.072 a	0.155
1.1	30	63	17.942 b	0.025
1.1	30	73	18.792 c	0.029
1.1	30	53	15.798 a	0.247
1.1	30	63	16.486 b	0.277
1.1	30	73	17.913 c	0.025
1.1	30	53	14.670 a	0.093
1.1	30	63	15.706 b	0.239
1.1	30	73	16.606 c	0.022

*Means followed by same letter within a column at the same bed height and solvent temperature are not significantly different ($p>0.05$)

**Standard error

Table 3.14 Statistical analysis of the effect of solvent flow rate on liquid holdup for the given bed height and solvent temperature

Bed height	Temperature	Flow rate	Liquid holdup, ml	
m	°C	ml/min	Mean	S.E.*
0.5	30	53	145 a	15
0.5	30	63	167 ab	12
0.5	30	73	190 b	10
0.5	40	53	135 a	5
0.5	40	63	140 a	0
0.5	40	73	165 b	5
0.5	50	53	110 a	10
0.5	50	63	120 a	10
0.5	50	73	135 a	5
0.8	30	53	270 a	10
0.8	30	63	290 a	0
0.8	30	73	315 b	5
0.8	40	53	240 a	0
0.8	40	63	260 ab	0
0.8	40	73	280 b	0
0.8	50	53	215 a	5
0.8	50	63	225 a	5
0.8	50	73	242 a	5
1.1	30	53	385 a	5
1.1	30	63	425 b	5
1.1	30	73	455 c	5
1.1	40	53	360 a	10
1.1	40	63	375 a	15
1.1	40	73	390 a	10
1.1	50	53	330 a	0
1.1	50	63	345 a	5
1.1	50	73	360 a	10

*Standard error

3.5 Total tar removal

The total tar removal was determined by integrating the absorption data of benzene, toluene and ethylbenzene over the time of experimental run. The liquid phase concentration of benzene, toluene and ethylbenzene at the best case (packed bed height of 1.1 m, solvent temperature of 30°C, and solvent flow rate of 73 ml/min) and the worst case (packed bed height of 0.5 m, solvent temperature of 50°C, and solvent flow rate of 53 ml/min) removal efficiencies are shown in Figures 3.36-3.38. As shown in the figures, the total absorption of benzene, toluene and ethylbenzene was the maximum at the best case because the solubility of these tar compounds was the highest due to the low solvent temperature; while the opposite effect was observed at the worst case due to the highest solvent temperature.

The saturated concentration of benzene (14.6 g/l) and toluene (21.3 g/l) in soybean oil at the solvent temperature of 30°C was determined by extrapolating the experimental data. For comparison, the saturation limit of benzene (10 g/l) and toluene (20 g/l) in sunflower oil at the temperature of 25°C were also determined using the study published by Ozturk & Yilmaz (2006) and is given in Appendix C. The deviation of the saturation limit of benzene and toluene from the published data could be due to differences in oil type, operating conditions, and/or experimental set-up.

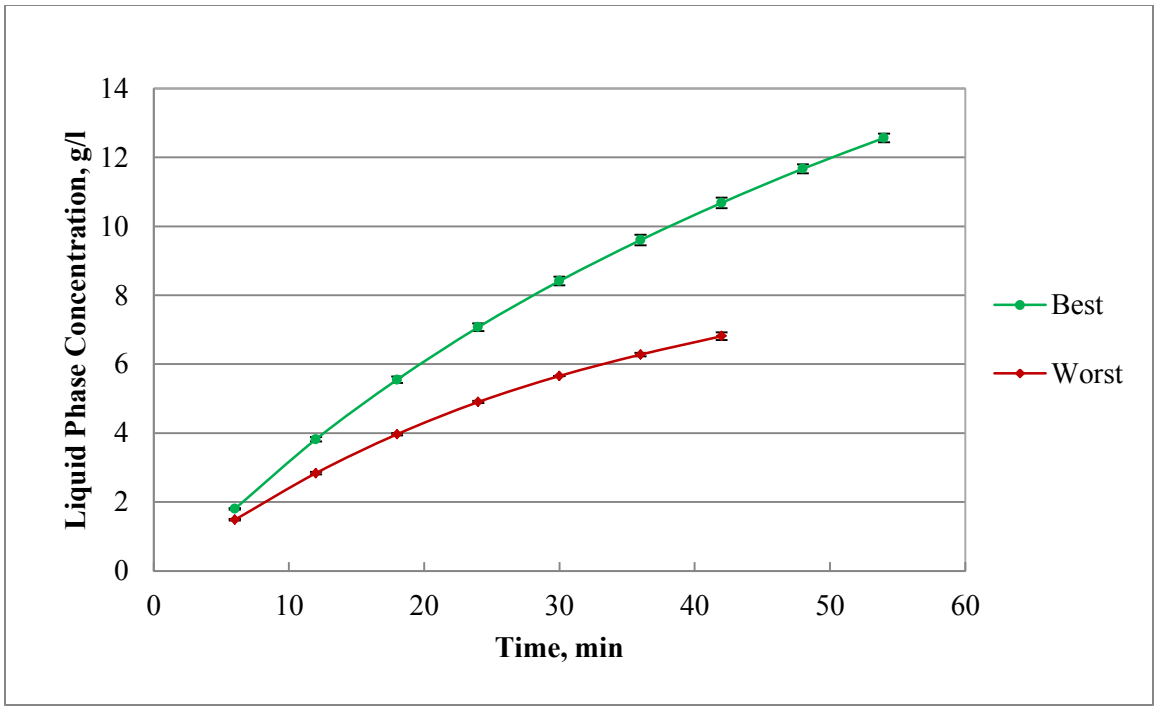

Figure 3.36 Liquid phase benzene concentration at the best and worst case removal efficiences

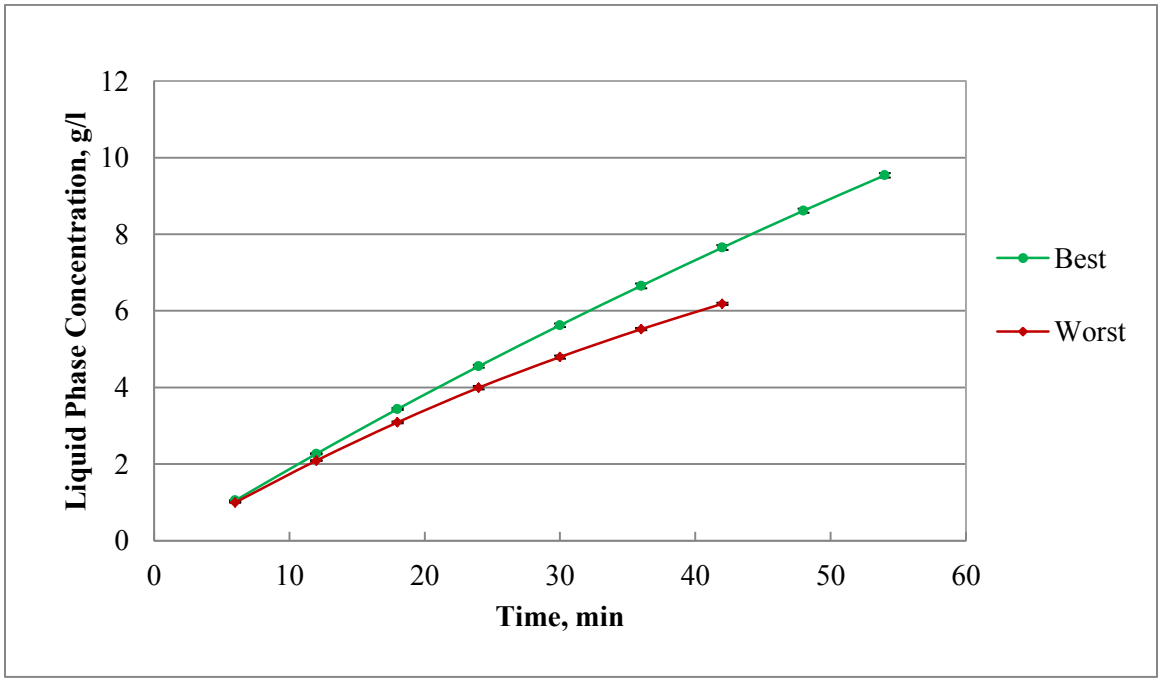

Figure 3.37 Liquid phase toluene concentration at the best and worst case removal efficiences

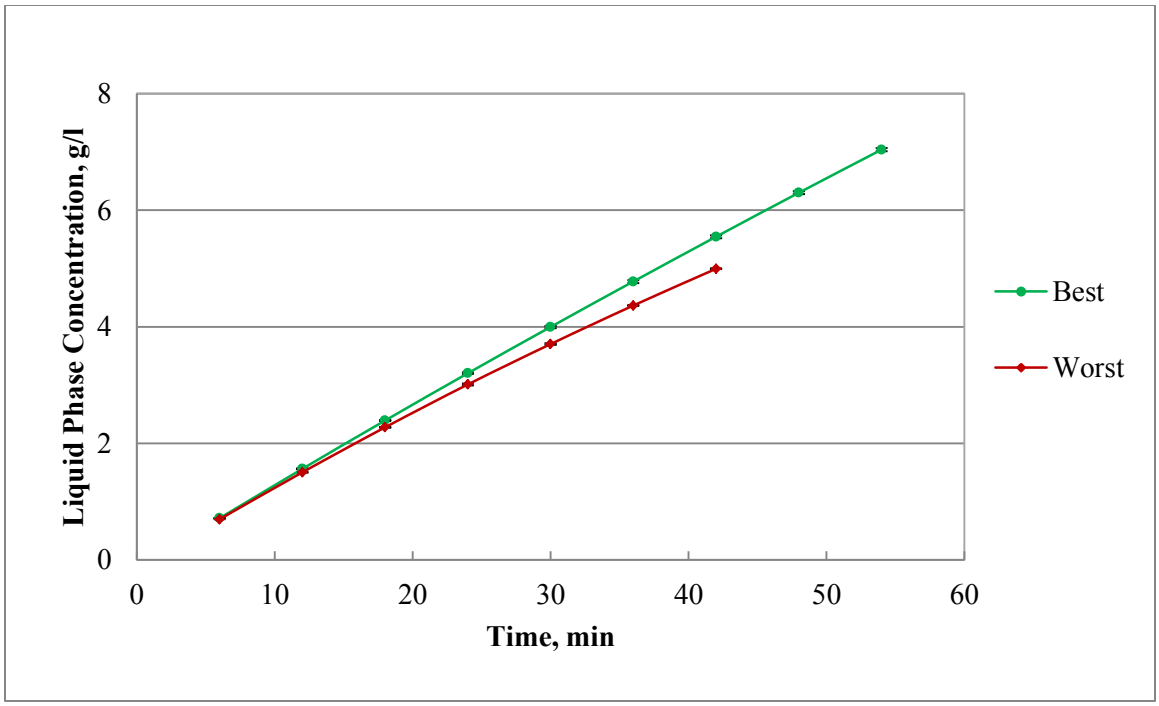

Figure 3.38 Liquid phase ethylbenzene concentration at the best and worst case removal efficiences

3.6 Solvent loss

Solvent plays an important role in the wet scrubbing processes. Millions of tons of solvent are used and disposed each year and, therefore, the government and industries have focused on replacing, recycling or minimizing solvent use to reduce the impact on human health and environment (Curzons et al., 1999). Efficient and economical operation of wet scrubbing unit is directly associated with the rate of solvent loss. In addition, due to stringent environmental regulations, industries are forced to adopt the solvent loss reduction scheme which is expensive.

Figure 3.39 Measurement of solvent loss using a dry ice condenser trap

To measure the solvent loss in the present system, a dry ice condenser trap shown in Figure 3.39 was used to maintain a temperature of -78.5°C. Exiting air stream of wet scrubbing system passed through the outer annular space of the dry ice shell to condense the solvent vapor before exiting to the exhaust. The condensed solvent was removed from the bottom shell and measured through

a graduated centrifuge tube at the end of experiment. Experimental results showed that the solvent loss of 1-2 ml, i.e., 0.1-0.25 %, was observed at solvent temperatures of 30 to 50°C. A low solvent loss was observed with vegetable oil due to its low vapor pressure, i.e., 0.005, 0.007 and 0.01 atmosphere, at the solvent temperature of 30, 40 and 50°C (Ndiaye et al., 2005), respectively.

3.7 Model results of the removal efficiency of tar compounds

A process model was developed using an equilibrium stage based approach and a "RadFrac" block of the Aspen Plus™ software. Non-random two-liquid (NRTL) was considered as the thermodynamic property model and the missing binary interaction parameters of the NRTL model were predicted through UNIQUAC (UNIversal QUAsiChemical) Functional-group Activity Coefficients (UNIFAC) model. The solvent, i.e., vegetable oil and raschig rings of 6 mm size were specified using supplier information as shown in Table 2.1 and Table 2.3, respectively. A steady state model was developed in Aspen Plus™ software to study the removal efficiency of model tar compounds. To generate dynamic data with time, liquid phase model tar concentration was determined through a mass balance calculation using experimental data. As an example, liquid phase benzene, toluene and ethylbenzene concentrations for the best and worst case removal efficiencies are given in Section 3.5. The concentration levels of model tar compounds at the outlet air stream of the wet scrubbing system with time were predicted using the calculated liquid phase concentration as an input to the steady state model. The other process variables such as solvent temperature, solvent flow rate, bed height and the pressure drop across the column were specified per experimental conditions.

Two extreme conditions, i.e., the best case scenario and the worst case scenario, were predicted and compared with the experimental results. Accordingly, two bed heights (0.5 and 1.1 m), two solvent temperatures (30 and 50°C) at each bed height, and two solvent flow rates (53 and 73 ml/min) at each solvent temperature were predicted through model. The experimental and

model results are shown in Figures 3.40-3.47. As shown in Figure 3.40, the model slightly under predicted removal efficiencies for benzene (2-6%), toluene (1-4%) and ethylbenzene (1-2%) of experimental data at the solvent temperature of 30°C, solvent flow rate of 53 ml/min and bed height of 0.5 m. The differences in the experimental and the model values could be due to three major reasons. First, there is a dilution effect in the upper section of the packed bed column due to short packed bed height, i.e., 0.5 m, compared to overall packed bed column height, i.e., 1.4 m. Second, in the selected thermodynamic model, i.e., NRTL, the missing binary interaction parameters (a_{ij} and b_{ij}) were predicted through a UNIFAC method in the absence of experimental values. The error in these binary interaction parameters could lead to a deviation from experimental values. Third, there is a possibility of liquid maldistribution at the bottom of the column which has a direct impact on the interfacial area for the mass transfer of the model tar compounds. However, as the solvent flow rate increased to 73 ml/min, the model prediction shows a very good fit with experimental results and the deviation was reduced to +/- 1%. This occurs because as the solvent flow rate increased to 73 ml/min, it increases the mass transfer area due to improved wetting of the packing materials. In addition, a required theoretical numbers of stages also reduce as the solvent flow rate increases.

At the higher solvent temperature, i.e., 50°C (Figure 3.42), the model predicted removal efficiencies within 1-7%, 1-4%, and 1-6% of experimental data for benzene, toluene, and ethylbenzene, respectively. It was determined that the temperature controller deviated after 36 minutes of operation at the higher solvent temperature, i.e., 50°C. Therefore, experimental and predicted data after 36 minutes of operation is not included in Figures 3.42 and 3.43.

The differences in the model and experimental results further increases as the solvent flow rate increases (Figure 3.43). It was observed that the deviation of the experimental and the model removal efficiency results for the benzene, toluene and ethylbenzene are 7-13%, 3-8% and 2-4%, respectively. In addition, it was also observed that the model over predicted the removal

efficiency of all three tar compounds. The major reason could be left over traces of tar compounds from previous experiments. In addition, liquid maldistribution could also have impact on the interfacial mass transfer area at the higher solvent temperature and solvent flow rate.

Similarly, model predictions were compared to experimental results at the highest bed height of 1.1 m at the solvent temperature of 30°C and the solvent flow rate of 53 and 73 ml/min (Figures 3.44 and 3.45). As shown in Figure 3.44, the model predictions are good fits with the experimental values for benzene (1-6%), toluene (1-3%) and ethylbenzene (1-2%). However, initially, up to 18 minutes of operation the benzene removal efficiency deviated to 5-11% of experimental data. This occurs because in the experimental results, the liquid phase model tar concentration with time changes gradually and thus initial liquid phase model tar compounds are low. While in the case of the model, a stepwise increment in the liquid phase model tar compounds was considered as an input. At higher solvent flow rate, i.e., 73 ml/min, the model predicted the tar removal efficiency within the range of 2-6%, 0-4% and 1-2% of experimental data for benzene, toluene and ethylbenzene, respectively. As the solvent temperature increased to 50°C (Figure 3.46), the model under predicted the tar removal efficiency within the range of 2-14%, 2-10% and 3-11% of experimental data for benzene, toluene and ethylbenzene, respectively. These differences in the model versus experimental values could be due mainly to a liquid maldistribution at the higher solvent temperature as explained earlier. However, as the solvent flow rate increased to 73 ml/min, the differences in the model and experimental values reduce considerably (Figure 3.47). As shown, the model prediction deviates from the experimental values within the range of 1-4%, 4-14% and 2-11% of experimental data for benzene, toluene, and ethylbenzene, respectively. As shown in Figure 3.46 and 3.47, a large difference was observed in both toluene and ethylbenzene removal efficiencies. This occurs because the initial efficiency reduced by 4-6% of theoretical prediction for both toluene and ethylbenzene cases which could have been occurred due to the presence of traces of toluene and ethylbenzene from

previous experimental tests. At the higher packed bed of 1.1 m, it was determined that the temperature controller was deviated after 36 minutes of operation; therefore, experimental and model prediction were removed after 36 minutes of operation at higher solvent temperature of 50°C as explained earlier.

Overall, the model prediction of removal efficiency shows the best fit with experimental data at the solvent temperature of 30°C. The maximum deviation between experimental and model was observed at the higher solvent temperature of 50°C.

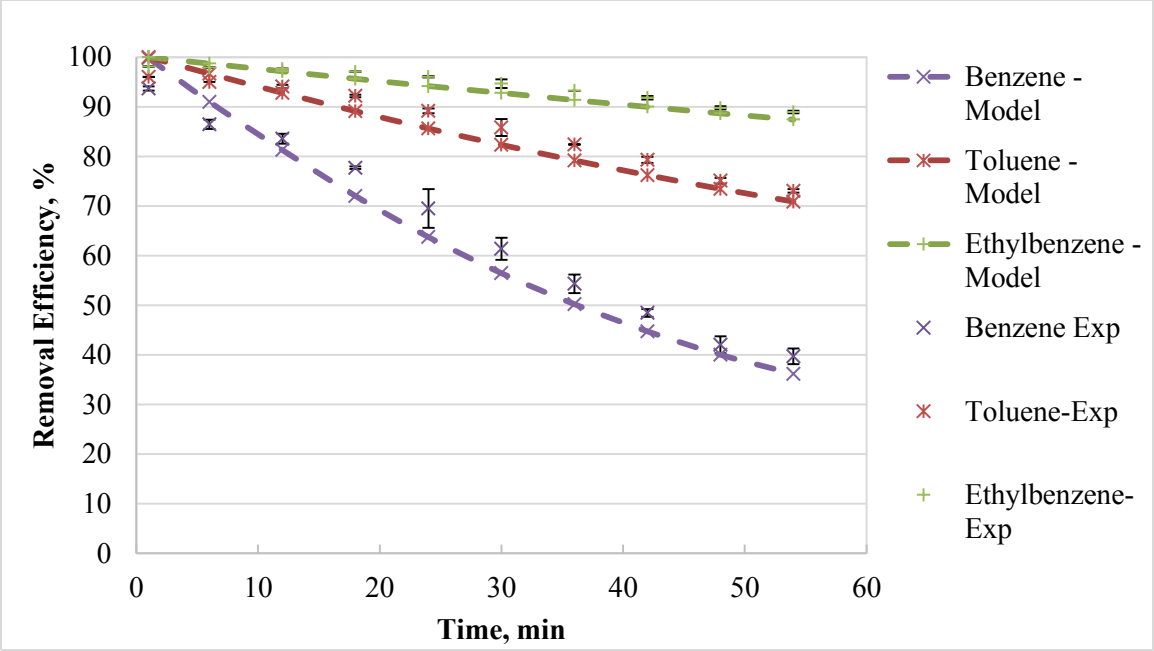

Figure 3.40 Predicted and experimental removal efficiencies of benzene, toluene, and ethylbenzene at the packed bed height of 0.5 m, solvent temperature of 30°C, solvent flow rate of 53 ml/min, and using soybean oil as a solvent

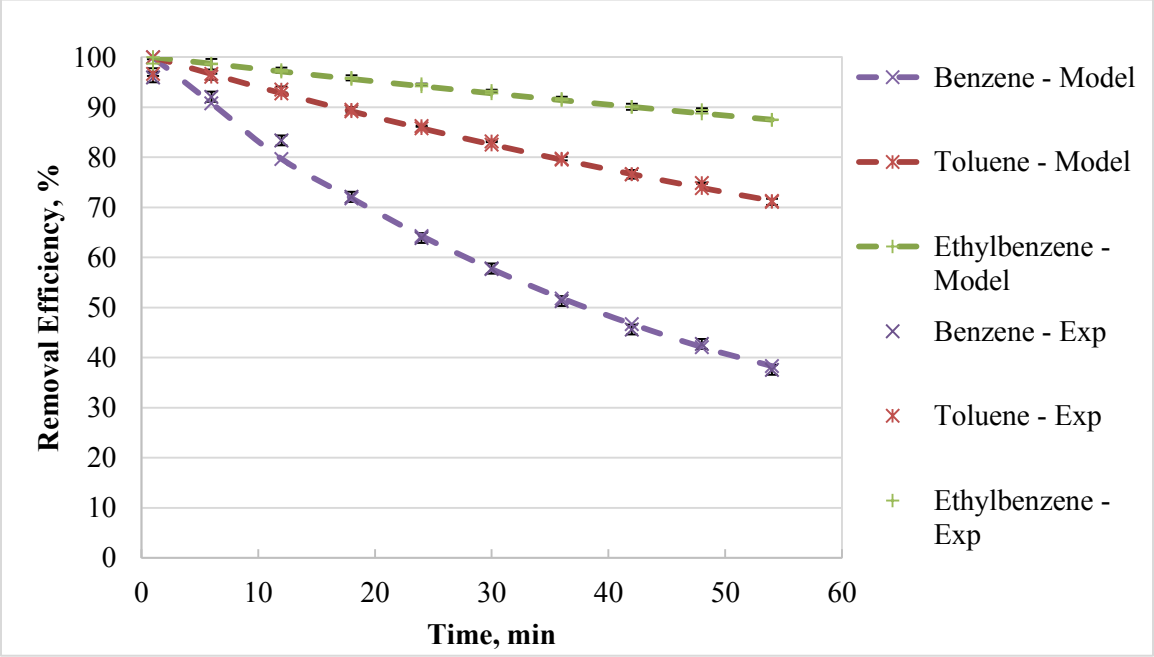

Figure 3.41 Predicted and experimental removal efficiencies of benzene, toluene, and ethylbenzene at the packed bed height of 0.5 m, solvent temperature of 30°C, solvent flow rate of 73 ml/min, and using soybean oil as a solvent

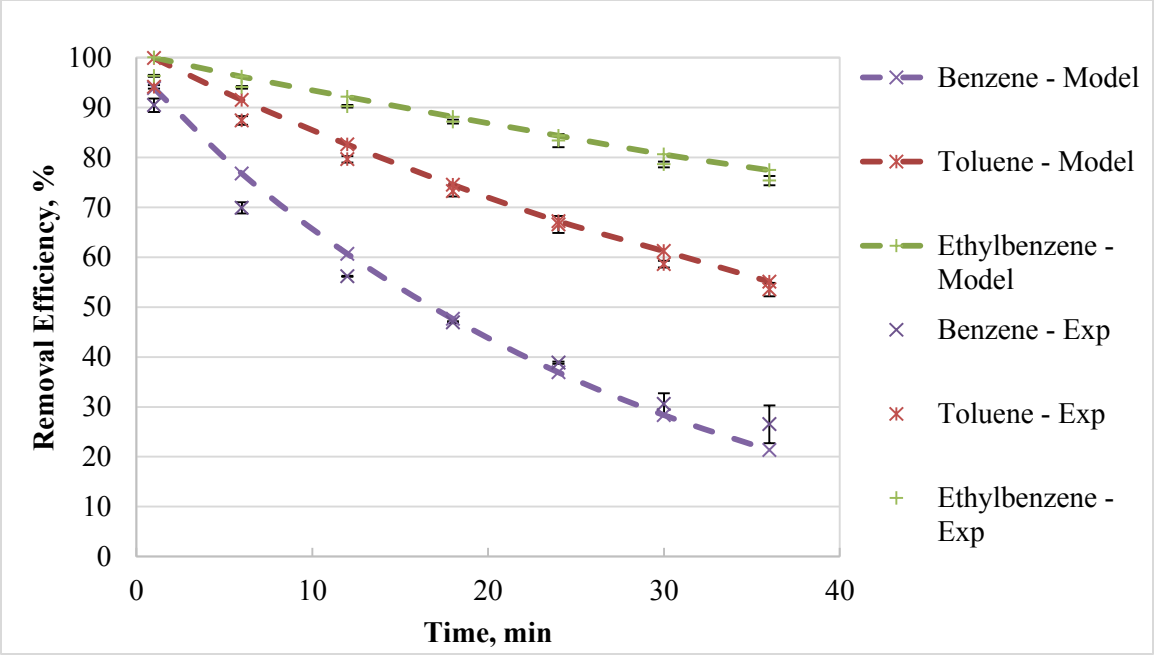

Figure 3.42 Predicted and experimental removal efficiencies of benzene, toluene, and ethylbenzene at the packed bed height of 0.5 m, solvent temperature of 50°C, solvent flow rate of 53 ml/min, and using soybean oil as a solvent

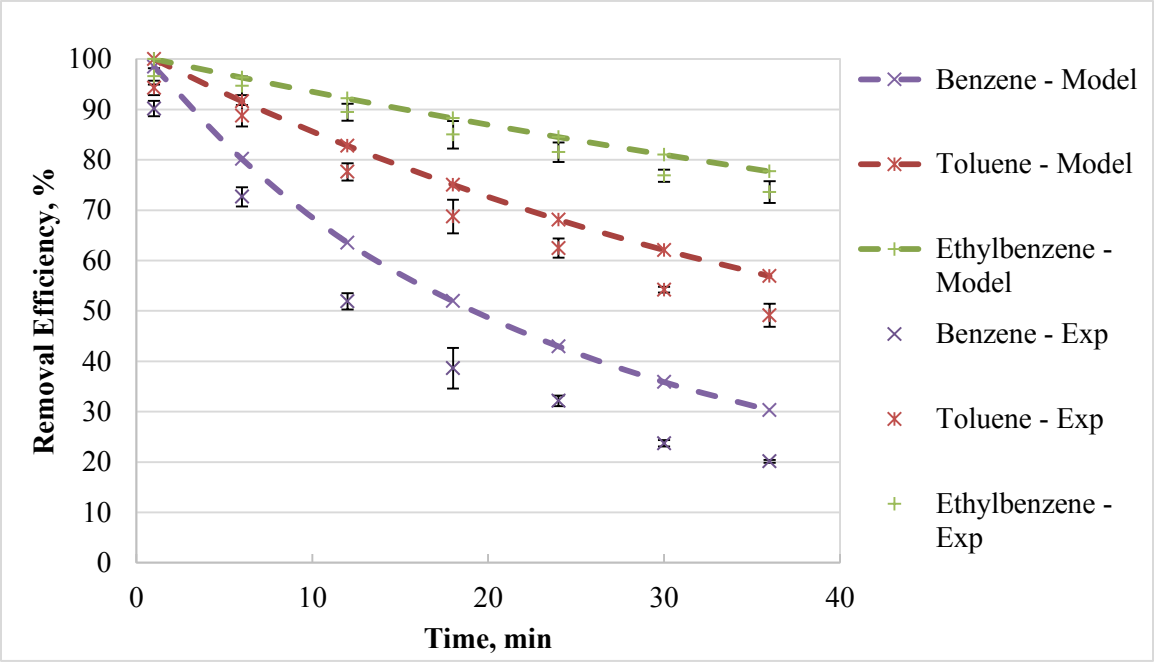

Figure 3.43 Predicted and experimental removal efficiencies of benzene, toluene, and ethylbenzene at the packed bed height of 0.5 m, solvent temperature of 50°C, solvent flow rate of 73 ml/min, and using soybean oil as a solvent

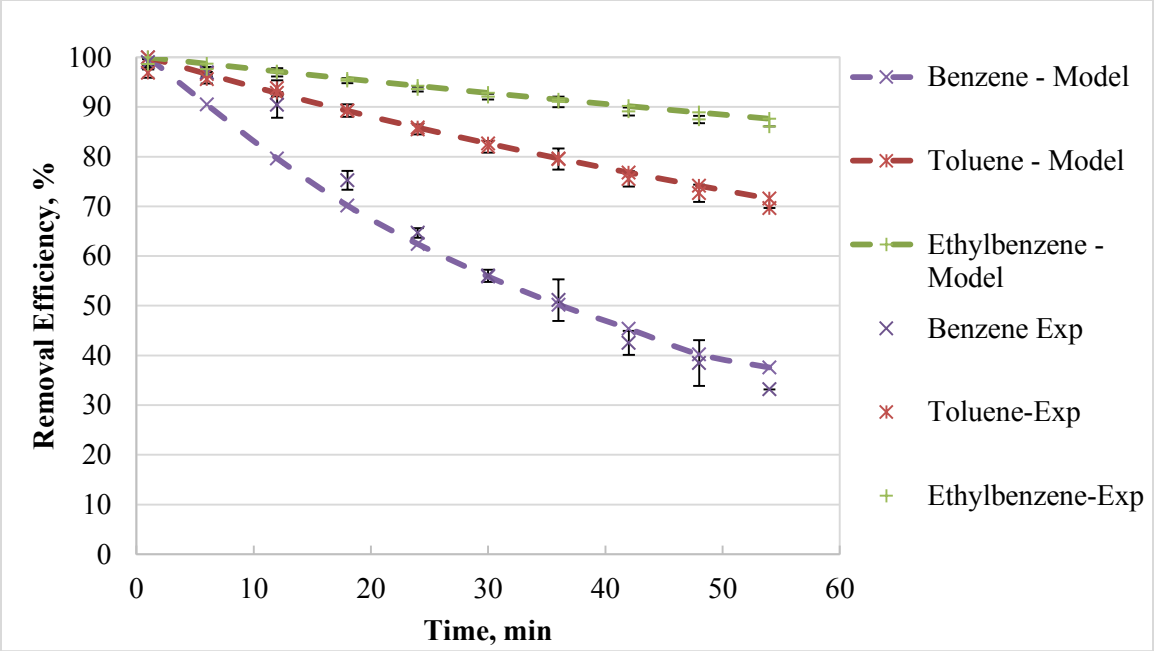

Figure 3.44 Predicted and experimental removal efficiencies of benzene, toluene, and ethylbenzene at the packed bed height of 1.1 m, solvent temperature of 30°C, solvent flow rate of 53 ml/min, and using soybean oil as a solvent

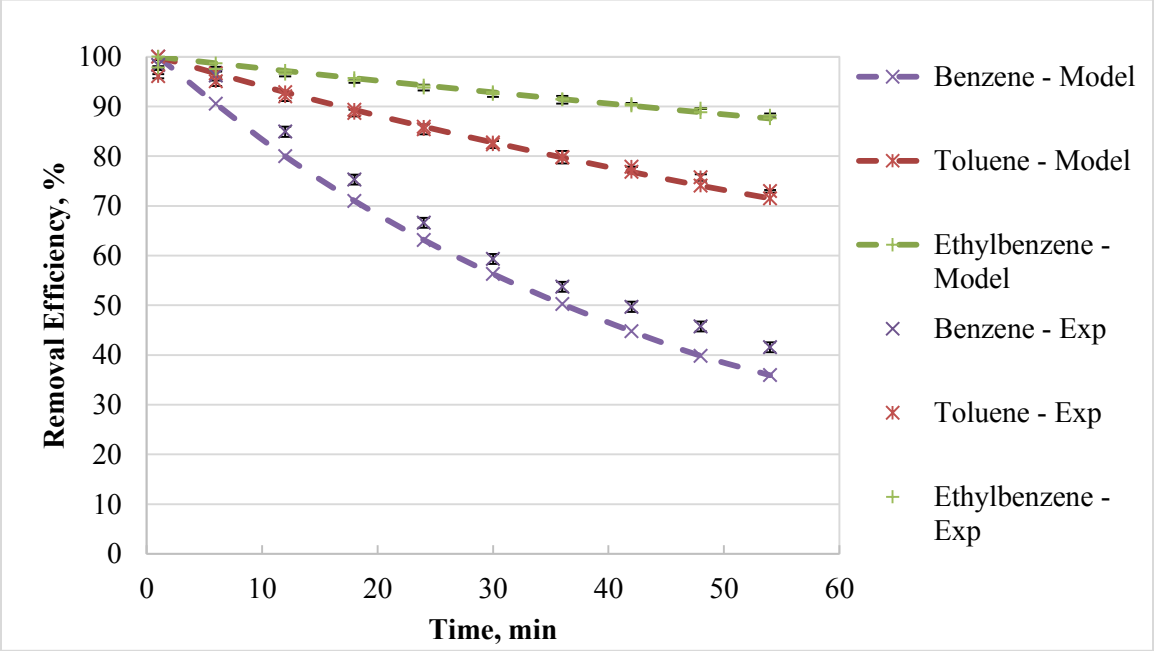

Figure 3.45 Predicted and experimental removal efficiencies of benzene, toluene, and ethylbenzene at the packed bed height of 1.1 m, solvent temperature of 30°C, solvent flow rate of 73 ml/min, and using soybean oil as a solvent

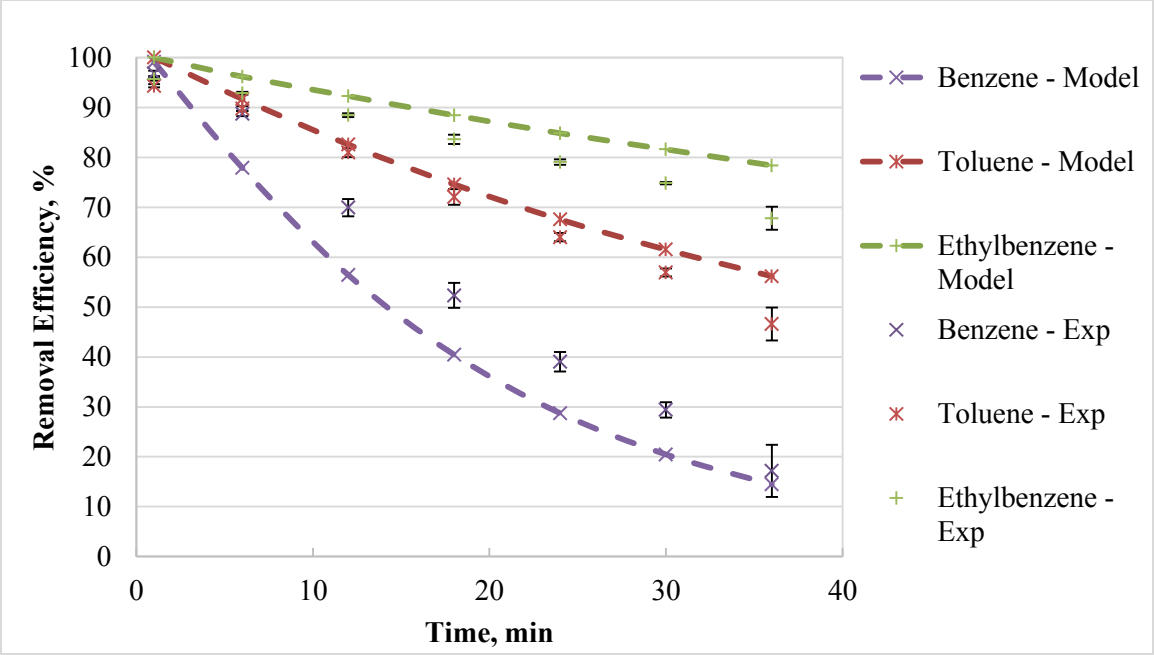

Figure 3.46 Predicted and experimental removal efficiencies of benzene, toluene, and ethylbenzene at the packed bed height of 1.1 m, solvent temperature of 50°C, solvent flow rate of 53 ml/min, and using soybean oil as a solvent

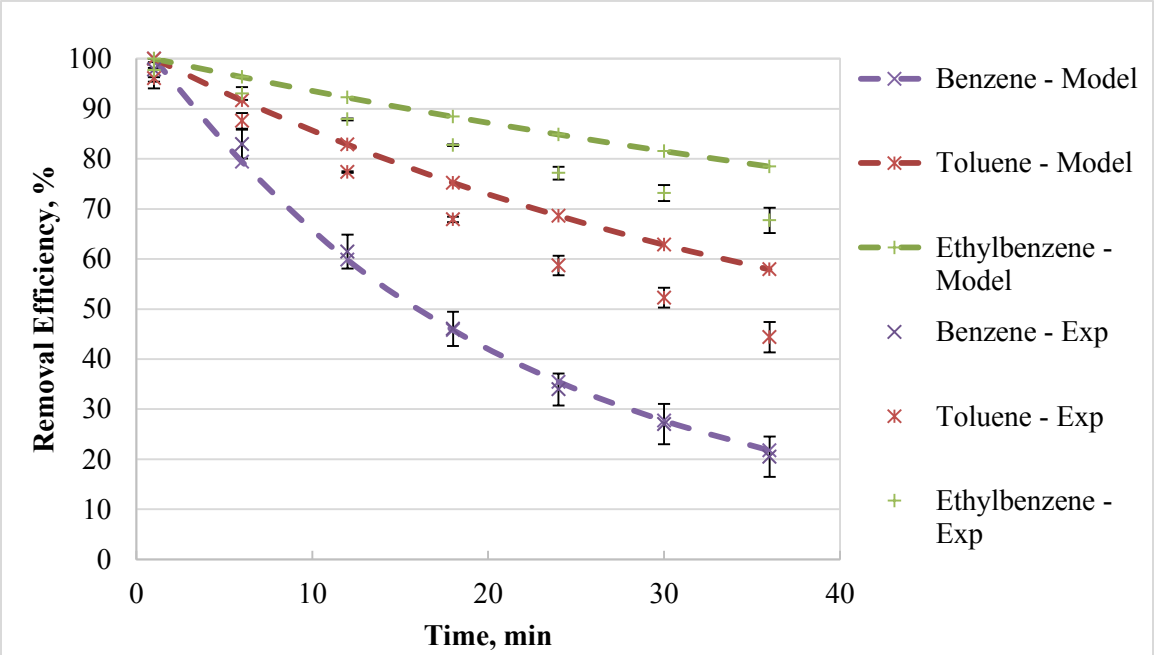

Figure 3.47 Predicted and experimental removal efficiencies of benzene, toluene and ethylbenzene at the packed bed height of 1.1 m, solvent temperature of 50°C, solvent flow rate of 73 ml/min, and using soybean oil as a solvent

CHAPTER IV

SUMMARY AND CONCLUSIONS

This chapter provides a summary of major findings for the vegetable oil based wet scrubbing system in the removal of model tar compounds. An experimental wet scrubbing system was designed, fabricated and used to evaluate the design and operating variables: height of the packed bed and solvent type, temperature and flow rate through the system. A liquid distributor was designed and fabricated to distribute high viscous vegetable oil uniformly. Model tar compounds used in this research were benzene, toluene and ethylbenzene. A tar mixing section was also designed and installed prior to wet scrubbing column to generate a desired tar concentrations in the inlet air stream. An equilibrium stage-based process model was also developed using a non-random two-liquid (NRTL) thermodynamic property model and validated using experimental data.

Based on the analysis of the experimental results, following conclusions are made:

1. Both soybean and canola oils are good candidates as solvents for the removal of model tar compounds. Both oils provide comparable removal efficiency of model tar compounds. Soybean oil is recommended as a solvent for the removal of model tar compounds based on its low cost and availability in large quantities compared to canola oil.

2. A gas chromatography/mass spectroscopy method was developed to analyze the model tar compounds concentrations. This method is useful in quantification of tar compounds in the range of 27-8355, 54-4206 and 54-2439 ppmv for benzene, toluene and ethylbenzene, respectively. A protocol was developed to calibrate model tar compounds using US EPA method 18 (EPA, 1987) will be useful in developing calibration of other tar compounds.
3. The packed bed height had a highly significant (p<0.0001) effect on the removal efficiency of model tar compounds. It was observed that an incremental change in the removal efficiency of model tar compounds decreases as the packed bed height increases.
4. Ten theoretical stages of the packed bed column height were determined using an equilibrium stage-based process model and Kremser's method (Perry et al., 1984). The experimental height equivalent to a theoretical plate (HETP) was determined as 0.11 m using ten equilibrium stages and an effective bed height of 1.1 m.
5. Solvent temperature had a highly significant (p<0.0001) effect on the removal efficiency of model tar compounds because the solvent temperature significantly influences the K-value of model tar compounds. It was also observed that the viscosity reduces and the surface tension increases as the solvent temperature increases which can lead to a liquid misdistribution. Thus, a low solvent temperature is recommended for the design of vegetable oil based wet scrubbing system for the removal of model tar compounds.
6. Solvent flow rate did not have a significant (p>0.05) effect on the removal efficiency of model tar compounds.
7. An equilibrium stage based process model was developed in Aspen Plus^{TM} software. The model uses a non-random two-liquid (NRTL) as thermodynamic model, while the missing binary interaction parameters of NRTL model were predicted using UNIQUAC functional-group activity coefficients (UNIFAC) method. The model was validated for the extreme conditions of the selected experimental variables. It was observed that the model predicted

the removal efficiency of benzene, toluene and ethylbenzene within 1-6%, 1-4%, and 1-2%, respectively, for the solvent temperature of 30°C. Therefore, NRTL-PR as a property model and UNIFAC model for missing binary interaction parameters are recommended for modeling absorption of tar compounds in vegetable oils.

8. Packed bed height, solvent temperature and solvent flow rates had a highly significant (p<0.0001) effects on the pressure drop across the column. Pressure drop was predicted using Billet & Schultes (1999) pressure drop correlation. The packing specific constants, i.e., C_h and $C_{P,0}$, were determined as 2.52 and 2.93 using experimental values of pressure drop across the column. A very good fit was observed using these packing specific parameters.
9. A low solvent loss of 0.1-0.25% was observed which favors the use of vegetable oils as solvents for tar removal.

CHAPTER V

RECOMMENDATIONS FOR FUTURE RESEARCH

A vegetable oil based wet scrubbing system has been designed, fabricated and used to evaluate the removal of model tar compounds. The following recommendations are provided for further development of the vegetable oil based wet scrubbing system to a pilot or commercial scale for the removal of tar compounds.

1. This study used raschig rings as packing materials which is a basic packing material. Data from a laboratory or pilot scale system using advanced packings would be more useful for commercial applications.
2. In this study, packing specific constants (C_h and $C_{P,0}$) of Billet & Schultes (1999) pressure drop correlation were determined for air-vegetable oil system at a constant air flow rate. A detailed study on hydrodynamics of air-vegetable oil system including all region of operation (i.e., below loading point, above loading point and flooding point) will be useful to develop holdup and pressure drop correlations for all region.
3. The process model uses a non-random two-liquid (NRTL) thermodynamic property model, while the missing binary interaction parameters were predicted using UNIQUAC functional-group activity coefficients (UNIFAC) method. Even though the model prediction was very good compared to experimental data, it can be improved further through either using a regressed binary interaction parameters from experimental data or predicted through a novel quantitative structure-property relationship (QSPR) model which will improve the thermodynamic properties of the used components.

4. The wet packed bed column was operated in a batch system and the solvent was recirculated through a solvent recycling pump. Thus, the removal efficiency curves showed continuous decreasing trends. However, in commercial applications, a waste solvent stream is regenerated using a stripping column and routed back to the absorption column. Therefore, a design, fabrication and evaluation of a stripping column along with absorption column will be beneficial for industrial applications.

REFERENCES

Ahmed, A., Cateni, B. G., Huhnke, R. L., & Lewis, R. S. (2006). Effects of biomass-generated producer gas constituents on cell growth, product distribution and hydrogenase activity of *Clostridium carboxidivorans* P7^{T}. *Biomass and Bioenergy, 30*(7), 665-672.

Anis, S., & Zainal, Z. (2011). Tar reduction in biomass producer gas via mechanical, catalytic and thermal methods: A review. *Renewable and Sustainable Energy Reviews, 15*(5), 2355-2377.

AspenTech. (2001). Aspen Plus 11.1. Unit Operation Models, Aspen Technology Inc. Cambridge, MA.

Baker, E., Brown, M., Elliott, D., & Mudge, L. (1988). Characterization and treatment of tars and biomass gasifiers: Pacific Northwest Lab., Richland, WA, USA.

Baker, E., Brown, M., Moore, R., Mudge, L., & Elliott, D. (1986). Engineering analysis of biomass gasifier product gas cleaning technology: Pacific Northwest Lab., Richland, WA, USA.

Barratt, R. (1981). The preparation of standard gas mixtures. A review. *Analyst, 106*(1265), 817-849.

Bergman, P. C., van Paasen, S. V., & Boerrigter, H. (2002). The novel "OLGA" technology for complete tar removal from biomass producer gas. Pyrolysis and Gasification of Biomass and Waste, Expert Meeting, Strasbourg, France.

Bhave, A., Vyas, D., & Patel, J. (2008). A wet packed bed scrubber-based producer gas cooling-cleaning system. *Renewable Energy, 33*(7), 1716-1720.

Billet, R., & Schultes, M. (1999). Prediction of mass transfer columns with dumped and arranged packings. *Trans IChemE, 77*(Part A), 498-504.

Boerrigter, H., Van Paasen, S., Bergman, P., Könemann, J., Emmen, R., & Wijnands, A. (2005). OLGA tar removal technology. *Energy Research Centre of the Netherlands, ECN-C--05-009*.

Brage, C., Yu, Q., Chen, G., & Sjöström, K. (2000). Tar evolution profiles obtained from gasification of biomass and coal. *Biomass and Bioenergy, 18*(1), 87-91.

Brandt, P., & Henriksen, U. B. (2000). Decomposition of tar in gas from updraft gasifier by thermal cracking. 1st World Conference on Biomass for Energy and Industry, Sevilla, Spain.

Bridgwater, A. (1995). The technical and economic feasibility of biomass gasification for power generation. *Fuel, 74*(5), 631-653.

Bui, T., Loof, R., & Bhattacharya, S. (1994). Multi-stage reactor for thermal gasification of wood. *Energy, 19*(4), 397-404.

Carlson, E. C. (1996). Don't gamble with physical properties for simulations. *Chemical Engineering Progress, 92*(10), 35-46.

Cateni, B. G. (2007). Effects of feed composition and gasification parameters on product gas from a pilot scale fluidized bed gasifier (Doctoral dissertation). Retrieved from ProQuest Dissertations and Theses (UMI Number: 3302329). Oklahoma State University, Stillwater, OK.

Coll, R., Salvado, J., Farriol, X., & Montané, D. (2001). Steam reforming model compounds of biomass gasification tars: conversion at different operating conditions and tendency towards coke formation. *Fuel Processing Technology, 74*(1), 19-31.

Curzons, A., Constable, D., & Cunningham, V. (1999). Solvent selection guide: a guide to the integration of environmental, health and safety criteria into the selection of solvents. *Clean Technologies and Environmental Policy, 1*(2), 82-90.

de Jong, W., Ünal, Ö., Andries, J., Hein, K. R., & Spliethoff, H. (2003). Biomass and fossil fuel conversion by pressurised fluidised bed gasification using hot gas ceramic filters as gas cleaning. *Biomass and Bioenergy, 25*(1), 59-83.

Devi, L., Ptasinski, K. J., & Janssen, F. J. J. G. (2003). A review of the primary measures for tar elimination in biomass gasification processes. *Biomass and Bioenergy, 24*(2), 125-140.

Doan, H., & Fayed, M. (2001). Dispersion-concentric model for mass transfer in a packed bed with a countercurrent flow of gas and liquid. *Industrial & Engineering Chemistry Research, 40*(21), 4673-4680.

DOE. (2012). Biomass Multi-Year Program Plan: Office of the Biomass Program, US DOE Washington, DC.

Dogru, M., Midilli, A., & Howarth, C. R. (2002). Gasification of sewage sludge using a throated downdraft gasifier and uncertainty analysis. *Fuel Processing Technology, 75*(1), 55-82.

Eckert, J. (1963). Tower packings… comparative performance. *Chem. Eng. Prog., 59*(5), 76-82.

Eckert, J. (1970). Selecting the proper distillation column packing. *Chem. Eng. Prog., 66*(3), 39.

Eckert, J. (1975). How tower packings behave. *Chem. Eng., 82*(8), 70-76.

EIA. (2012). http://www.eia.gov/oiaf/aeo/otheranalysis/aeo_2006analysispapers/nlf.html. Accessed during September 2012.

Elliott, D. C. (1988). *Relation of Reaction Time and Temperature to Chemical Composition of Pyrolysis Oils* (Vol. 376): ACS Publications.

EPA. (1987). U.S. Environmental Protection Agency. Method 18. Code of Federal Regulations, Part 60; Title 40; Appendix A; U.S. GPO: Washington, DC.

Esteban, B., Riba, J. R., Baquero, G., Puig, R., & Rius, A. (2012). Characterization of the surface tension of vegetable oils to be used as fuel in diesel engines. *Fuel, 102*, 231-238.

Gebreyohannes, Yerramsetty, K., Neely, B. J., & Gasem, K. A. (2012). Improved QSPR Generalized Interaction Parameters for the Nonrandom Two-Liquid Activity Coefficient Model. *Fluid Phase Equilibria, 339*, 20-30.

Gebreyohannes, S. (2011). Process design and economic evaluation of an ethanol production process by biomass gasification (Master's thesis). Retrieved from ProQuest Dissertations and Theses (UMI Number: 1488891): Oklahoma State University, Stillwater, OK.

Gil, J., Aznar, M. P., Caballero, M. A., Francés, E., & Corella, J. (1997). Biomass gasification in fluidized bed at pilot scale with steam-oxygen mixtures. Product distribution for very different operating conditions. *Energy & Fuels, 11*(6), 1109-1118.

Hasler, P., & Nussbaumer, T. (1999). Gas cleaning for IC engine applications from fixed bed biomass gasification. *Biomass and Bioenergy, 16*(6), 385-395.

Henriksen, U., & Christensen, O. (1994). Gasification of straw in a two-stage 50 kW gasifier. Proceedings of the 8th European Conference on Biomass for Energy, Environment, Agriculture and Industry. Pergamon, Elsevier Science Ltd.: Oxford, UK.

Herguido, J., Corella, J., & Gonzalez-Saiz, J. (1992). Steam gasification of lignocellulosic residues in a fluidized bed at a small pilot scale. Effect of the type of feedstock. *Industrial & Engineering Chemistry Research, 31*(5), 1274-1282.

Heymes, F., Manno-Demoustier, P., Charbit, F., Fanlo, J. L., & Moulin, P. (2006). A new efficient absorption liquid to treat exhaust air loaded with toluene. *Chemical Engineering Journal, 115*(3), 225-231.

Hindsgaul, C., Schramm, J., Gratz, L., Henriksen, U., & Dall Bentzen, J. (2000). Physical and chemical characterization of particles in producer gas from wood chips. *Bioresource Technology, 73*(2), 147-155.

Hoekman, S. K. (2009). Biofuels in the US - Challenges and Opportunities. *Renewable Energy, 34*(1), 14-22.

Janzen, A., Schubert, M., Barthel, F., Hampel, U., & Kenig, E. (2013). Investigation of dynamic liquid distribution and hold-up in structured packings using ultrafast electron beam X-ray tomography. *Chemical Engineering and Processing: Process Intensification, 66*, 20-26.

Kenkel, P., Godsey, C., Epplin, F., Gregory, M., Holcomb, R., & Huhnke, R. (2006). Potential for Production of Biofuel Feedstocks in Oklahoma: Working Paper, Dept. Agr. Econ., Oklahoma State University.

Khummongkol, D., & Tangsathitkulchai, C. (1989). A model for tar-removal efficiency from biomass-produced gas impinging on a water surface. *Energy, 14*(3), 113-121.

Kinoshita, C., Wang, Y., & Zhou, J. (1994). Tar formation under different biomass gasification conditions. *Journal of Analytical and Applied Pyrolysis, 29*(2), 169-181.

Kister, H. (1992). *Distillation Design* (Vol. 1): McGraw-Hill New York.

Kister, H., Scherffius, J., Afshar, K., & Abkar, E. (2007). Realistically predict capacity and pressure drop for packed columns. AIChE meeting, Houston, TX.

Knight, R. A. (2000). Experience with raw gas analysis from pressurized gasification of biomass. *Biomass and Bioenergy, 18*(1), 67-77.

Kuramochi, H., Maeda, K., Kato, S., Osako, M., Nakamura, K., & Sakai, S. (2009). Application of UNIFAC models for prediction of vapor–liquid and liquid–liquid equilibria relevant to separation and purification processes of crude biodiesel fuel. *Fuel, 88*(8), 1472-1477.

Lettner, F., Timmerer, H., & Haselbacher, P. (2007). Biomass gasification–State of the art description. Intelligent Energy Europe, Austria.

Mateescu, C. M., Muzenda, E., Belaid, M., Abdulkareem, S., & Afolabi, A. S. (2011). Estimating the Absorption of Volatile Organic Compounds in Four Biodiesels Using the UNIFAC

Procedure. *International Journal of Chemical, Materials Science and Engineering, 5*(2), 1-6.

Milne, T., Abatzoglou, N., & Evans, R. (1998). Biomass gasifier "tars": their nature, formation, and conversion (NREL/TP-570-25357). National Renewable Energy Laboratory, Golden, Colorado.

Minkova, V., Marinov, S., Zanzi, R., Bjornbom, E., Budinova, T., Stefanova, M., & Lakov, L. (2000). Thermochemical treatment of biomass in a flow of steam or in a mixture of steam and carbon dioxide. *Fuel Processing Technology, 62*(1), 45-52.

Mudinoor, A. R. (2010). Conversion of Toluene (model Tar) in the Presence of Syngas Using Selected Steam Reforming Catalysts (Master's thesis). Retrieved from ProQuest Dissertations and Theses (UMI Number: 1480999): Oklahoma State University, Stillwater, OK.

Myrén, C., Hörnell, C., Björnbom, E., & Sjöström, K. (2002). Catalytic tar decomposition of biomass pyrolysis gas with a combination of dolomite and silica. *Biomass and Bioenergy, 23*(3), 217-227.

Narvaez, I., Orio, A., Aznar, M. P., & Corella, J. (1996). Biomass gasification with air in an atmospheric bubbling fluidized bed. Effect of six operational variables on the quality of the produced raw gas. *Industrial & Engineering Chemistry Research, 35*(7), 2110-2120.

Ndiaye, P. M., Tavares, F. W., Dalmolin, I., Dariva, C., Oliveira, D., & Oliveira, J. V. (2005). Vapor pressure data of soybean oil, castor oil, and their fatty acid ethyl ester derivatives. *Journal of Chemical & Engineering Data, 50*(2), 330-333.

Noureddini, H., Teoh, B., & Clements, L. D. (1992). Viscosities of vegetable oils and fatty acids. *Journal of the American Oil Chemists Society, 69*(12), 1189-1191.

O'Meara, M. (2012). Determination of the Interfacial Tension between Oil-Steam and Oil-Air at Elevated Temperatures (Master's thesis). Retrived from

http://www.lib.ncsu.edu/resolver/1840.16/8150: North Carolina State University, Raleigh, North Carolina

Ozturk, B., & Yilmaz, D. (2006). Absorptive removal of volatile organic compounds from flue gas streams. *Process Safety and Environmental Protection, 84*(5), 391-398.

Pan, Y., Roca, X., Velo, E., & Puigjaner, L. (1999). Removal of tar by secondary air in fluidised bed gasification of residual biomass and coal. *Fuel, 78*(14), 1703-1709.

Pathak, B., Kapatel, D., Bhoi, P., Sharma, A., & Vyas, D. (2007). Design and development of sand bed filter for upgrading producer gas to IC engine quality fuel. *International Energy Journal, 8*, 15-20.

Perry, R. H., Green, D. W., & Maloney, J. O. (1984). *Perry's Chemical Engineers' Handbook - 8th ed. (Retrived from www.knovel.com)*: McGraw-Hill, New York.

Phuphuakrat, T., Namioka, T., & Yoshikawa, K. (2011). Absorptive removal of biomass tar using water and oily materials. *Bioresource Technology, 102*(2), 543-549.

Phuphuakrat, T., Nipattummakul, N., Namioka, T., Kerdsuwan, S., & Yoshikawa, K. (2010). Characterization of tar content in the syngas produced in a downdraft type fixed bed gasification system from dried sewage sludge. *Fuel, 89*(9), 2278-2284.

Pierucci, S., Del Rosso, R., Bombardi, D., Concu, A., & Lugli, G. (2005). An innovative sustainable process for VOCs recovery from spray paint booths. *Energy, 30*(8), 1377-1386.

Rabou, L. P., Zwart, R. W., Vreugdenhil, B. J., & Bos, L. (2009). Tar in biomass producer gas, the Energy research Centre of the Netherlands (ECN) experience: an enduring challenge. *Energy & Fuels, 23*(12), 6189-6198.

Ravindranath, D., Neely, B. J., Robinson, R. L., & Gasem, K. A. M. (2007). QSPR generalization of activity coefficient models for predicting vapor–liquid equilibrium behavior. *Fluid Phase Equilibria, 257*(1), 53-62.

Renon, H., & Prausnitz, J. (1969). Estimation of parameters for the NRTL equation for excess Gibbs energies of strongly nonideal liquid mixtures. *Industrial & Engineering Chemistry Process Design and Development, 8*(3), 413-419.

Sandler, S. I. (1999). *Chemical and Engineering Thermodynamics*: Wiley, New York.

Seader, J., Henley, E. J., & Keith, D. (2011). *Separation Process Principles - 3rd ed.*: John Wiley & Sons, Inc., Hoboken, NJ.

Seethamraju, S., Field, R. P., & Herzog, H. J. (2013). Modeling tar handling options in biomass gasification. *Energy & Fuels, 27*(6), 2859–2873.

Smith, J. M., & Ness, H. C. V. (2011). Introduction to chemical engineering thermodynamics.

Stichlmair, J., Bravo, J., & Fair, J. (1989). General model for prediction of pressure drop and capacity of countercurrent gas/liquid packed columns. *Gas Separation & Purification, 3*(1), 19-28.

Strigle, R. F. (1994). *Packed Tower Design and Applications: Random and Structured Packings - 2nd ed.*: Gulf Publishing Company, Houston, TX.

Susanto, H., & Beenackers, A. A. (1996). A moving-bed gasifier with internal recycle of pyrolysis gas. *Fuel, 75*(11), 1339-1347.

Sutton, D., Kelleher, B., & Ross, J. R. (2001). Review of literature on catalysts for biomass gasification. *Fuel Processing Technology, 73*(3), 155-173.

Taylor, R., Krishna, R., & Kooijman, H. (2003). Real-world modeling of distillation. *Transfer, 1000*, 1.

Tisdale, J. (2004). Simulations and modeling of biomass gasification processes (Master's thesis): Massachusetts Institute of Technology, Cambridge, MA.

Torres, W., Pansare, S. S., & Goodwin Jr, J. G. (2007). Hot gas removal of tars, ammonia, and hydrogen sulfide from biomass gasification gas. *Catalysis Reviews, 49*(4), 407-456.

USDA. (2012). http://www.ers.usda.gov/topics/crops/soybeans-oil-crops.aspx. Accessed during September 2012.

Wu, H., Feng, T. C., & Chung, T. W. (2010). Studies of VOCs removed from packed-bed absorber by experimental design methodology and analysis of variance. *Chemical Engineering Journal, 157*(1), 1-17.

Xu, C. C., Donald, J., Byambajav, E., & Ohtsuka, Y. (2010). Recent advances in catalysts for hot-gas removal of tar and NH3 from biomass gasification. *Fuel, 89*(8), 1784-1795.

Yin, F., Wang, Z., Afacan, A., Nandakumar, K., & Chuang, K. T. (2000). Experimental studies of liquid flow maldistribution in a random packed column. *The Canadian Journal of Chemical Engineering, 78*(3), 449-457.

Yu, Q., Brage, C., Chen, G., & Sjöström, K. (1997). Temperature impact on the formation of tar from biomass pyrolysis in a free-fall reactor. *Journal of Analytical and Applied Pyrolysis, 40*, 481-489.

APPENDICES

Appendix A: GC/MS calibration charts

A.1 Calibration of benzene

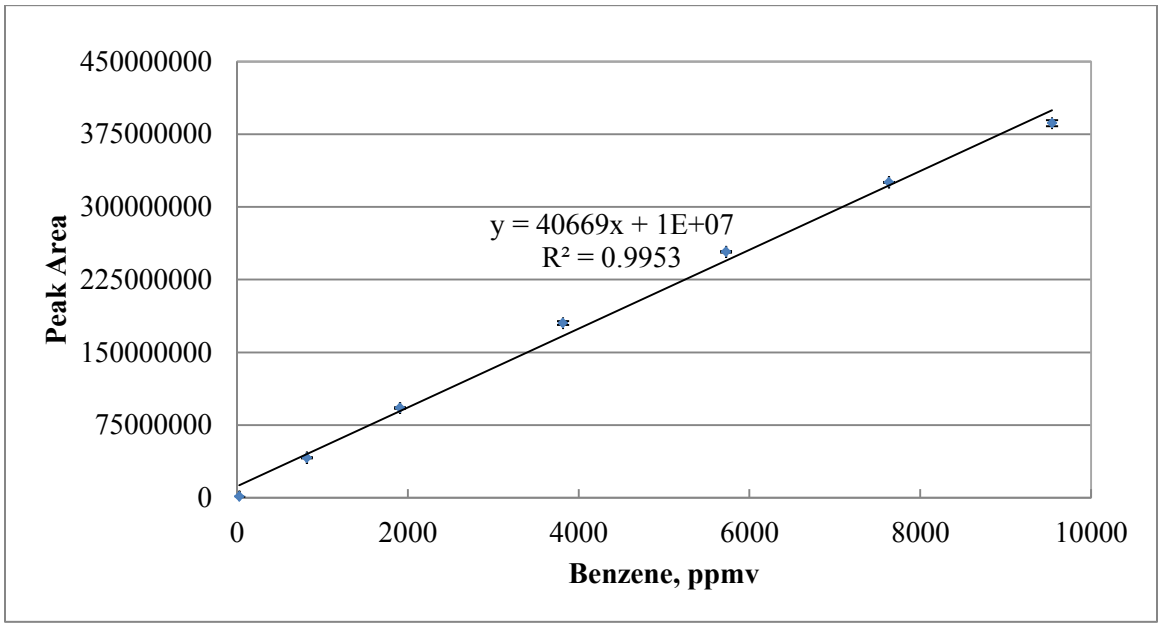

A.2 Calibration of toluene

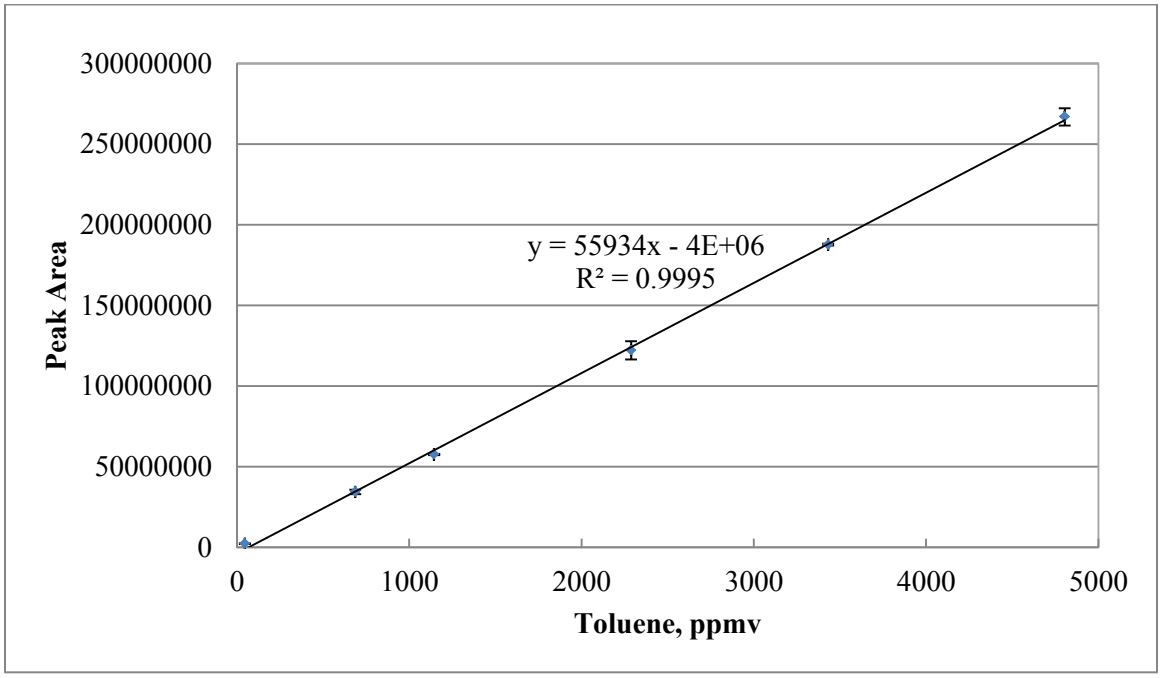

A.3 Calibration of ethylbenzene

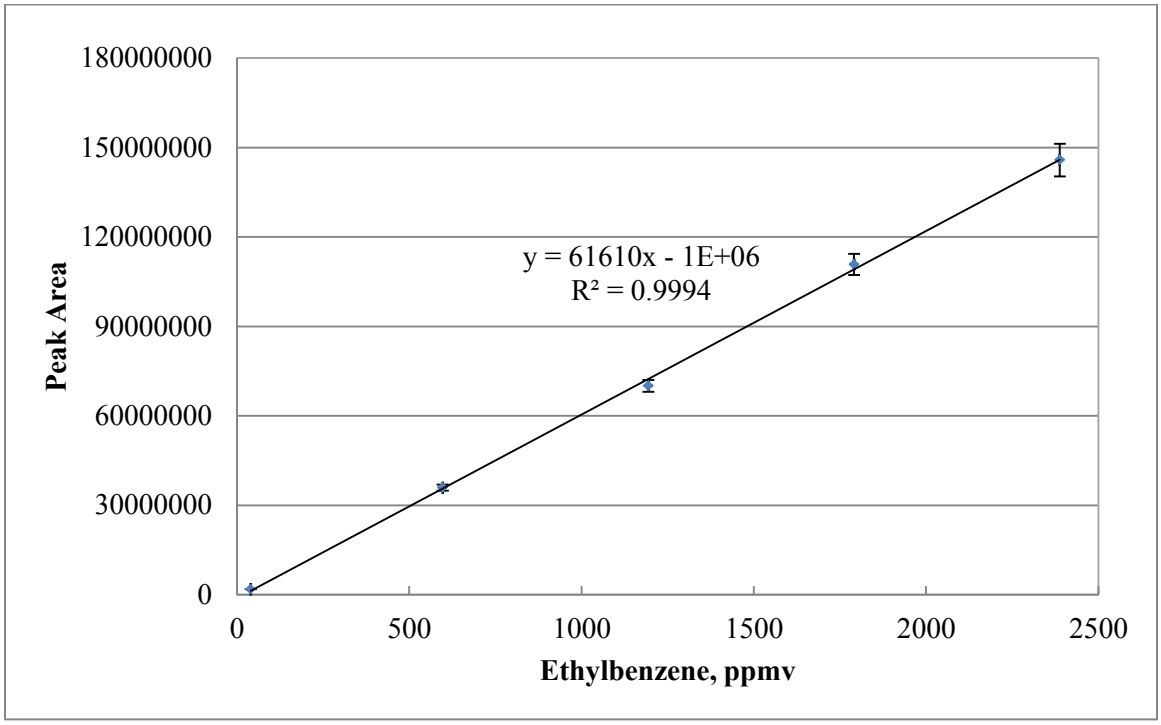

Appendix B: Experimental data on removal efficiencies of model tar compounds with time and as a function of solvent type, bed height, solvent temperature and solvent flow rate

					Removal efficiencies of model tar compounds					
					Benzene		Toluene		Ethylbenzene	
Solvent	Bed height	Solvent temp.	Solvent flow rate	Time	Mean	S.E.*	Mean	S.E.*	Mean	S.E.*
	m	C	ml/min	min	%		%		%	
Soybean	0.5	30	53	1	93.7	0.4	96.0	0.0	98.1	0.1
Soybean	0.5	30	53	6	86.4	0.9	95.0	0.0	97.9	0.1
Soybean	0.5	30	53	12	83.6	1.0	94.1	0.4	97.6	0.1
Soybean	0.5	30	53	18	77.7	0.2	92.2	0.3	97.1	0.1
Soybean	0.5	30	53	24	69.5	3.9	89.2	0.5	96.0	0.1
Soybean	0.5	30	53	30	61.4	2.2	85.8	1.7	94.7	0.9
Soybean	0.5	30	53	36	54.3	1.9	82.4	0.0	93.2	0.0
Soybean	0.5	30	53	42	48.4	0.8	79.3	0.6	91.8	0.3
Soybean	0.5	30	53	48	42.0	1.7	75.1	0.6	89.8	0.3
Soybean	0.5	30	53	54	39.7	1.6	73.0	0.3	88.9	0.3
Soybean	0.5	30	63	1	95.5	1.4	97.1	1.7	98.7	1.0
Soybean	0.5	30	63	6	90.6	2.1	96.0	1.4	98.6	1.1
Soybean	0.5	30	63	12	83.8	0.3	94.1	0.6	97.7	0.5
Soybean	0.5	30	63	18	72.2	3.4	90.1	0.5	96.2	0.0
Soybean	0.5	30	63	24	69.4	3.9	88.1	1.6	95.4	0.8
Soybean	0.5	30	63	30	57.4	3.9	83.2	0.7	93.3	0.1
Soybean	0.5	30	63	36	53.1	2.6	80.8	0.3	92.3	0.1
Soybean	0.5	30	63	42	45.8	3.0	76.9	0.5	90.5	0.1
Soybean	0.5	30	63	48	42.2	3.4	74.3	0.8	89.3	0.0
Soybean	0.5	30	63	54	38.6	2.2	71.6	0.1	87.9	0.4
Soybean	0.5	30	73	1	96.0	0.1	96.7	0.4	98.7	0.9
Soybean	0.5	30	73	6	92.1	0.2	96.1	0.6	98.6	1.0
Soybean	0.5	30	73	12	83.4	0.0	93.6	0.6	97.4	0.5
Soybean	0.5	30	73	18	72.1	0.4	89.5	0.6	95.9	0.5
Soybean	0.5	30	73	24	63.9	0.8	86.2	0.1	94.6	0.1
Soybean	0.5	30	73	30	57.8	0.9	83.2	0.2	93.3	0.3
Soybean	0.5	30	73	36	51.3	0.3	79.7	0.3	91.7	0.4
Soybean	0.5	30	73	42	45.6	1.3	76.6	0.9	90.1	0.6
Soybean	0.5	30	73	48	42.7	0.1	74.9	0.1	89.5	0.3
Soybean	0.5	30	73	54	37.5	0.9	71.1	0.6	87.4	0.0
Soybean	0.5	40	53	1	91.6	3.0	94.8	0.6	97.1	0.1
Soybean	0.5	40	53	6	79.1	0.5	92.1	0.3	96.5	0.2

Soybean	0.5	40	53	12	68.4	0.2	86.4	0.4	93.9	0.3
Soybean	0.5	40	53	18	58.8	1.0	81.7	0.9	91.9	0.6
Soybean	0.5	40	53	24	50.1	2.2	76.5	1.6	89.4	0.9
Soybean	0.5	40	53	30	42.7	0.8	71.8	1.4	87.0	0.7
Soybean	0.5	40	53	36	38.0	0.3	68.5	0.2	85.3	0.0
Soybean	0.5	40	53	42	35.2	2.5	66.2	2.1	84.2	1.0
Soybean	0.5	40	53	48	29.7	1.9	61.1	2.7	81.4	1.6
Soybean	0.5	40	53	54	25.8	1.0	57.4	1.7	78.8	-
Soybean	0.5	40	63	1	93.3	2.7	96.1	0.8	98.0	0.6
Soybean	0.5	40	63	6	79.1	3.5	92.9	0.0	97.2	0.4
Soybean	0.5	40	63	12	70.2	1.6	89.3	0.1	95.9	0.2
Soybean	0.5	40	63	18	58.8	2.6	83.5	1.5	93.3	0.7
Soybean	0.5	40	63	24	50.0	0.7	78.7	0.3	91.1	0.2
Soybean	0.5	40	63	30	42.3	0.4	73.7	0.3	88.8	0.3
Soybean	0.5	40	63	36	41.3	4.4	71.6	0.8	87.6	0.1
Soybean	0.5	40	63	42	32.3	0.4	65.5	2.0	84.7	1.5
Soybean	0.5	40	63	48	27.0	1.5	60.6	1.8	81.9	1.7
Soybean	0.5	40	63	54	24.4	1.1	57.1	2.9	79.9	2.0
Soybean	0.5	40	73	1	92.1	0.1	95.9	2.0	98.2	1.6
Soybean	0.5	40	73	6	80.8	0.1	93.0	2.1	97.1	1.5
Soybean	0.5	40	73	12	66.1	1.7	86.5	3.0	94.4	1.9
Soybean	0.5	40	73	18	56.4	1.4	82.0	0.9	92.5	1.0
Soybean	0.5	40	73	24	47.7	1.7	76.7	3.7	90.0	2.5
Soybean	0.5	40	73	30	41.8	1.1	73.2	3.2	88.4	2.5
Soybean	0.5	40	73	36	35.8	0.3	68.0	1.7	85.7	1.6
Soybean	0.5	40	73	42	30.7	0.3	63.5	2.8	83.3	2.5
Soybean	0.5	40	73	48	27.4	0.7	59.9	1.8	81.4	1.7
Soybean	0.5	40	73	54	23.8	0.3	55.8	3.8	79.2	3.5
Soybean	0.5	50	53	1	90.4	1.4	94.1	0.3	96.3	0.2
Soybean	0.5	50	53	6	69.9	1.1	87.4	0.9	94.0	0.2
Soybean	0.5	50	53	12	56.2	0.1	79.6	0.6	90.2	0.3
Soybean	0.5	50	53	18	46.9	0.2	73.2	1.1	87.1	0.4
Soybean	0.5	50	53	24	38.8	0.2	66.5	1.7	83.3	1.3
Soybean	0.5	50	53	30	30.6	2.2	58.6	0.7	78.6	0.6
Soybean	0.5	50	53	36	26.5	3.8	53.5	1.3	75.3	0.9
Soybean	0.5	50	53	42	23.6	2.0	48.9	0.1	72.0	0.2
Soybean	0.5	50	53	48	19.1	2.6	41.5	1.3	66.4	0.8
Soybean	0.5	50	53	54	19.2	4.8	39.6	3.2	65.2	2.0
Soybean	0.5	50	63	1	85.7	3.9	92.3	2.4	95.6	1.1

Soybean	0.5	50	63	6	71.2	1.6	87.5	2.0	94.1	1.1
Soybean	0.5	50	63	12	58.2	1.6	79.9	2.5	90.3	1.4
Soybean	0.5	50	63	18	45.2	1.5	71.3	2.3	86.1	1.5
Soybean	0.5	50	63	24	33.6	1.5	62.4	0.8	81.1	1.0
Soybean	0.5	50	63	30	27.8	0.0	55.6	2.0	76.6	1.9
Soybean	0.5	50	63	36	22.9	0.4	48.8	2.7	72.3	3.0
Soybean	0.5	50	63	42	19.6	1.2	43.6	2.3	68.8	2.3
Soybean	0.5	50	63	48	16.5	1.8	38.4	3.0	64.9	4.1
Soybean	0.5	50	63	54	15.9	4.5	35.1	0.4	62.3	1.7
Soybean	0.5	50	73	1	89.4	2.6	94.3	1.4	96.6	1.6
Soybean	0.5	50	73	6	72.6	1.9	88.7	2.1	94.7	1.8
Soybean	0.5	50	73	12	51.9	1.6	77.6	1.7	89.5	1.7
Soybean	0.5	50	73	18	38.6	4.0	68.8	3.3	85.0	2.7
Soybean	0.5	50	73	24	32.1	1.1	62.5	1.9	81.5	1.9
Soybean	0.5	50	73	30	23.7	0.6	54.2	0.6	76.8	1.2
Soybean	0.5	50	73	36	20.1	0.3	49.1	2.3	73.6	2.2
Soybean	0.5	50	73	42	19.7	2.5	47.3	3.9	72.2	3.7
Soybean	0.5	50	73	48	18.3	2.7	44.5	2.5	69.8	0.5
Soybean	0.5	50	73	54	20.0	6.1	44.9	6.3	70.3	3.5
Canola	0.5	30	53	1	93.7	1.6	96.6	0.3	98.4	0.1
Canola	0.5	30	53	6	85.9	3.7	95.5	0.8	98.3	0.1
Canola	0.5	30	53	12	85.2	5.2	95.0	1.0	98.2	0.2
Canola	0.5	30	53	18	76.1	2.1	92.5	1.1	97.4	0.4
Canola	0.5	30	53	24	70.1	0.2	90.3	1.1	96.6	0.7
Canola	0.5	30	53	30	62.9	0.6	87.3	1.3	95.6	0.8
Canola	0.5	30	53	36	54.6	4.8	83.6	2.9	94.0	1.6
Canola	0.5	30	53	42	51.4	0.6	81.5	2.1	93.0	1.5
Canola	0.5	30	53	48	43.6	3.5	77.6	3.4	91.3	2.2
Canola	0.5	30	53	54	40.7	4.6	75.2	3.8	90.2	2.4
Canola	0.5	30	63	1	91.6	1.2	96.6	1.1	98.7	0.9
Canola	0.5	30	63	6	85.6	0.5	95.7	1.1	98.7	0.9
Canola	0.5	30	63	12	80.3	1.8	94.2	0.6	98.0	0.5
Canola	0.5	30	63	18	73.9	0.7	92.1	0.9	97.3	0.7
Canola	0.5	30	63	24	63.1	1.1	87.9	0.7	95.8	0.6
Canola	0.5	30	63	30	56.9	1.1	85.0	0.5	94.6	0.6
Canola	0.5	30	63	36	50.1	0.6	81.4	0.7	93.1	0.5
Canola	0.5	30	63	42	45.1	1.3	78.2	0.4	91.6	0.4
Canola	0.5	30	63	48	39.2	-	73.8	-	89.2	-
Canola	0.5	30	63	54	37.1	-	72.4	-	89.0	-

Canola	0.5	30	73	1	92.0	1.0	96.1	0.5	98.3	0.3
Canola	0.5	30	73	6	86.3	0.8	95.2	0.6	98.2	0.4
Canola	0.5	30	73	12	81.6	0.2	93.9	0.9	97.8	0.6
Canola	0.5	30	73	18	74.3	1.4	91.6	1.0	97.0	0.6
Canola	0.5	30	73	24	66.5	0.7	88.4	0.2	95.8	0.3
Canola	0.5	30	73	30	60.5	3.3	85.7	0.9	94.7	0.2
Canola	0.5	30	73	36	52.1	3.1	81.7	1.4	93.1	0.4
Canola	0.5	30	73	42	48.5	5.2	79.1	2.3	91.7	0.9
Canola	0.5	30	73	48	46.6	-	78.0	-	91.0	-
Canola	0.5	30	73	54	44.0	-	75.9	-	89.9	-
Canola	0.5	40	53	1	90.9	1.1	94.8	0.5	97.2	0.2
Canola	0.5	40	53	6	79.4	2.4	92.2	0.5	96.5	0.1
Canola	0.5	40	53	12	67.2	1.6	86.6	0.0	94.2	0.0
Canola	0.5	40	53	18	57.7	0.7	81.8	0.3	92.1	0.3
Canola	0.5	40	53	24	48.7	0.2	76.6	0.4	89.6	0.4
Canola	0.5	40	53	30	42.9	1.0	72.3	0.1	87.4	0.1
Canola	0.5	40	53	36	38.1	3.0	69.1	2.0	85.9	1.1
Canola	0.5	40	53	42	33.5	4.3	65.0	2.9	83.6	2.0
Canola	0.5	40	53	48	29.5	1.4	60.8	1.2	81.2	0.9
Canola	0.5	40	53	54	26.7	1.1	57.2	0.7	79.0	0.5
Canola	0.5	40	63	1	89.0	0.1	95.9	0.8	98.6	1.1
Canola	0.5	40	63	6	77.6	1.7	93.3	1.0	97.6	0.6
Canola	0.5	40	63	12	70.5	2.0	89.9	0.2	96.3	0.2
Canola	0.5	40	63	18	59.9	0.1	84.4	0.2	94.0	0.0
Canola	0.5	40	63	24	52.7	1.9	80.9	0.7	92.7	0.1
Canola	0.5	40	63	30	43.2	0.4	75.6	0.2	90.5	0.2
Canola	0.5	40	63	36	37.7	1.9	70.9	1.1	88.1	0.5
Canola	0.5	40	63	42	31.0	5.0	65.7	2.8	85.4	1.6
Canola	0.5	40	63	48	27.7	3.1	61.8	1.4	83.1	0.9
Canola	0.5	40	63	54	24.5	3.3	58.1	1.4	81.1	0.8
Canola	0.5	40	73	1	91.9	5.1	95.5	1.4	97.9	0.7
Canola	0.5	40	73	6	81.1	0.6	93.5	1.0	97.5	0.7
Canola	0.5	40	73	12	69.1	2.6	87.8	2.3	95.1	1.3
Canola	0.5	40	73	18	57.5	3.3	81.9	3.1	92.4	2.1
Canola	0.5	40	73	24	48.2	2.2	77.0	1.9	90.2	1.3
Canola	0.5	40	73	30	41.5	2.2	72.3	1.6	87.8	1.2
Canola	0.5	40	73	36	35.8	1.4	67.8	1.6	85.5	1.7
Canola	0.5	40	73	42	30.8	1.9	63.5	1.5	83.4	1.2
Canola	0.5	40	73	48	27.0	0.6	59.5	1.2	81.2	1.1

Canola	0.5	40	73	54	23.7	1.2	55.7	0.8	79.2	0.9
Canola	0.5	50	53	1	84.1	0.3	93.3	0.0	96.4	0.0
Canola	0.5	50	53	6	70.7	0.1	88.1	0.4	94.6	0.2
Canola	0.5	50	53	12	58.7	1.5	81.5	1.4	91.5	0.8
Canola	0.5	50	53	18	46.8	1.3	73.3	0.8	87.3	0.4
Canola	0.5	50	53	24	37.4	2.2	65.7	1.8	82.8	1.5
Canola	0.5	50	53	30	31.2	0.2	60.1	0.8	79.9	0.5
Canola	0.5	50	53	36	24.5	1.0	52.6	0.7	75.0	1.3
Canola	0.5	50	53	42	21.9	0.4	49.1	0.5	72.7	0.0
Canola	0.5	50	53	48	19.6	1.4	44.7	2.8	69.1	2.4
Canola	0.5	50	53	54	17.7	1.4	40.5	2.1	65.5	1.9
Canola	0.5	50	63	1	85.9	0.4	93.2	0.4	96.2	0.4
Canola	0.5	50	63	6	71.1	3.4	88.3	1.6	94.6	0.8
Canola	0.5	50	63	12	56.9	2.6	80.1	1.3	90.9	0.9
Canola	0.5	50	63	18	42.9	3.8	71.4	1.8	86.6	1.1
Canola	0.5	50	63	24	35.9	3.1	64.9	2.1	83.0	1.4
Canola	0.5	50	63	30	26.8	5.1	56.3	3.8	77.9	2.8
Canola	0.5	50	63	36	22.8	0.7	50.5	1.3	74.0	2.1
Canola	0.5	50	63	42	20.0	0.7	45.2	1.1	70.3	1.6
Canola	0.5	50	63	48	17.1	2.2	40.2	0.8	66.2	0.0
Canola	0.5	50	63	54	16.1	2.6	36.9	3.9	62.8	3.2
Canola	0.5	50	73	1	82.3	8.1	94.5	2.8	97.7	2.3
Canola	0.5	50	73	6	71.6	0.7	89.7	2.1	96.0	1.7
Canola	0.5	50	73	12	61.0	2.7	83.2	2.8	93.0	2.0
Canola	0.5	50	73	18	46.0	2.5	73.2	1.7	87.9	1.2
Canola	0.5	50	73	24	36.4	0.3	65.4	0.7	83.9	0.8
Canola	0.5	50	73	30	29.8	0.0	59.8	0.4	81.0	0.6
Canola	0.5	50	73	36	23.3	0.9	51.7	1.2	75.5	0.6
Canola	0.5	50	73	42	17.8	0.8	45.1	1.3	71.4	1.6
Canola	0.5	50	73	48	15.2	0.2	39.2	0.2	66.9	0.2
Canola	0.5	50	73	54	13.2	0.1	34.8	1.9	63.7	2.1
Soybean	0.8	30	53	1	98.2	0.1	96.3	0.1	98.0	0.0
Soybean	0.8	30	53	6	95.8	0.2	95.9	0.0	97.9	0.0
Soybean	0.8	30	53	12	89.3	1.0	94.0	0.4	97.2	0.1
Soybean	0.8	30	53	18	79.9	1.9	91.2	0.7	96.2	0.1
Soybean	0.8	30	53	24	70.7	0.6	88.1	0.0	95.0	0.1
Soybean	0.8	30	53	30	61.9	1.5	84.5	0.8	93.4	0.3
Soybean	0.8	30	53	36	57.7	0.5	82.5	0.3	92.6	0.0
Soybean	0.8	30	53	42	51.2	0.3	79.4	0.2	91.1	0.1

Soybean	0.8	30	53	48	46.1	0.4	76.9	0.2	90.1	0.0
Soybean	0.8	30	53	54	41.6	0.3	74.1	0.3	88.8	0.1
Soybean	0.8	30	63	1	98.9	0.6	97.1	0.8	98.7	0.9
Soybean	0.8	30	63	6	97.1	0.9	96.6	0.9	98.6	1.0
Soybean	0.8	30	63	12	89.9	0.7	94.5	0.7	97.6	0.5
Soybean	0.8	30	63	18	79.6	0.6	91.6	0.9	96.6	0.6
Soybean	0.8	30	63	24	71.2	0.9	88.4	1.1	95.3	0.6
Soybean	0.8	30	63	30	63.8	0.3	85.5	0.9	94.1	0.5
Soybean	0.8	30	63	36	57.1	2.0	82.6	0.3	92.7	0.3
Soybean	0.8	30	63	42	51.7	1.0	79.9	0.7	91.6	0.4
Soybean	0.8	30	63	48	50.4	1.1	78.7	1.4	91.0	0.7
Soybean	0.8	30	63	54	43.5	4.1	75.1	0.6	89.4	0.0
Soybean	0.8	30	73	1	98.2	0.2	96.3	0.1	98.0	0.1
Soybean	0.8	30	73	6	96.0	1.0	95.6	0.3	97.7	0.1
Soybean	0.8	30	73	12	84.5	0.0	92.3	0.0	96.5	0.0
Soybean	0.8	30	73	18	76.7	1.9	89.8	0.9	95.6	0.5
Soybean	0.8	30	73	24	66.5	0.7	86.1	0.5	94.1	0.2
Soybean	0.8	30	73	30	60.4	0.1	83.3	0.5	92.8	0.3
Soybean	0.8	30	73	36	52.6	1.2	79.9	0.1	91.2	0.0
Soybean	0.8	30	73	42	47.5	2.0	77.2	0.4	90.0	0.3
Soybean	0.8	30	73	48	43.0	1.9	74.3	0.0	88.6	0.1
Soybean	0.8	30	73	54	39.6	1.3	72.1	0.2	87.5	0.1
Soybean	0.8	40	53	1	95.8	0.9	95.2	0.4	97.0	0.2
Soybean	0.8	40	53	6	88.3	1.3	92.7	0.4	95.9	0.2
Soybean	0.8	40	53	12	74.1	0.7	87.0	0.5	93.2	0.4
Soybean	0.8	40	53	18	61.6	0.7	81.8	0.2	90.7	0.0
Soybean	0.8	40	53	24	52.1	0.9	77.1	0.5	88.3	0.4
Soybean	0.8	40	53	30	42.9	0.8	71.8	0.3	85.6	0.0
Soybean	0.8	40	53	36	35.8	2.3	67.1	1.4	82.9	0.9
Soybean	0.8	40	53	42	30.1	2.8	62.5	1.9	80.2	1.1
Soybean	0.8	40	53	48	25.7	1.2	58.3	1.0	77.9	0.6
Soybean	0.8	40	53	54	21.2	2.2	53.9	2.1	75.2	1.0
Soybean	0.8	40	63	1	95.6	1.2	95.2	1.0	97.2	0.5
Soybean	0.8	40	63	6	86.8	0.2	91.8	0.7	95.6	0.4
Soybean	0.8	40	63	12	70.4	2.8	85.4	0.8	92.8	0.6
Soybean	0.8	40	63	18	61.5	0.3	81.7	0.6	91.2	0.5
Soybean	0.8	40	63	24	51.5	1.3	77.0	0.2	89.0	0.0
Soybean	0.8	40	63	30	40.2	5.6	70.5	2.3	85.5	1.5
Soybean	0.8	40	63	36	35.0	3.9	66.3	1.4	83.2	0.9

Soybean	0.8	40	63	42	33.3	0.0	64.2	0.0	82.7	0.0
Soybean	0.8	40	63	48	23.4	5.8	56.9	3.0	78.3	1.9
Soybean	0.8	40	63	54	19.4	7.6	52.8	4.7	75.7	3.4
Soybean	0.8	40	73	1	94.5	1.4	94.7	0.5	97.0	0.2
Soybean	0.8	40	73	6	86.5	0.4	91.2	0.3	95.5	0.0
Soybean	0.8	40	73	12	71.5	2.3	85.3	1.3	92.8	0.6
Soybean	0.8	40	73	18	60.5	3.0	80.4	1.4	90.5	0.6
Soybean	0.8	40	73	24	51.2	2.5	75.7	0.9	88.2	0.2
Soybean	0.8	40	73	30	42.9	1.1	70.6	0.2	85.6	0.1
Soybean	0.8	40	73	36	37.5	3.2	66.7	1.8	83.6	0.7
Soybean	0.8	40	73	42	32.5	2.3	62.9	0.9	81.6	0.3
Soybean	0.8	40	73	48	26.2	4.4	57.2	3.0	78.4	2.0
Soybean	0.8	40	73	54	23.2	1.5	53.1	0.6	75.4	0.2
Soybean	0.8	50	53	1	95.1	1.0	94.2	0.2	95.9	0.2
Soybean	0.8	50	53	6	83.0	0.5	90.5	0.6	94.0	0.6
Soybean	0.8	50	53	12	63.7	1.1	81.5	1.1	89.6	0.8
Soybean	0.8	50	53	18	48.6	1.0	73.1	0.2	85.1	0.2
Soybean	0.8	50	53	24	37.9	1.1	65.9	0.9	81.0	1.0
Soybean	0.8	50	53	30	28.6	0.3	58.4	0.8	76.7	0.9
Soybean	0.8	50	53	36	23.0	1.4	52.1	2.1	72.2	2.3
Soybean	0.8	50	53	42	17.4	0.7	45.6	0.1	67.7	0.3
Soybean	0.8	50	53	48	14.4	1.5	40.1	0.3	63.9	0.5
Soybean	0.8	50	53	54	11.7	0.3	35.0	1.0	59.4	1.7
Soybean	0.8	50	63	1	94.1	0.2	94.7	0.1	96.3	0.2
Soybean	0.8	50	63	6	81.6	2.0	89.8	1.2	93.9	1.0
Soybean	0.8	50	63	12	62.7	2.5	80.8	1.2	89.5	1.1
Soybean	0.8	50	63	18	49.3	3.3	72.9	1.3	85.4	1.1
Soybean	0.8	50	63	24	37.2	3.2	64.6	1.2	80.7	0.9
Soybean	0.8	50	63	30	31.1	3.3	58.6	1.5	77.1	1.6
Soybean	0.8	50	63	36	24.7	3.0	52.3	2.0	73.3	1.8
Soybean	0.8	50	63	42	22.3	6.4	48.0	4.8	70.2	3.8
Soybean	0.8	50	63	48	20.9	2.9	45.2	0.9	68.8	0.6
Soybean	0.8	50	63	54	16.7	4.7	37.8	3.4	62.3	3.0
Soybean	0.8	50	73	1	93.9	0.3	94.7	0.5	96.3	0.1
Soybean	0.8	50	73	6	79.3	1.5	88.5	0.3	92.7	0.9
Soybean	0.8	50	73	12	57.0	4.9	78.1	1.7	87.7	1.7
Soybean	0.8	50	73	18	45.4	0.6	71.0	0.3	84.2	0.7
Soybean	0.8	50	73	24	38.9	5.5	65.4	3.0	81.2	1.1
Soybean	0.8	50	73	30	28.8	3.1	57.3	1.8	76.9	0.3

Soybean	0.8	50	73	36	22.8	1.2	51.2	1.7	72.5	0.2
Soybean	0.8	50	73	42	20.4	0.5	46.8	2.8	69.5	1.6
Soybean	0.8	50	73	48	19.2	1.6	45.9	2.4	68.8	1.3
Soybean	0.8	50	73	54	18.7	-	48.3	-	69.8	-
Soybean	1.1	30	53	1	99.0	0.7	96.9	1.0	98.6	1.0
Soybean	1.1	30	53	6	96.9	0.9	95.6	0.9	97.6	0.5
Soybean	1.1	30	53	12	90.4	2.6	93.8	1.6	97.0	0.9
Soybean	1.1	30	53	18	75.2	1.9	89.3	1.2	95.3	0.5
Soybean	1.1	30	53	24	64.7	0.9	85.5	1.0	93.6	0.5
Soybean	1.1	30	53	30	56.0	1.2	82.0	1.2	92.1	0.6
Soybean	1.1	30	53	36	51.1	4.2	79.5	2.1	91.0	1.1
Soybean	1.1	30	53	42	42.6	2.4	75.5	1.6	89.1	0.8
Soybean	1.1	30	53	48	38.5	4.6	72.6	1.7	87.5	0.8
Soybean	1.1	30	53	54	33.2	-	69.6	-	86.1	-
Soybean	1.1	30	63	1	98.9	0.1	96.6	0.1	97.9	0.0
Soybean	1.1	30	63	6	96.3	0.6	95.1	0.2	97.2	0.1
Soybean	1.1	30	63	12	87.0	0.8	92.5	0.5	96.3	0.2
Soybean	1.1	30	63	18	77.0	0.5	89.5	0.1	95.1	0.1
Soybean	1.1	30	63	24	68.8	0.7	86.6	0.5	93.9	0.3
Soybean	1.1	30	63	30	60.0	1.7	83.1	0.6	92.3	0.1
Soybean	1.1	30	63	36	52.5	1.1	79.7	0.2	90.7	0.1
Soybean	1.1	30	63	42	46.3	4.0	76.6	1.7	89.3	0.8
Soybean	1.1	30	63	48	39.6	2.3	72.7	0.9	87.4	0.5
Soybean	1.1	30	63	54	37.4	0.1	70.9	0.2	86.5	0.1
Soybean	1.1	30	73	1	98.4	0.7	96.1	0.4	97.9	0.3
Soybean	1.1	30	73	6	96.2	1.8	95.0	0.9	97.5	0.5
Soybean	1.1	30	73	12	84.9	1.5	92.0	0.9	96.5	0.5
Soybean	1.1	30	73	18	75.3	0.9	88.7	0.7	95.2	0.4
Soybean	1.1	30	73	24	66.6	1.2	85.4	1.0	93.8	0.6
Soybean	1.1	30	73	30	59.3	0.8	82.4	0.7	92.5	0.5
Soybean	1.1	30	73	36	53.7	1.6	79.8	1.3	91.4	0.7
Soybean	1.1	30	73	42	49.7	0.9	77.9	0.0	90.5	0.2
Soybean	1.1	30	73	48	45.7	1.7	75.7	0.6	89.6	0.1
Soybean	1.1	30	73	54	41.5	0.3	72.9	0.2	88.2	0.4
Soybean	1.1	40	53	1	98.3	1.1	96.4	1.3	98.3	1.5
Soybean	1.1	40	53	6	91.5	0.8	92.6	1.0	96.1	0.7
Soybean	1.1	40	53	12	76.6	1.0	86.8	1.2	93.5	0.8
Soybean	1.1	40	53	18	63.6	0.2	81.6	0.4	91.0	0.1
Soybean	1.1	40	53	24	49.6	1.8	74.7	0.2	87.4	0.1

Soybean	1.1	40	53	30	41.8	3.0	70.2	1.2	85.0	0.7
Soybean	1.1	40	53	36	35.8	2.4	66.2	0.9	83.2	0.6
Soybean	1.1	40	53	42	28.5	0.9	60.7	0.1	79.8	0.2
Soybean	1.1	40	53	48	24.8	1.2	57.2	0.7	77.8	0.5
Soybean	1.1	40	53	54	22.4	2.6	53.9	1.5	75.9	1.2
Soybean	1.1	40	63	1	96.8	0.2	95.3	0.2	97.2	0.0
Soybean	1.1	40	63	6	86.2	0.7	89.7	0.5	94.5	0.6
Soybean	1.1	40	63	12	67.1	3.8	81.9	1.9	90.6	0.9
Soybean	1.1	40	63	18	54.4	0.3	76.5	0.1	87.8	0.2
Soybean	1.1	40	63	24	40.7	2.2	69.7	1.3	84.4	0.4
Soybean	1.1	40	63	30	32.4	2.9	64.8	1.7	81.8	1.6
Soybean	1.1	40	63	36	25.1	0.0	60.3	0.6	79.3	0.1
Soybean	1.1	40	63	42	15.3	2.8	53.4	3.4	74.9	2.4
Soybean	1.1	40	63	48	6.1	-	45.6	-	69.7	-
Soybean	1.1	40	63	54	6.5	-	45.6	-	70.7	-
Soybean	1.1	40	73	1	97.0	0.0	95.2	0.1	96.8	0.0
Soybean	1.1	40	73	6	88.0	0.7	90.7	0.2	94.7	0.2
Soybean	1.1	40	73	12	72.4	0.2	85.1	0.4	92.2	0.4
Soybean	1.1	40	73	18	59.7	0.6	79.6	0.0	89.7	0.0
Soybean	1.1	40	73	24	50.0	2.6	75.1	1.2	87.6	0.7
Soybean	1.1	40	73	30	41.0	0.2	69.5	0.3	84.6	0.0
Soybean	1.1	40	73	36	36.2	2.3	66.0	0.7	82.7	0.5
Soybean	1.1	40	73	42	27.1	0.4	59.5	0.2	79.0	0.3
Soybean	1.1	40	73	48	23.4	4.6	56.0	2.9	77.0	2.0
Soybean	1.1	40	73	54	19.7	4.8	52.1	3.6	74.6	1.7
Soybean	1.1	50	53	1	96.8	0.6	94.3	0.3	95.6	0.3
Soybean	1.1	50	53	6	88.8	0.5	89.8	0.4	92.8	0.3
Soybean	1.1	50	53	12	69.9	1.7	81.0	1.0	88.5	0.4
Soybean	1.1	50	53	18	52.3	2.5	72.1	1.6	83.6	0.9
Soybean	1.1	50	53	24	39.0	2.0	64.0	0.8	79.1	0.5
Soybean	1.1	50	53	30	29.4	1.5	56.9	0.8	74.8	0.2
Soybean	1.1	50	53	36	17.2	5.2	46.6	3.3	67.8	2.3
Soybean	1.1	50	53	42	14.8	4.4	42.3	3.4	64.9	2.5
Soybean	1.1	50	53	48	11.5	5.4	37.0	4.5	60.6	4.1
Soybean	1.1	50	53	54	8.8	0.4	32.1	0.1	57.0	0.7
Soybean	1.1	50	63	1	96.1	0.3	94.0	0.7	95.4	0.7
Soybean	1.1	50	63	6	85.9	-	87.5	-	91.4	-
Soybean	1.1	50	63	12	62.4	2.1	77.5	0.9	86.9	0.3
Soybean	1.1	50	63	18	45.0	2.2	68.0	1.8	81.5	1.0

Soybean	1.1	50	63	24	33.7	1.8	60.6	2.2	77.5	1.7
Soybean	1.1	50	63	30	23.5	0.9	52.2	1.6	72.2	1.3
Soybean	1.1	50	63	36	19.6	1.1	47.5	0.2	69.0	0.6
Soybean	1.1	50	63	42	13.5	0.8	40.7	1.6	63.9	1.7
Soybean	1.1	50	63	48	12.4	2.3	37.3	1.8	60.8	1.6
Soybean	1.1	50	63	54	8.1	2.4	31.5	2.2	56.7	1.8
Soybean	1.1	50	73	1	97.8	1.5	96.1	2.0	97.7	2.3
Soybean	1.1	50	73	6	82.9	2.9	87.6	1.6	93.0	1.3
Soybean	1.1	50	73	12	61.5	3.4	77.3	0.2	87.9	0.2
Soybean	1.1	50	73	18	46.0	3.4	67.9	0.5	82.7	0.1
Soybean	1.1	50	73	24	33.9	3.2	58.7	1.9	77.1	1.3
Soybean	1.1	50	73	30	27.0	4.0	52.3	2.0	73.2	1.6
Soybean	1.1	50	73	36	20.5	4.0	44.4	3.1	67.7	2.5
Soybean	1.1	50	73	42	18.5	1.4	41.4	8.7	66.2	6.5
Soybean	1.1	50	73	48	18.7	3.8	39.5	14.4	63.5	11.8
Soybean	1.1	50	73	54	18.8	3.2	37.3	15.4	60.6	13.2
Canola	1.1	30	73	1	98.4	0.6	96.5	0.5	98.1	0.2
Canola	1.1	30	73	6	94.1	0.4	94.1	0.0	97.2	0.0
Canola	1.1	30	73	12	84.7	0.3	91.5	0.5	96.2	0.2
Canola	1.1	30	73	18	78.2	0.2	89.3	0.2	95.4	0.1
Canola	1.1	30	73	24	70.6	0.2	86.4	0.1	94.2	0.1
Canola	1.1	30	73	30	62.8	0.4	83.1	0.5	92.6	0.4
Canola	1.1	30	73	36	57.1	0.4	80.4	0.3	91.4	0.2
Canola	1.1	30	73	42	51.5	0.5	77.5	0.2	90.1	0.4
Canola	1.1	30	73	48	46.1	2.2	74.6	0.9	88.8	0.3
Canola	1.1	30	73	54	42.8	0.1	72.3	0.9	87.6	0.8
Canola	1.1	40	73	1	96.9	0.6	95.2	0.5	96.7	0.0
Canola	1.1	40	73	6	86.4	2.2	90.0	0.5	94.4	0.4
Canola	1.1	40	73	12	71.7	0.1	84.8	0.6	92.1	0.2
Canola	1.1	40	73	18	60.5	0.7	80.0	1.2	89.8	0.4
Canola	1.1	40	73	24	51.0	3.3	75.2	3.2	87.3	1.7
Canola	1.1	40	73	30	43.2	2.6	70.8	3.5	85.0	2.0
Canola	1.1	40	73	36	34.5	-	63.1	-	80.8	-
Canola	1.1	40	73	42	29.8	1.2	61.5	3.9	80.1	2.3
Canola	1.1	40	73	48	26.4	1.1	58.7	2.7	78.5	1.6
Canola	1.1	40	73	54	22.8	-	52.8	-	75.0	-
Canola	1.1	50	73	1	97.1	0.4	94.6	1.0	95.5	0.6
Canola	1.1	50	73	6	82.7	2.7	86.5	2.2	91.4	1.1
Canola	1.1	50	73	12	56.4	3.5	74.3	1.4	84.9	1.4

Canola	1.1	50	73	18	40.6	2.8	65.9	0.5	80.5	1.0
Canola	1.1	50	73	24	29.4	3.8	58.8	0.1	76.7	0.3
Canola	1.1	50	73	30	24.4	3.2	55.9	2.7	75.2	1.4
Canola	1.1	50	73	36	22.6	4.9	55.5	0.5	75.1	0.5
Canola	1.1	50	73	42	23.1	6.5	55.1	2.5	75.1	1.8
Canola	1.1	50	73	48	20.1	7.0	50.9	3.1	72.2	2.1
Canola	1.1	50	73	54	17.7	10.7	47.6	5.8	70.2	3.8

*Standard error

- missing data

Appendix C: Saturation limit of benzene and toluene determined using Ozturk & Yilmaz (2006) study

Saturated absorption limit of benzene in sunflower oil at 25°C temperature: 10 g/l

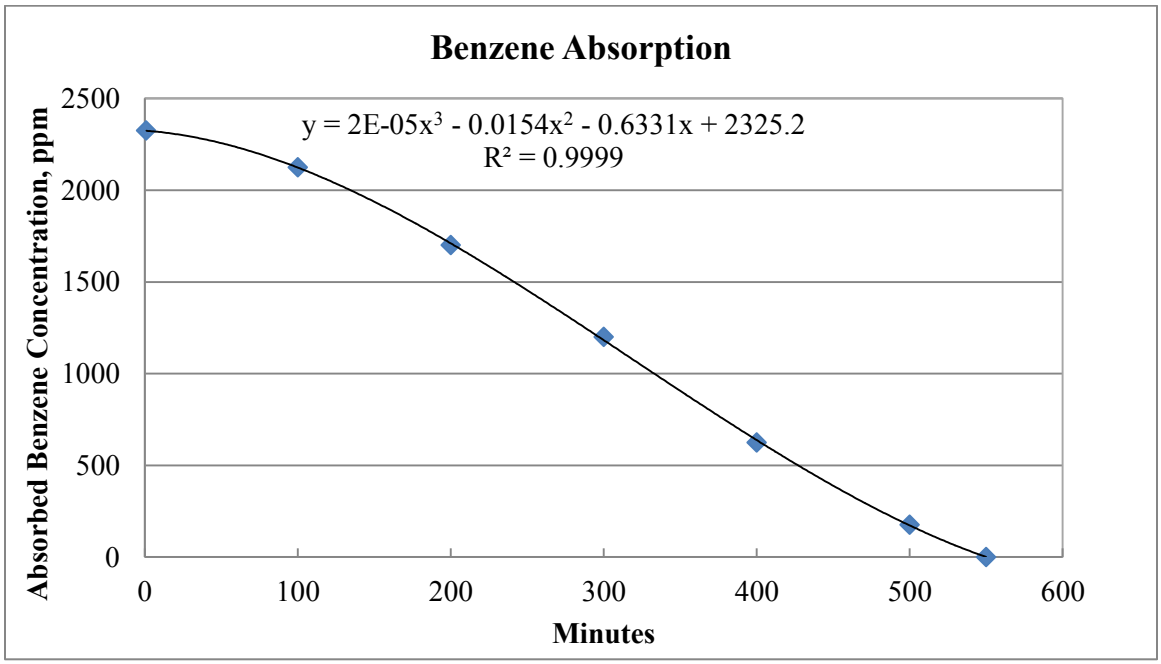

Saturated absorption limit of toluene in sunflower oil at 25°C temperature: 20 g/l

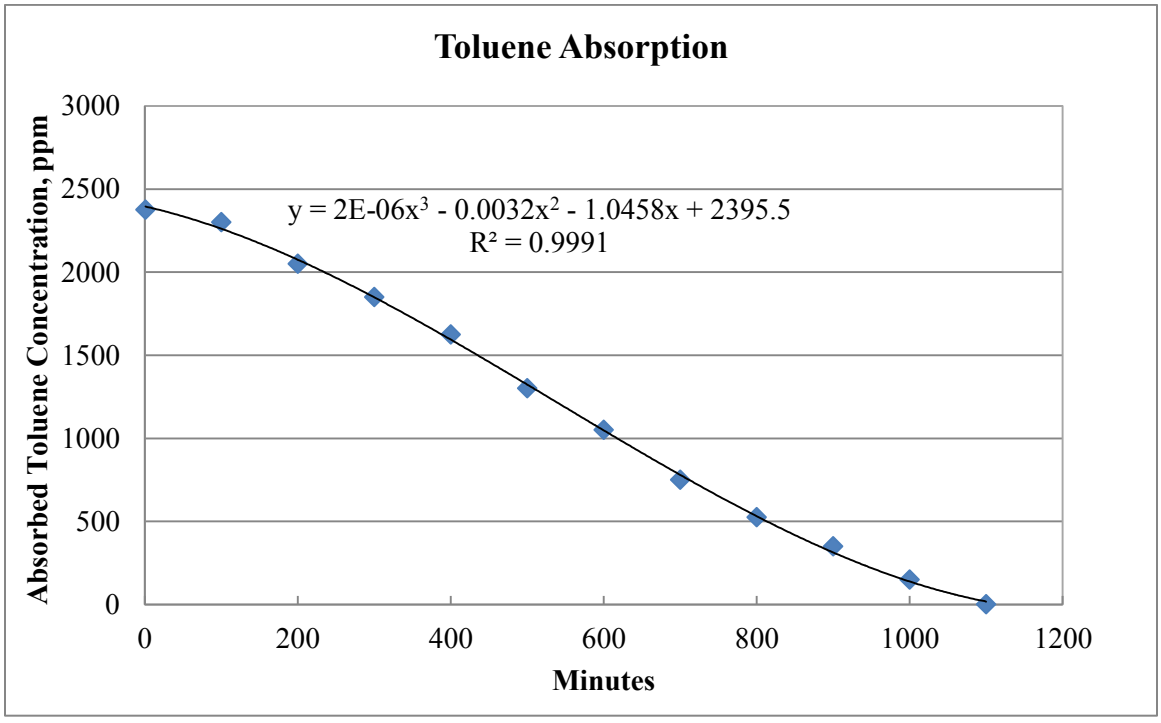

VITA

Prakashbhai Ramabhai Bhoi

Candidate for the Degree of

Doctor of Philosophy

Dissertation: WET SCRUBBING OF BIOMASS PRODUCER GAS TARS USING VEGETABLE OIL

Major Field: Biosystems Engineering

Biographical:

Education:
Completed the requirements for the Doctor of Philosophy in Biosystems Engineering at Oklahoma State University, Stillwater, Oklahoma in May, 2014.

Completed the requirements for the Master of Technology in Mechanical Engineering (Specialization: Turbo Machines) at Sardar Vallabhbhai National Institute of Technology, Surat, Gujarat, India in 2005.

Completed the requirements for the Bachelor of Engineering in Mechanical Engineering at Sardar Patel University, Vallabh Vidyanagar, Gujarat, India in 1999.

Experience:

- Research Engineer, Biosystems and Agricultural Engineering Department, Oklahoma State University, OK, USA [October 2009 – Present]
- Assistant Manager, Mechanical Engineering Department, L&T Sargent and Lundy limited, Vadodara, Gujarat, India [November 2006 – September 2009]
- Scientific Officer, Biomass Thermochemical Conversion Department, Sardar Patel Renewable Energy Research Institute, Vallabh Vidyanagar, Gujarat, India [April 2000 – October 2006]
- Apprentice Engineer, Eimco Elecon India Pvt. Ltd., Vallabh Vidyanagar, Gujarat, India [October 1999 – April 2000]

Professional Memberships:

- American Society of Agricultural and Biological Engineers (ASABE)
- Member of Institute of Industrial Engineers (IEE)